A multiscale restriction-smoothed basis method for high contrast porous media represented on unstructured grids

Olav Møyner and Knut–Andreas Lie

SINTEF Digital, Department of Mathematics & Cybernetics, Oslo, Norway

IPAM OILWS1 - Multiphysics, Multiscale, and Coupled Problems in Subsurface Physics, April 4 2017

Multiscale idea formulated as discrete operators

Illustration: cell-centered TPFA

$$A\boldsymbol{x} = \boldsymbol{q}$$

Initial fine-scale system, incorporating all details of geological model

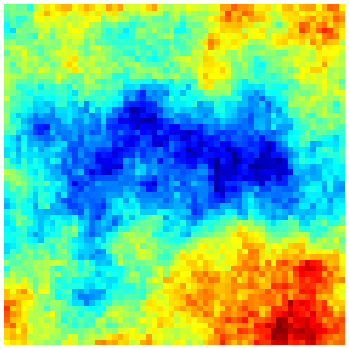

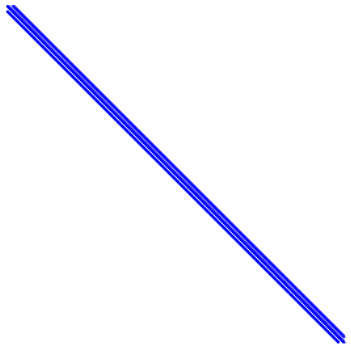

$$\boldsymbol{x} = P\boldsymbol{x}_c$$
$$P = \text{basis}(A)$$
$$A_c = RAP$$
$$\boldsymbol{q}_c = R\boldsymbol{q}$$

Multiscale expansion: generate basis functions, restrict fine-scale system and right-hand side

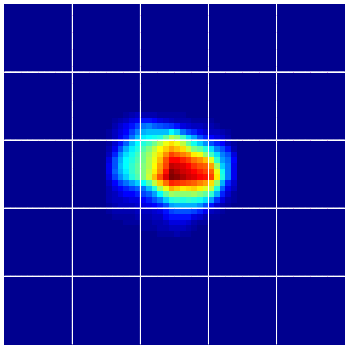

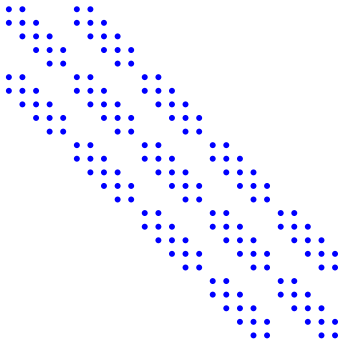

$$\boldsymbol{x}_c = A_c^{-1}\boldsymbol{q}_c$$
$$\boldsymbol{x} \approx P\boldsymbol{x}_c$$

Solve **reduced** system, **prolongate** to obtain approximate pressure

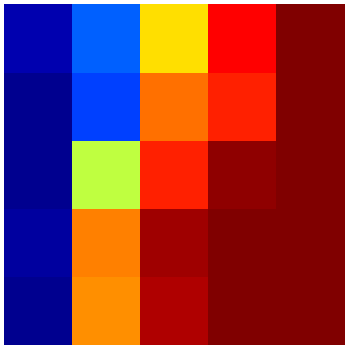

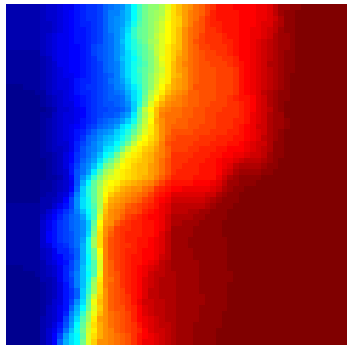

Lee, Lunati, Nordbotten, Tchelepi, Zhou, . . . (2008)

From Poisson's equation to reservoir simulation

Flow physics

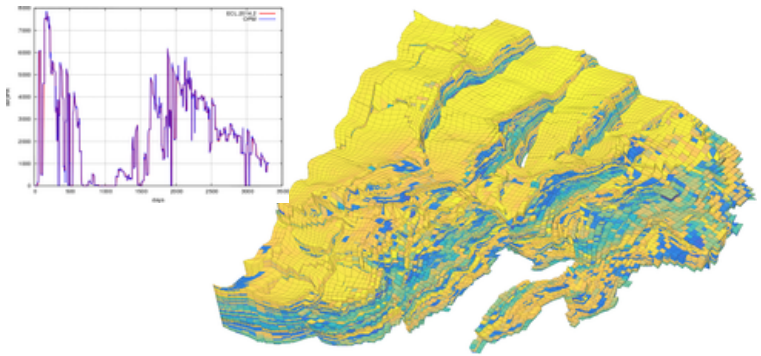

$$
\begin{aligned}
0 =& \partial_t(\phi b_o S_o) + \nabla \cdot (b_o \vec{v_o}) - b_o q_o \\
0 =& \partial_t(\phi b_w S_w) + \nabla \cdot (b_w \vec{v_w}) - b_w q_w \\
0 =& \partial_t\left[\phi(b_g S_b + b_o r_{so} S_o)\right] + \nabla \cdot (b_g \vec{v}_g) \\
& + \nabla \cdot (b_o r_{so} \vec{v_o}) - b_g q_g - b_o r_{so} q_o
\end{aligned}
$$

???

MsFV, MsMFE, 2003

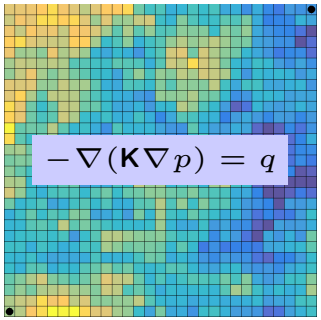

Geology

Why is this challenging?

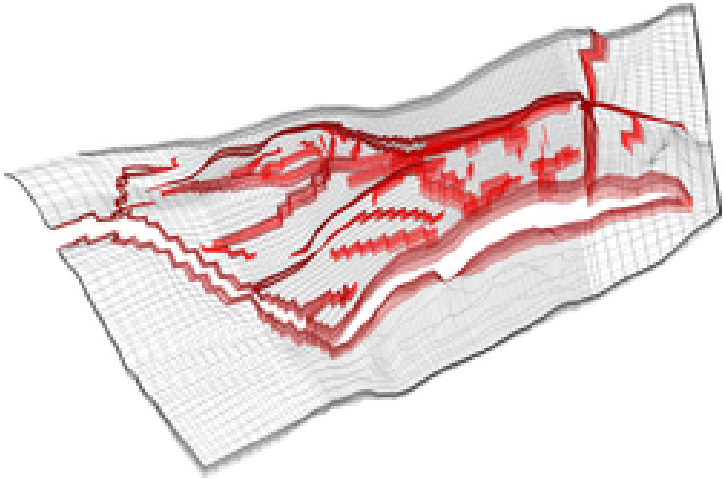

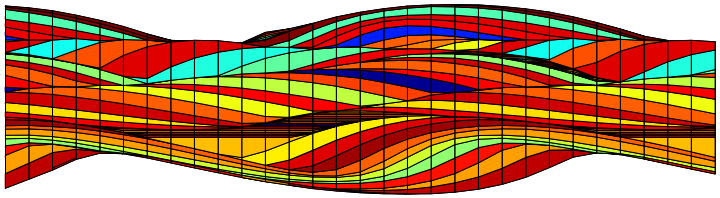

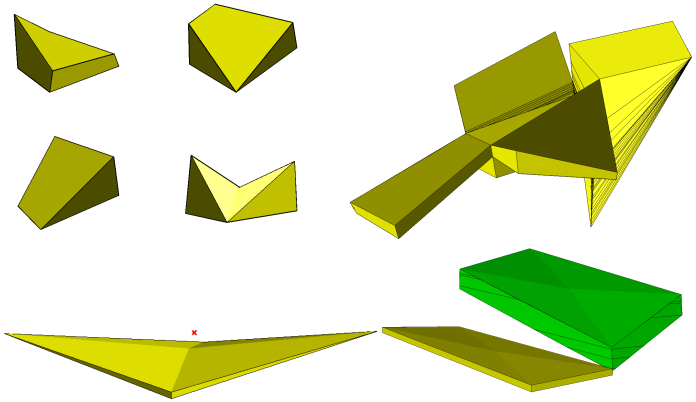

- Geological models: complex unstructured grids having many obscure challenges
- Flow models: system of highly nonlinear parabolic PDEs with elliptic and hyperbolic sub-character
- Well models: analytic sub-models, strong impact on flow

Challenges:

- Industry standard: corner-point / stratigraphic grids
- Grid topology is unstructured
- Geometry: deviates from box shape, high aspect ratios, many faces/neighbors, small faces, . . .
- As a general rule: coarse blocks *will* be unstructured
- Coarse blocks will have strange shapes, many special cases to be handled
- Coarse partition should adapt to features relevant to flow: petrophysical properties, faults, flow direction, wells, . . .

Qualitatively correct solution $\rightarrow$ small fine-scale residual

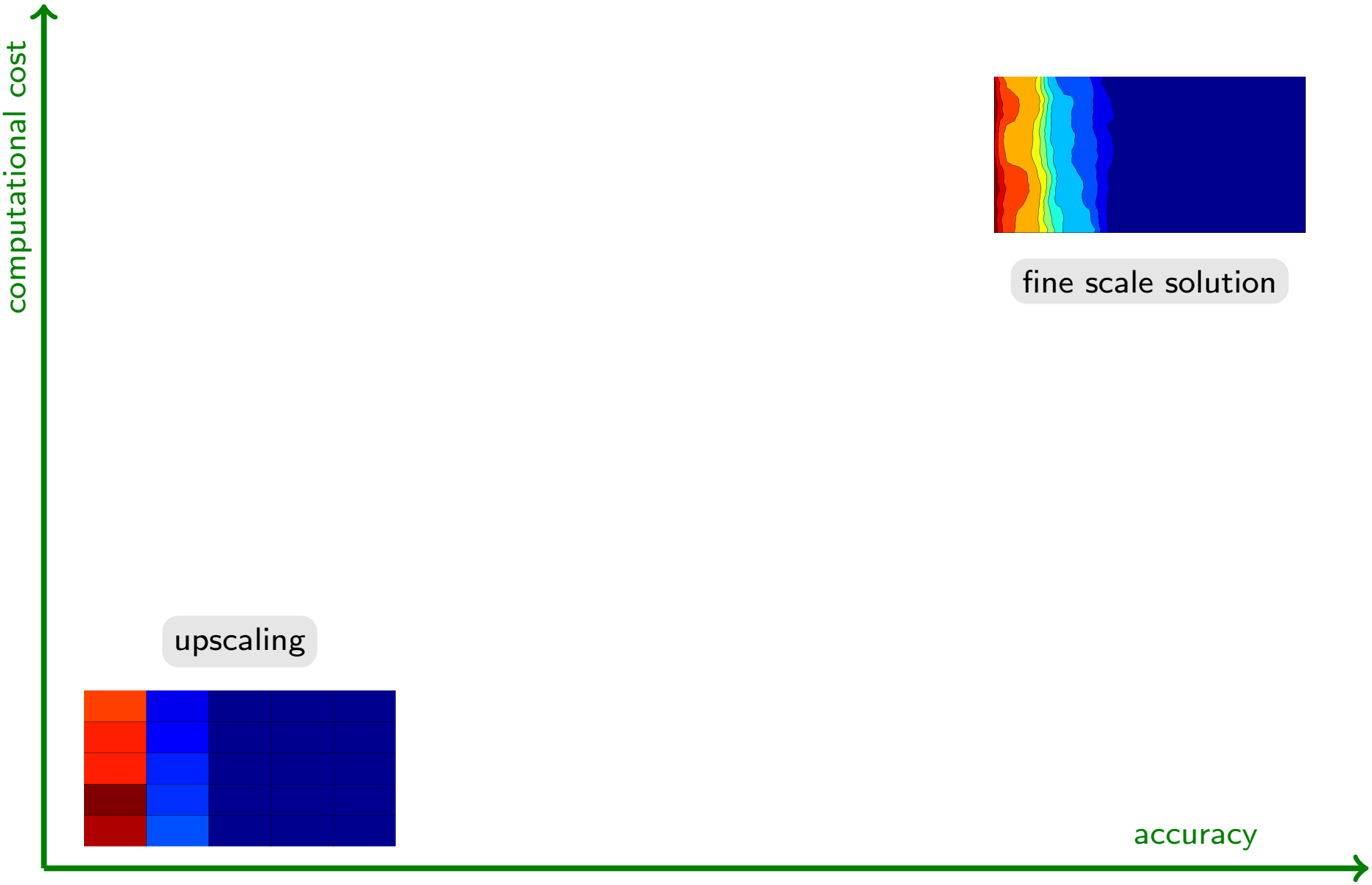

Qualitatively correct solution $\rightarrow$ small fine-scale residual

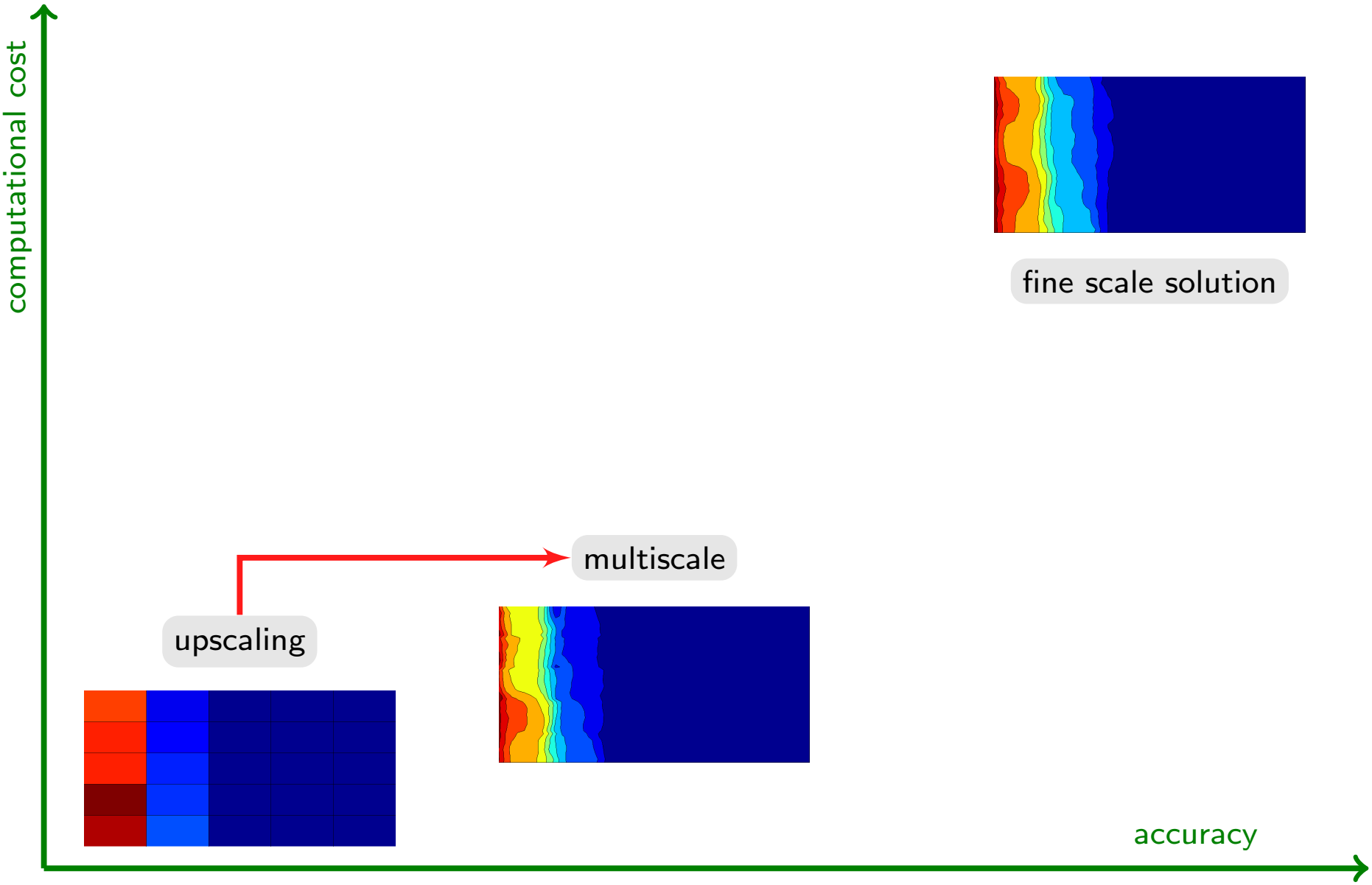

Qualitatively correct solution $\rightarrow$ small fine-scale residual

Residual iteration:

$$p^* = p^\nu + S(q - Ap^\nu)$$
$$p^{\nu+1} = p^* + A_{ms}^{-1}(q - Ap^*)$$

S is some inexpensive smoother, e.g., ILU(0)

Hajibeygi, Jenny, Tchelepi, Wang, ... (2008–2015)

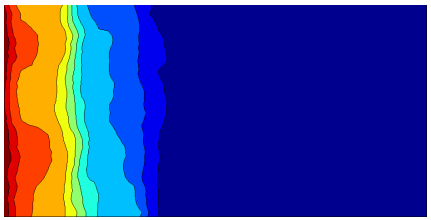

fine scale solution

extra iterations

multiscale

upscaling

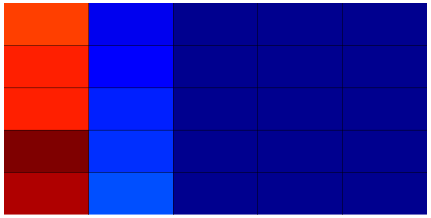

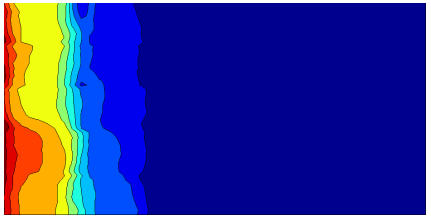

computational cost

accuracy

The multiscale finite-volume (MsFV) method

Developed by the INTERSECT research alliance (Chevron,Schlumberger,++)

In 2012: extensive research over the past decade, more than 40 papers by Jenny, Lee, Tchelepi, Lunati, Hajibeygi, etc:

- correction functions to handle non-elliptic features
- extension to compressible flow
- adaptive updating of basis functions (and transport equations)
- iterative formulation with smoothers (Jacobi, GMRES, ...)
- algebraic formulation

⋮

However...

- Monotonicity issues requires many iterations for strong heterogeneity
- Method only applied to Cartesian models with conceptual faults

Our focus: Extension to unstructured grids with realistic geology

MsFE/MsFV: prolongation operator in more detail

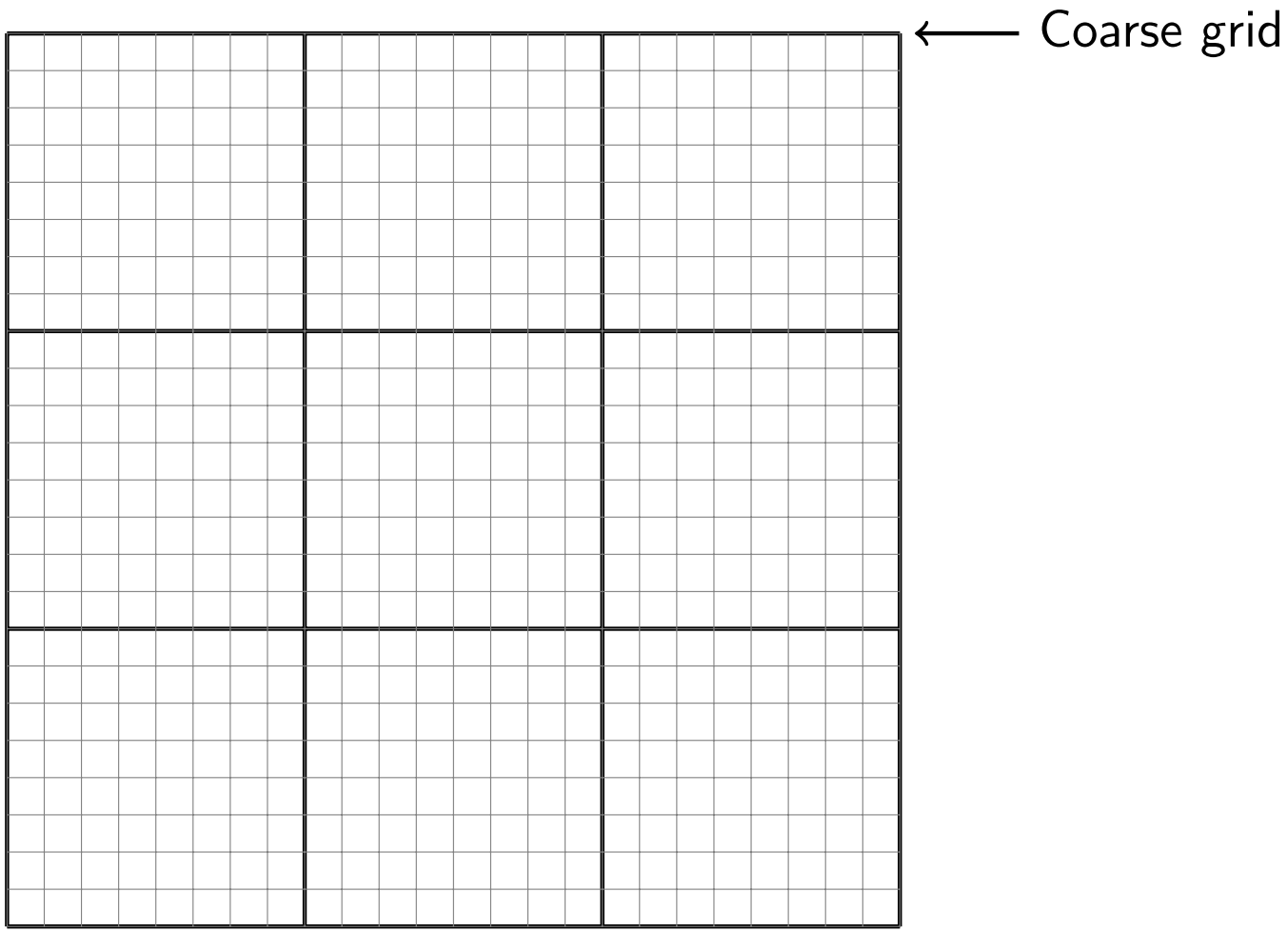

Hou & Wu (1997), Jenny, Lee, Tchelepi (2003)

MsFE/MsFV: prolongation operator in more detail

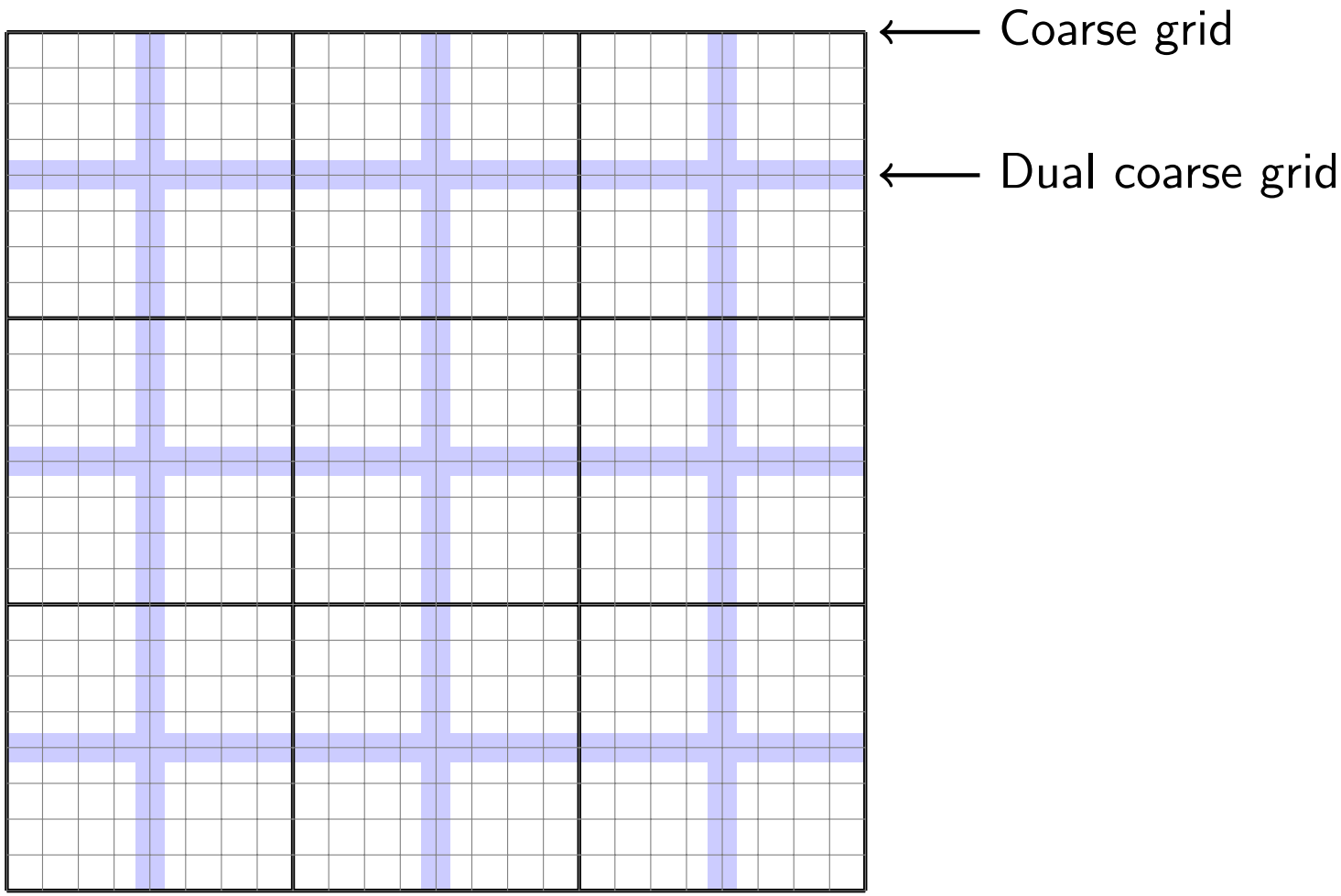

Hou & Wu (1997), Jenny, Lee, Tchelepi (2003)

MsFE/MsFV: prolongation operator in more detail

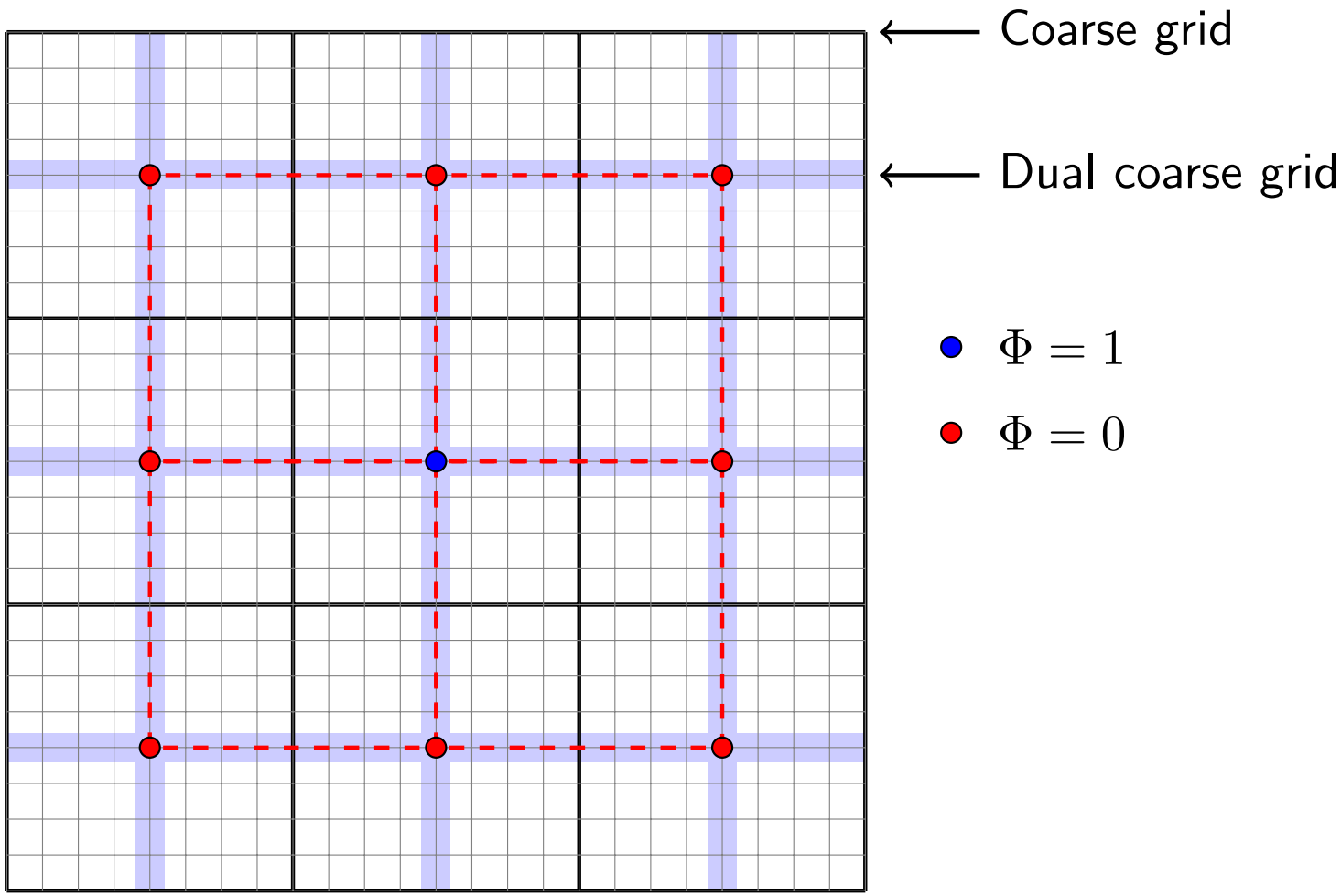

Hou & Wu (1997), Jenny, Lee, Tchelepi (2003)

MsFE/MsFV: prolongation operator in more detail

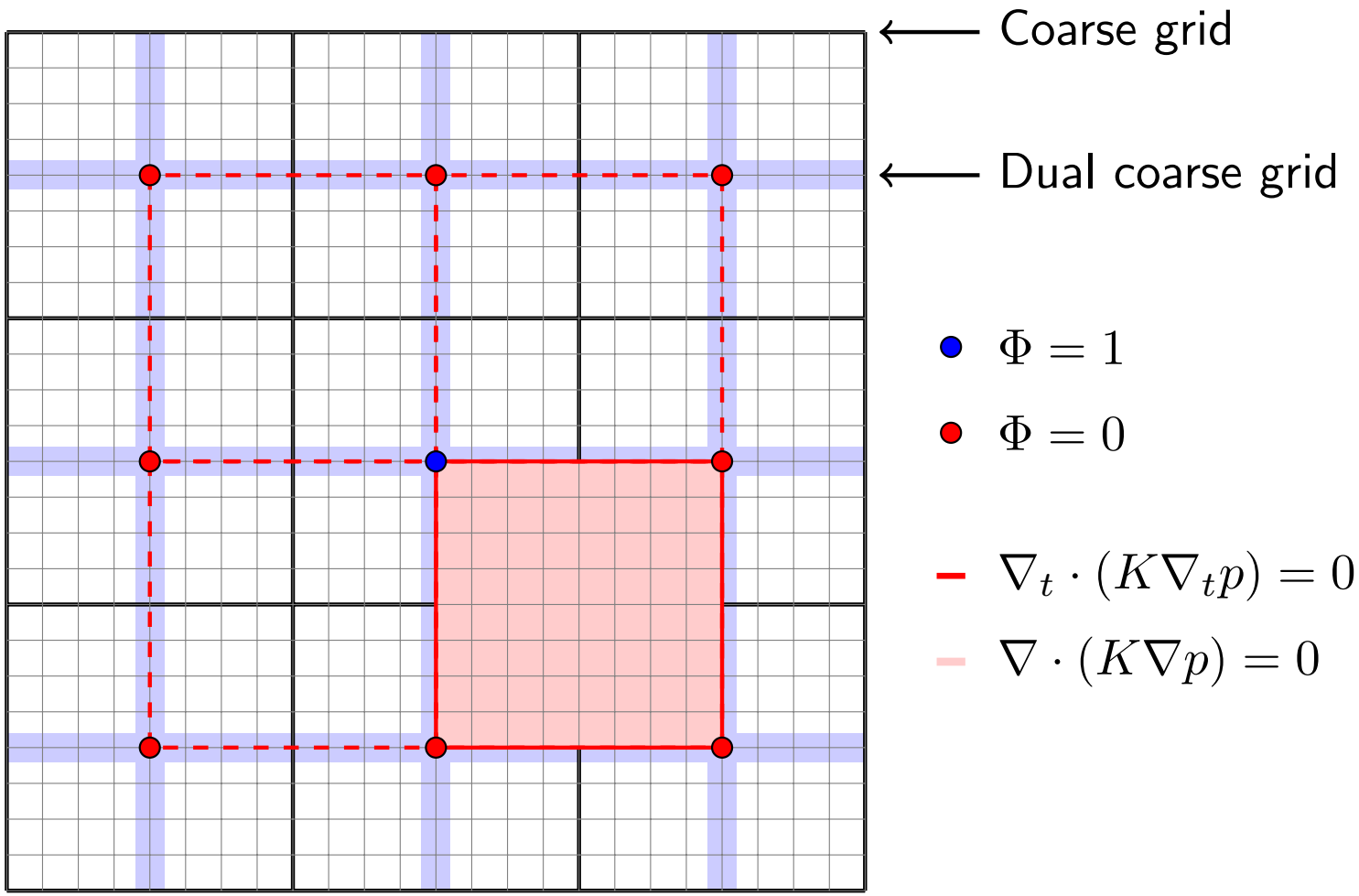

Hou & Wu (1997), Jenny, Lee, Tchelepi (2003)

MsFE/MsFV: prolongation operator in more detail

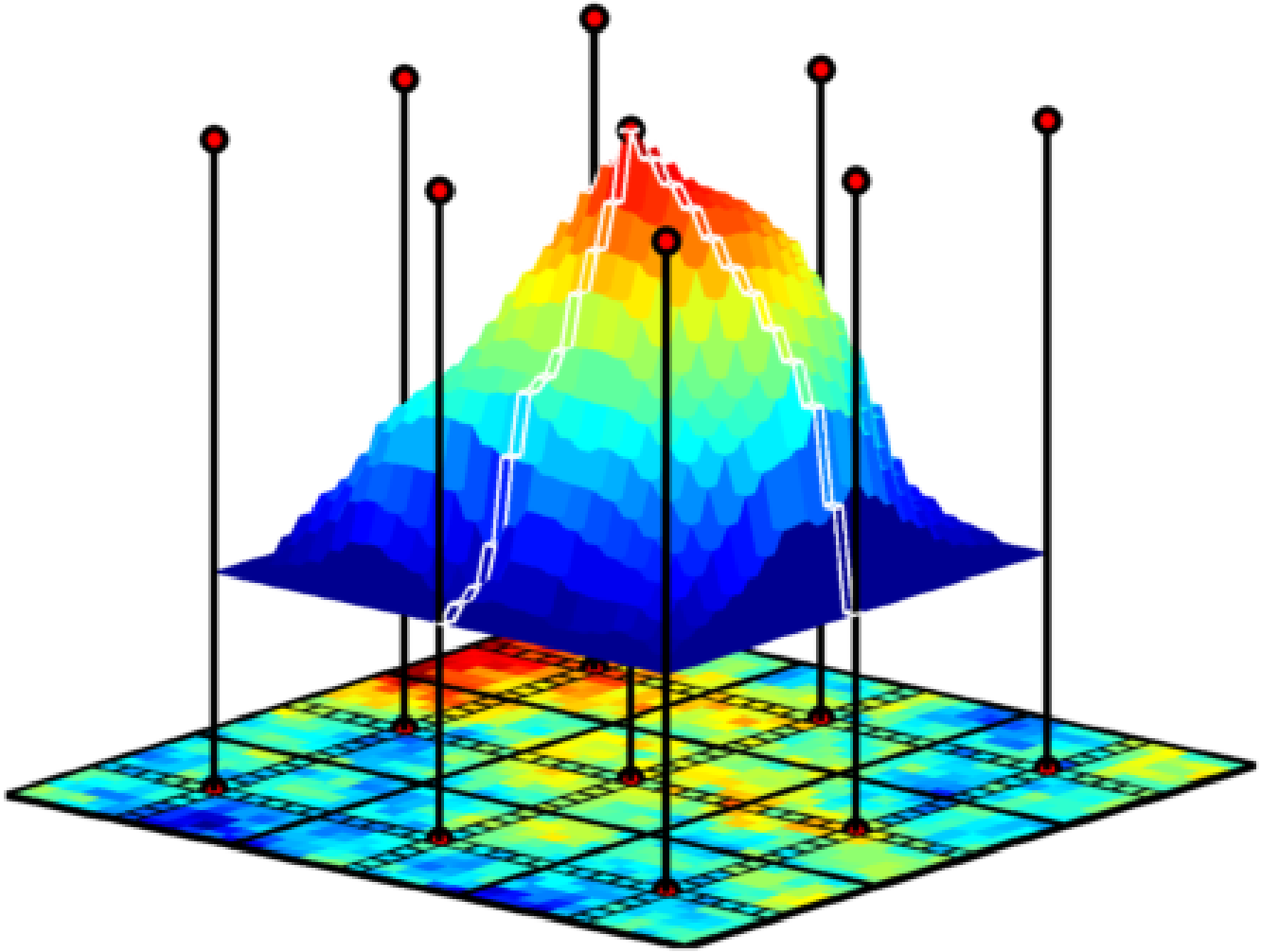

MsFV for unstructured grids (Møyner & Lie, 2013)

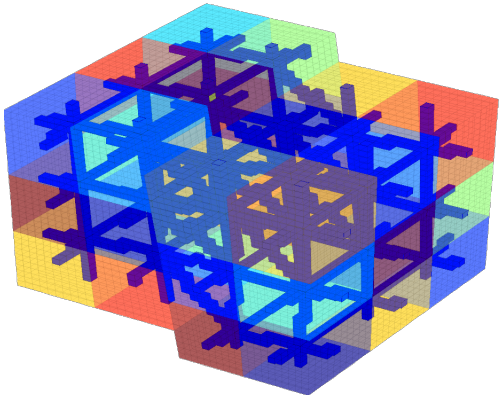

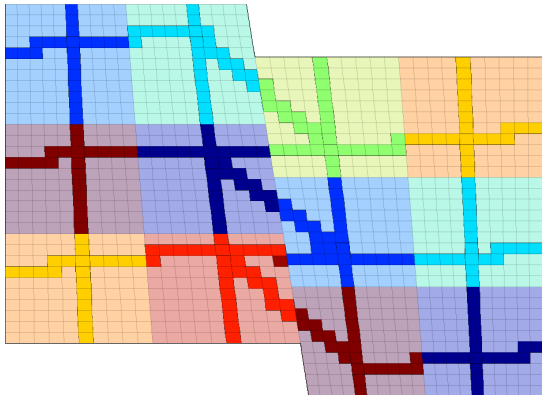

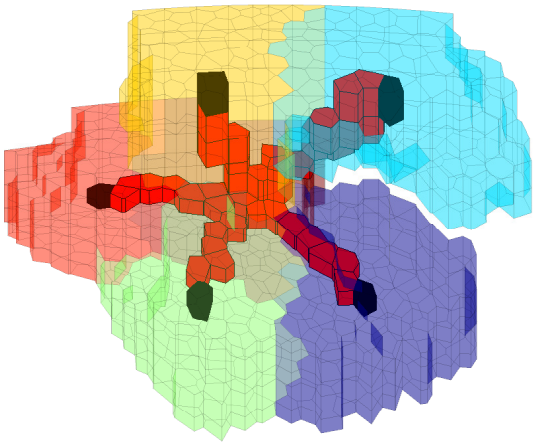

Algorithm for generating admissible primal–dual partitions on general grids

- automated on rectilinear, curvilinear, triangular, and Voronoi grids
- semi-automated on corner-point grids and grids with non-matching faces

Problems encountered: permeability contrasts

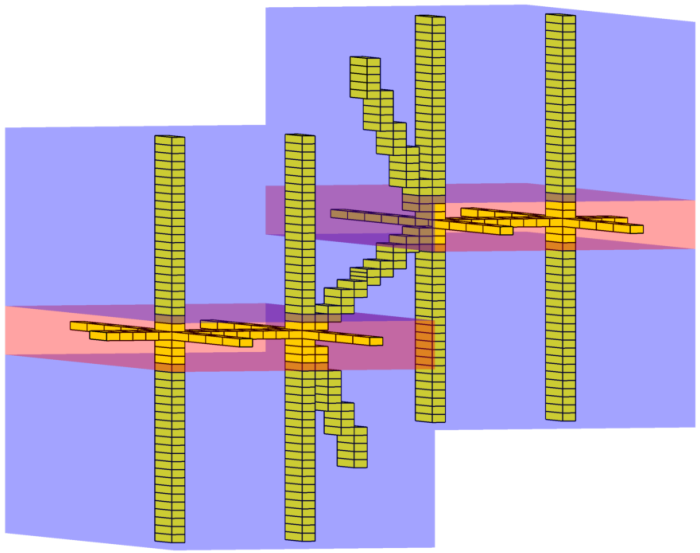

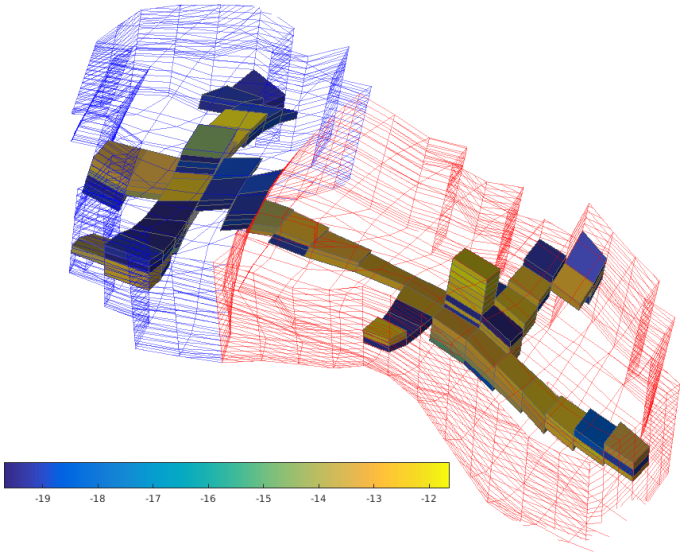

Automated algorithms will generally give:

- Dual block centers in low-permeable regions
- Dual edges crossing strong permeability contrasts (twice)
- Large number of cells categorized as edges

$\longrightarrow$ nonmonotone multipoint stencil for coarse-scale equations
$\longrightarrow$ poor decoupling, does not reproduce linear flow

Rethinking the basis functions: Requirements

What do we want from numerical basis functions P?

- Partition of unity to represent constant fields

$$\sum_j P_{ij} = 1 \rightarrow \text{Exact interpolation of constant modes}$$

- Algebraically smooth:

$$\text{Minimize } \|AP\|_1 \rightarrow APp_c \approx Ap \text{ locally.}$$

- Localization:

  Coarse system $A_c = RAP$ becomes dense as support of basis functions grow

Alternative approach: support regions (Møyner & Lie, 2015)

Basis functions require **a coarse grid** and **a support region**

- Support region: logical indices, topological search, distance measures,..
- Region constructed using triangulation of nodal coarse neighbors, resulting in a multipoint stencil on the coarse scale
- Avoid solving reduced flow problem along perimeter
- Main point: simple to implement in 3D for fully unstructured meshes

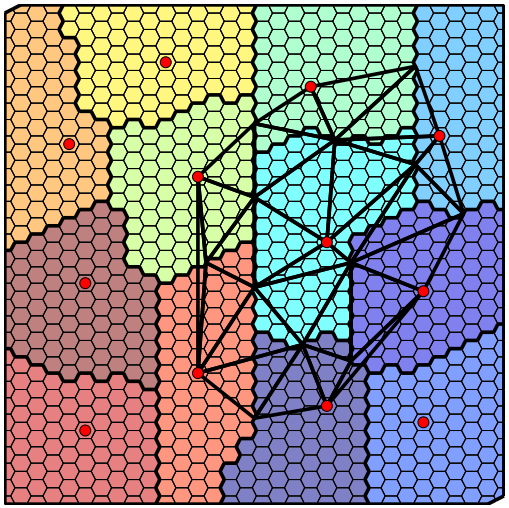

Coarse grid + triangulation

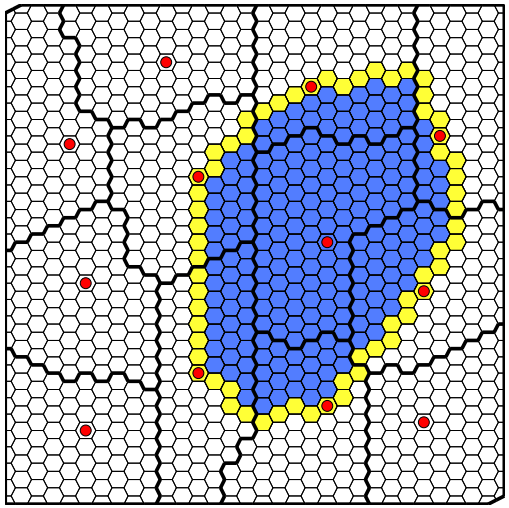

support region

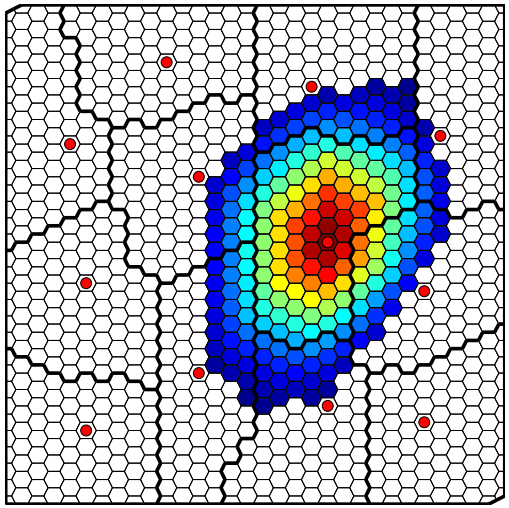

basis function

MsRSB: restricted, smoothed basis functions

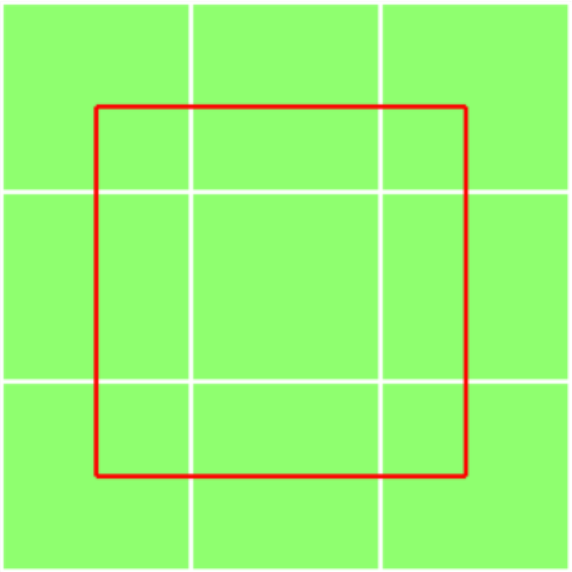

Permeability and grid

Ideally, operators are both *smooth* and *local*

1. Start with constant functions on primal grid
2. Apply Jacobi-like iterations as in algebraic multigrid methods (Vanek et al),

$$P^{n+1} = P^n - \omega D^{-1}(AP)$$

3. Restrict each function to its support region
4. Repeat steps 2 and 3 until convergence

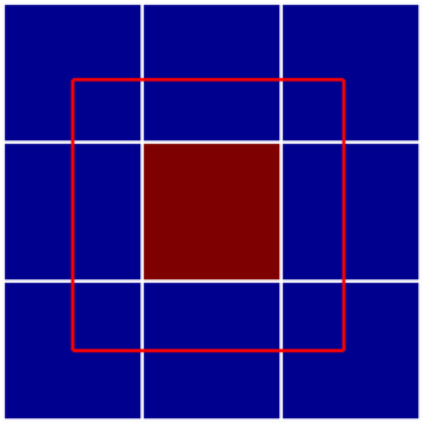

Initial constant basis

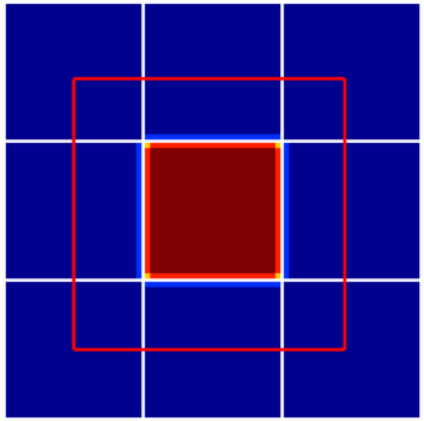

After one pass

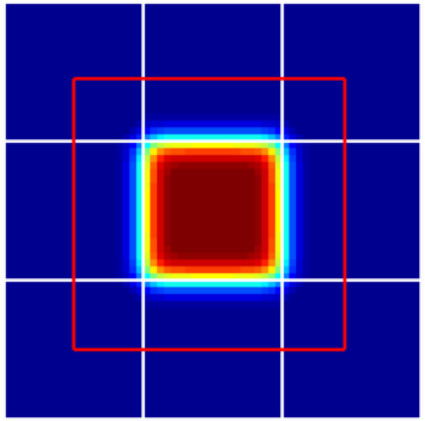

After 10 passes

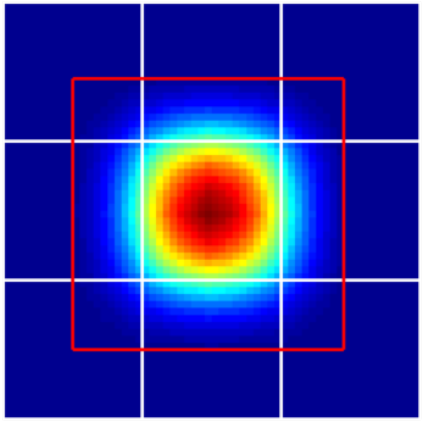

Converged ($n \approx 100$)

MsRSB: restricted, smoothed basis functions

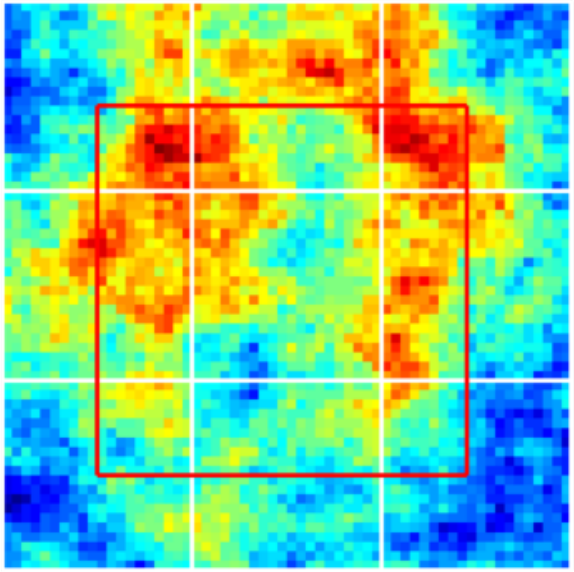

Permeability and grid

Ideally, operators are both *smooth* and *local*

1. Start with constant functions on primal grid
2. Apply Jacobi-like iterations as in algebraic multigrid methods (Vanek et al),

$$P^{n+1} = P^n - \omega D^{-1}(AP)$$

3. Restrict each function to its support region
4. Repeat steps 2 and 3 until convergence

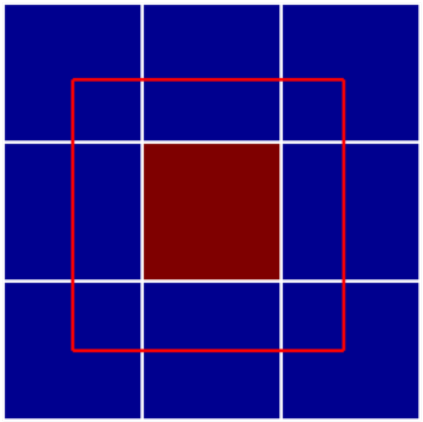

Initial constant basis

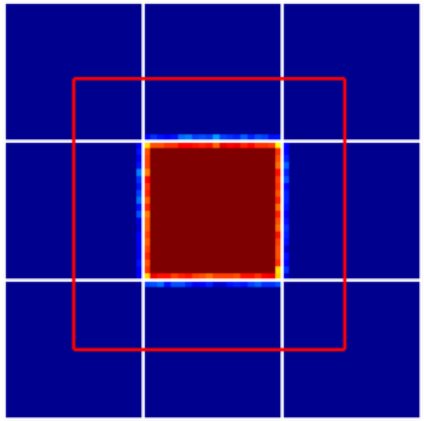

After one pass

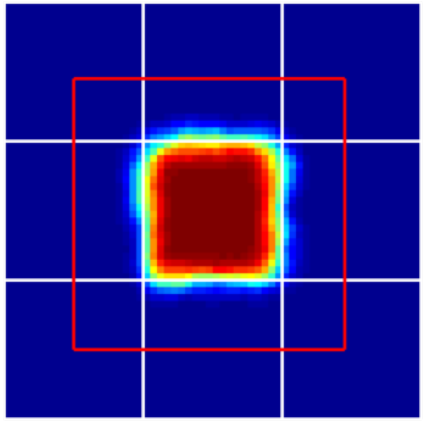

After 10 passes

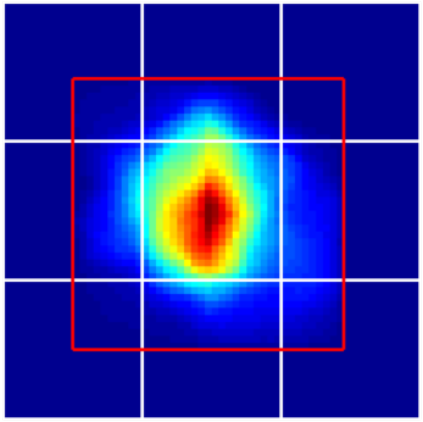

Converged ($n \approx 100$)

MsRSB: computing basis functions

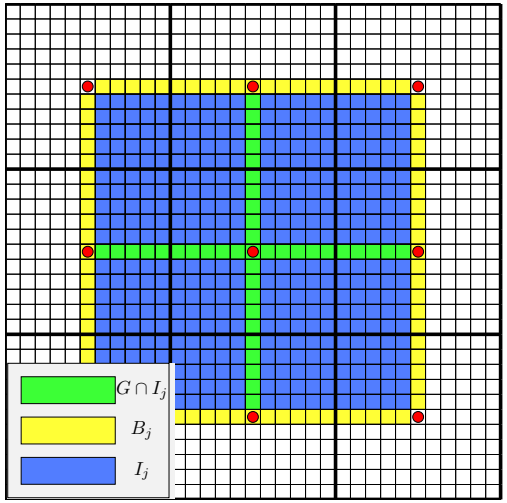

Define preliminary update by Jacobi relaxation,

$$\widehat{\mathbf{d}}_j = -\omega D^{-1} A P_j^n.$$

Modify the update according to cell category,

$$d_{ij} = \begin{cases} \frac{\widehat{d}_{ij} - P_{ij}^n \sum_{k \in H_i} \widehat{d}_{ik}}{1 + \sum_{k \in H_i} \widehat{d}_{ik}}, & i \in I_j, i \in G, \\ \widehat{d}_{ij}, & i \in I_j, i \notin G, \\ 0, & i \notin I_j. \end{cases}$$

Finally, apply the update and proceed to next iteration

$$P_{ij}^{n+1} = P_{ij}^n + d_{ij}$$

- Jacobi iteration ensures algebraic smoothness
- Limited support by construction
- Modified update for partition of unity

Examples: Single-phase flow

SPE10 full model

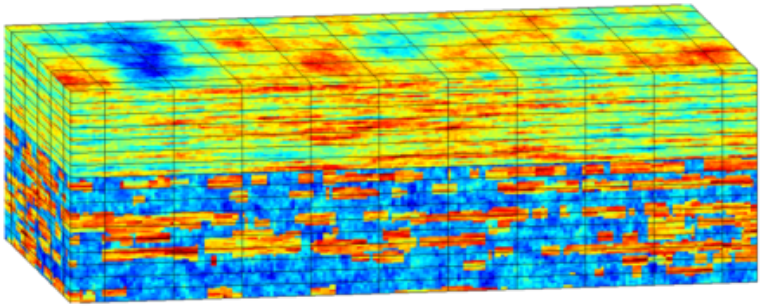

Horizontal permeability

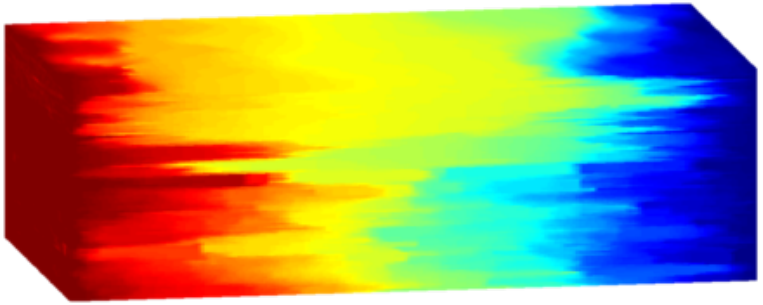

Reference solution

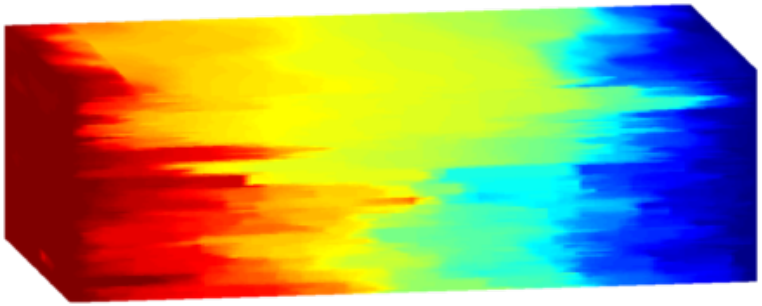

MsRSB

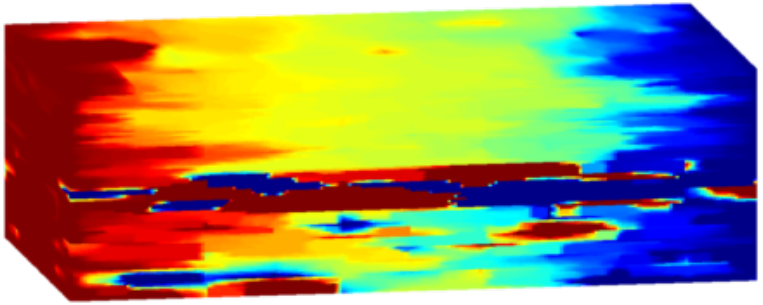

MsFV,

Error	Grid	p (L_2)	p (L_∞)	v (L_2)	v (L_∞)
MsFV	$6 \times 11 \times 17$	3.580	128.461	2.288	11.957
MsRSB	$6 \times 11 \times 17$	0.039	0.309	0.397	0.487

SPE10 full model

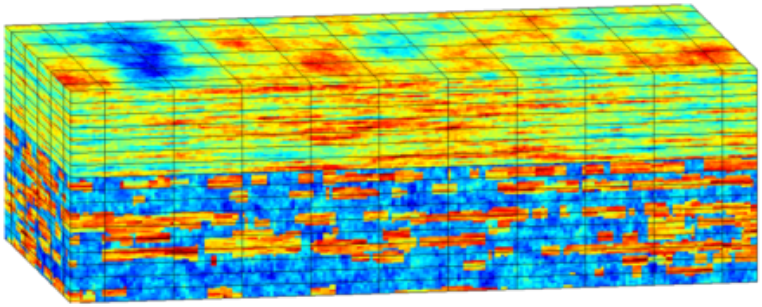

Horizontal permeability

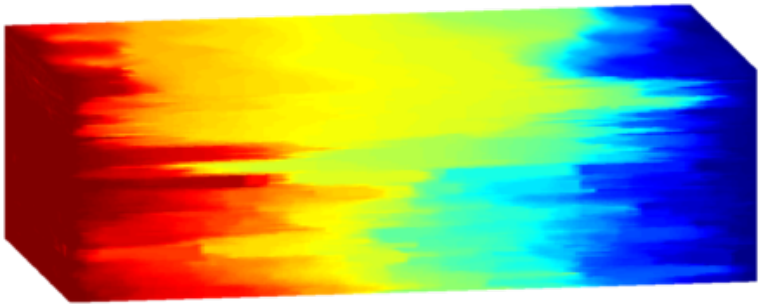

Reference solution

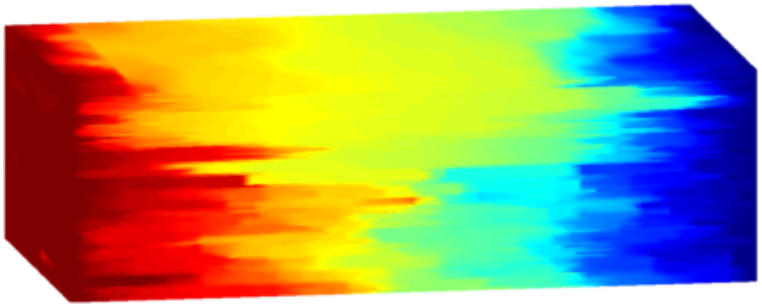

MsRSB

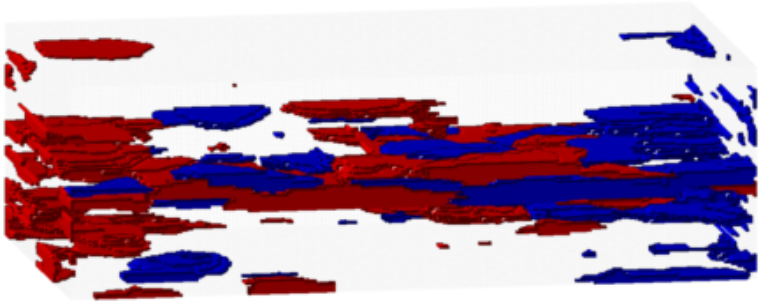

MsFV, $p \notin [0, 1]$

Error	Grid	p (L_2)	p (L_∞)	v (L_2)	v (L_∞)
MsFV	$6 \times 11 \times 17$	3.580	128.461	2.288	11.957
MsRSB	$6 \times 11 \times 17$	0.039	0.309	0.397	0.487

Example: unstructured PEBI grid

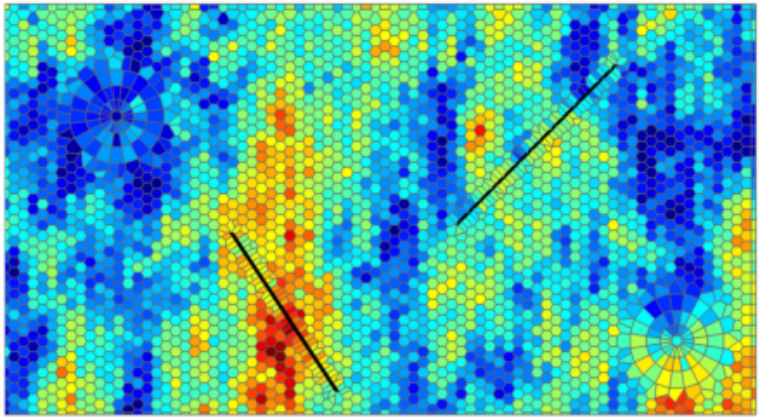

Porosity and grid

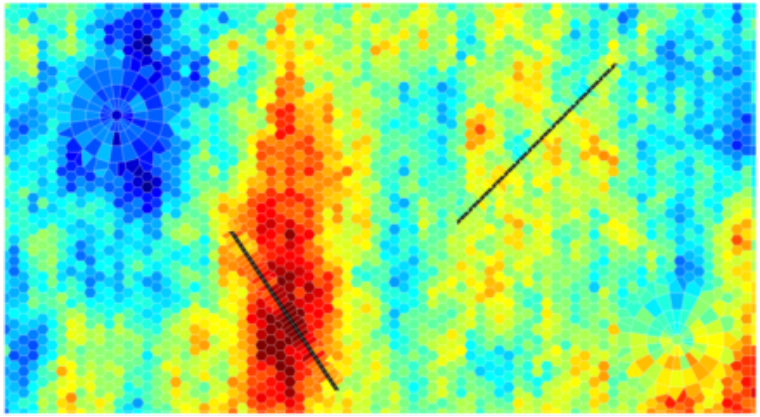

Permability from SPE 10, Layer 35

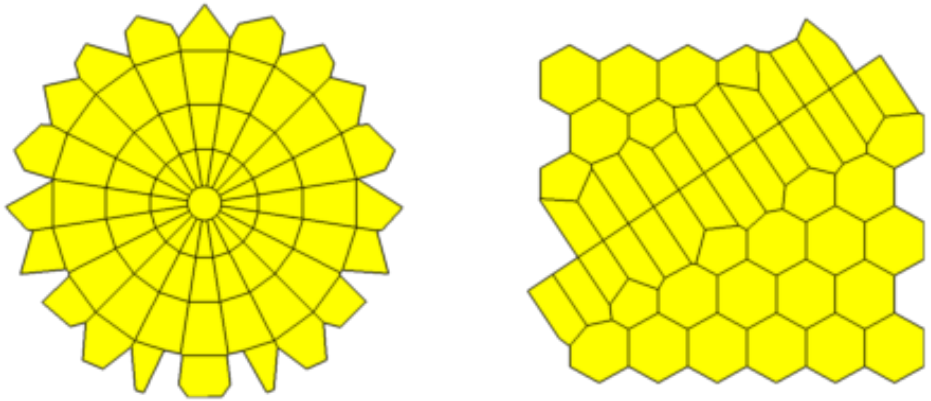

Detailed view of refinement

- Unstructured grid designed to minimize grid orientation effects
- Two embedded radial grids near wells
- Fine grid adapts to faults
- The faults are sealed, i.e. allow no fluid flow through

Example: unstructured PEBI grid

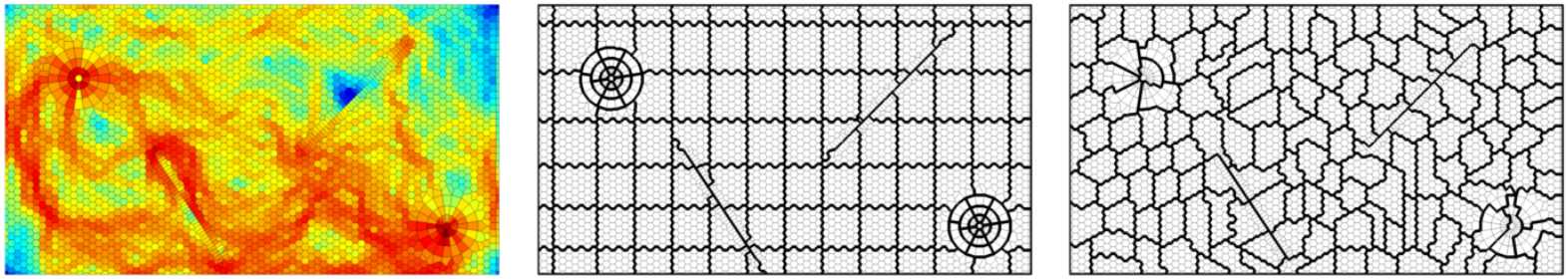

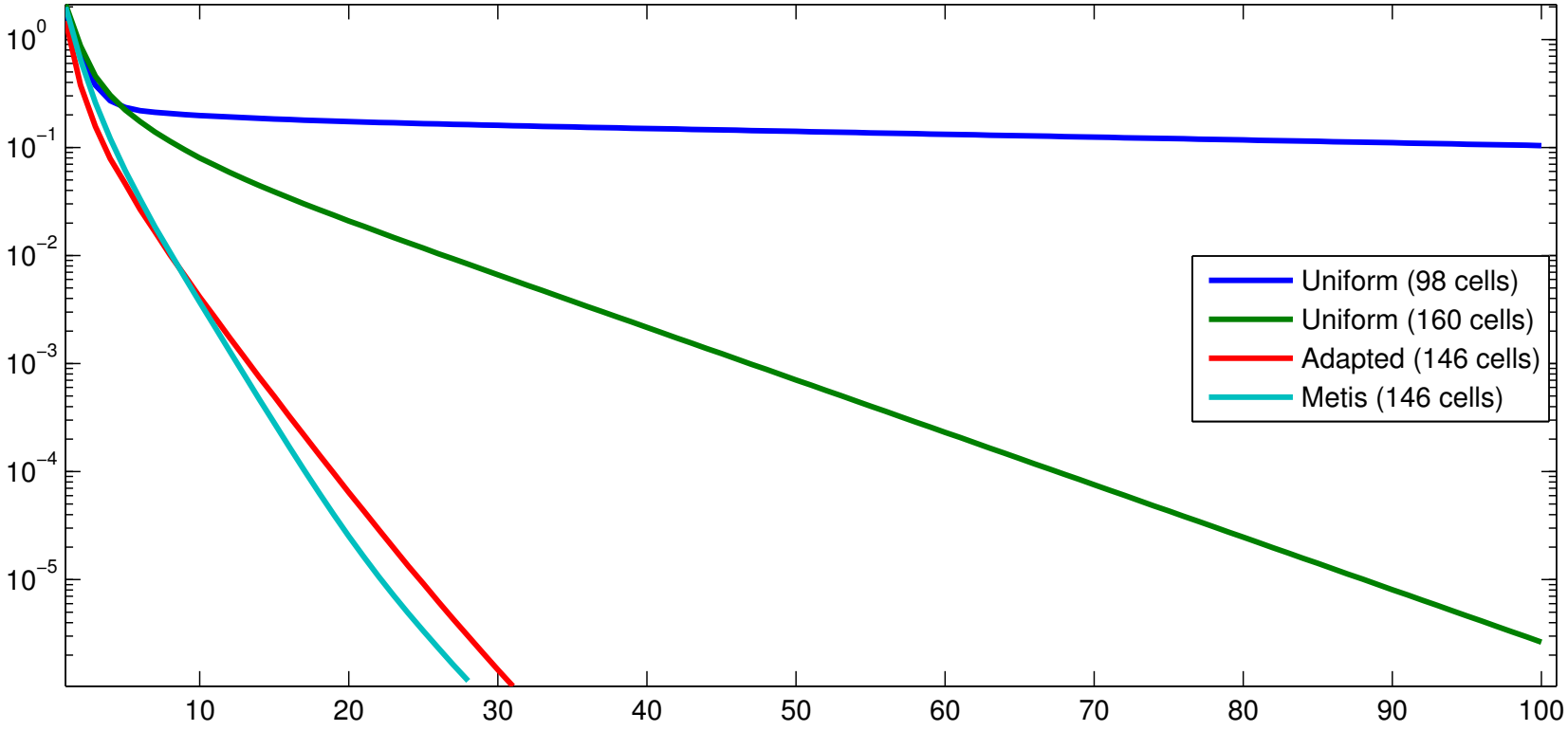

Two-step preconditioner, ILU(0) as 2nd stage, Richardson iterations

Example: unstructured PEBI grid

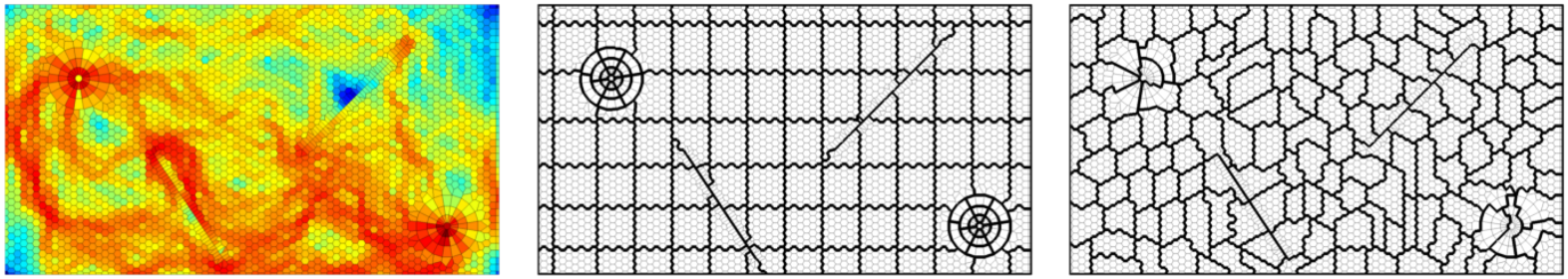

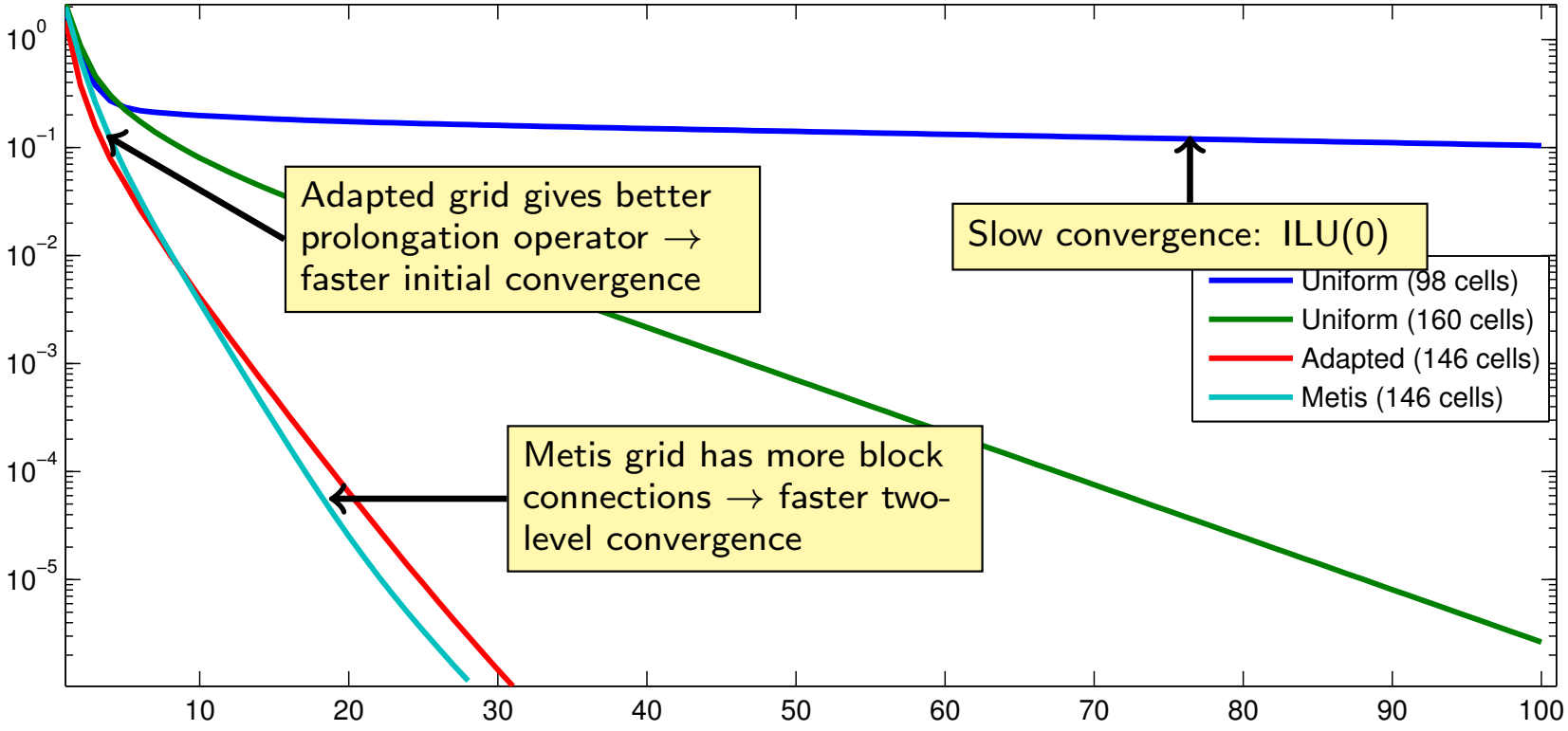

Two-step preconditioner, ILU(0) as 2nd stage, Richardson iterations

Example: Gullfaks field

- Early field model of a giant reservoir from the Norwegian North Sea
- 216 000 cells with a large number of faults and eroded layers
- Very challenging anisotropic permeability and grid
- Model includes cells with nearly 40 faces
- Synthetic well configuration with four vertical wells

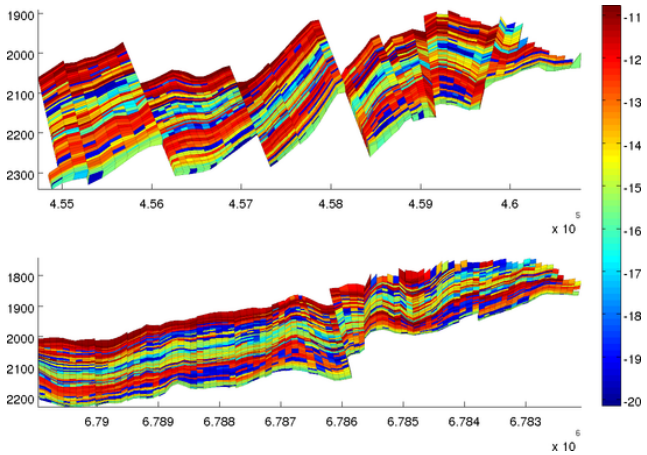

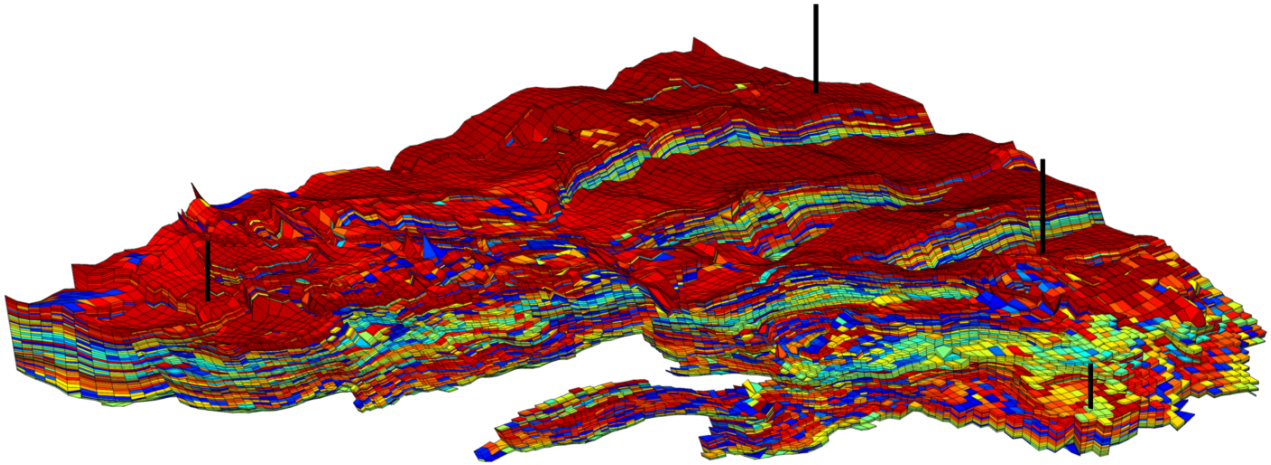

MsRSB: Gullfaks field

- First coarsening strategy:
  Uniform blocks, split over faults
- Second coarsening strategy:
  Use Metis with same number of DoF

Grid type	DoF	p (L_2)	p (L_∞)
$15 \times 15 \times 20$	416	0.032	0.102
Metis	416	0.032	0.100
$10 \times 10 \times 10$	1028	0.028	0.597
Metis	1028	0.015	0.112

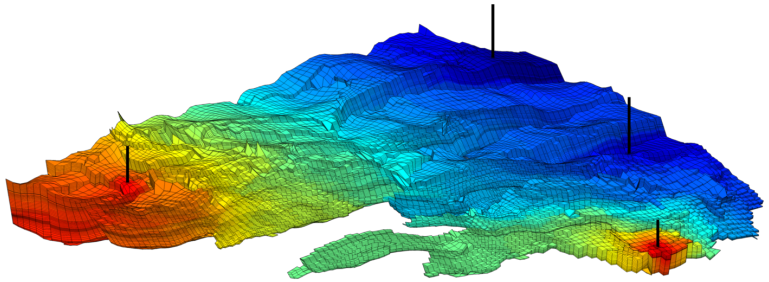

Fine scale (216 000 DoF)

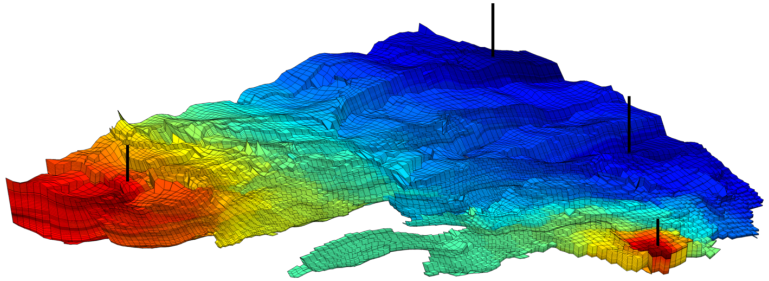

MsRSB (416 DoF)

MsRSB: Gullfaks field

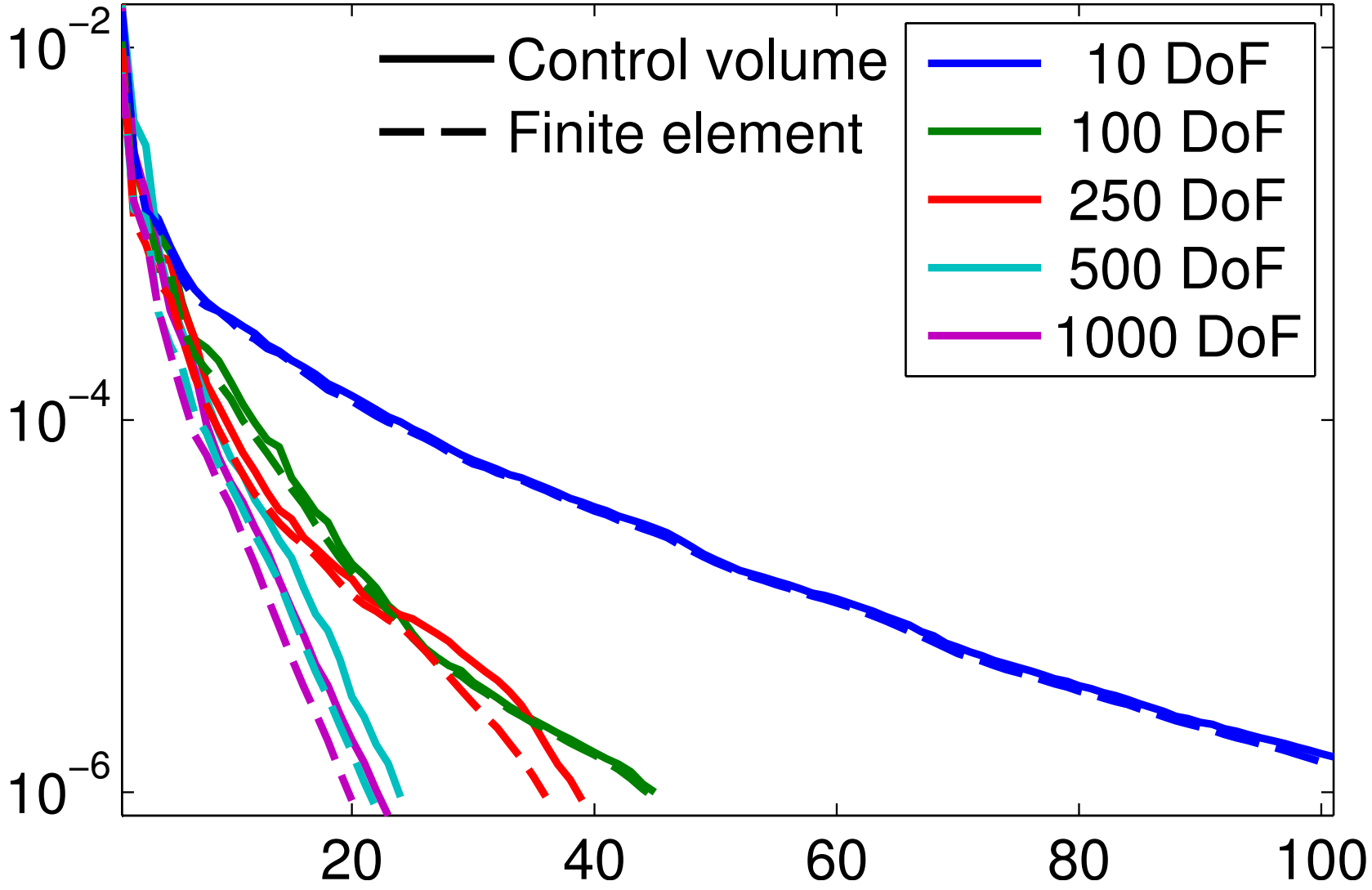

Examples: Compressible, multi-phase flow

Industry-standard flow simulation

The black-oil equations on residual form:

$$\begin{aligned}
\mathcal{R}_w &= \frac{1}{\Delta t}\left[(\phi\, b_w S_w)^{n+1} - (\phi\, b_w S_w)^n\right] + \nabla\cdot(b_w \vec{v}_w)^{n+1} - (b_w q_w)^{n+1} = 0,\\
\mathcal{R}_o &= \frac{1}{\Delta t}\left[(\phi\, b_o S_o)^{n+1} - (\phi\, b_o S_o)^n\right] + \nabla\cdot(b_o \vec{v}_o)^{n+1} - (b_o q_o)^{n+1} = 0,\\
\mathcal{R}_g &= \frac{1}{\Delta t}\left[(\phi\, b_g S_g + \phi\, r_{so} b_o S_o)^{n+1} - (\phi\, b_g S_g + \phi\, r_{so} b_o S_o)^n\right]\\
&\quad + \nabla\cdot(b_g \vec{v}_g + b_o r_{so} \vec{v}_o)^{n+1} - (b_g q_g + b_o r_{so} q_o)^{n+1} = 0.
\end{aligned}$$

Pressure equation found by eliminating saturation values at the next time step,

$$\mathcal{R}_p = \frac{\mathcal{R}_w}{b_w^{n+1}} + \left[\frac{1}{b_o^{n+1}} - \frac{r_{so}^{n+1}}{b_g^{n+1}}\right]\mathcal{R}_o + \frac{\mathcal{R}_g}{b_g^{n+1}} = 0,$$

Transport step: fractional flow formulation with standard two-point, upstream-mobility weighting.

Sequentially-implicit solution strategy

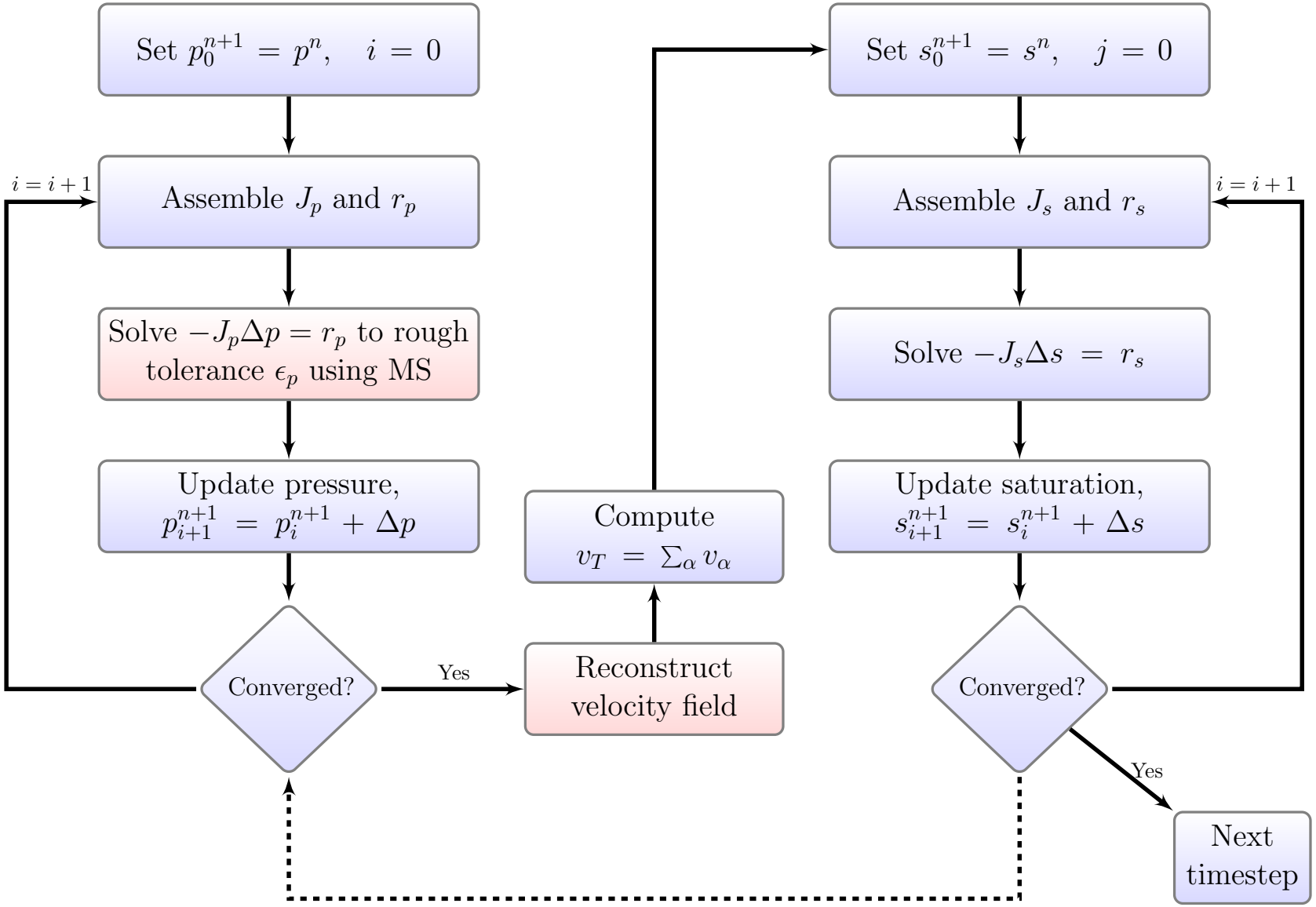

Example: SPE 10 model 2 benchmark

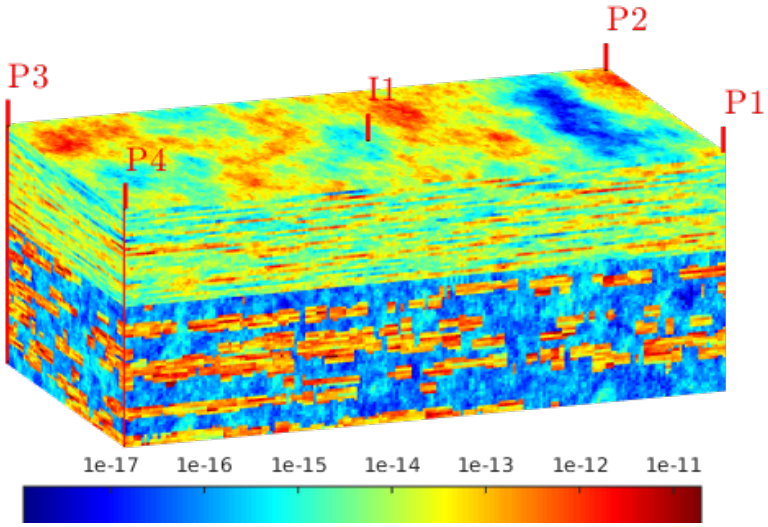

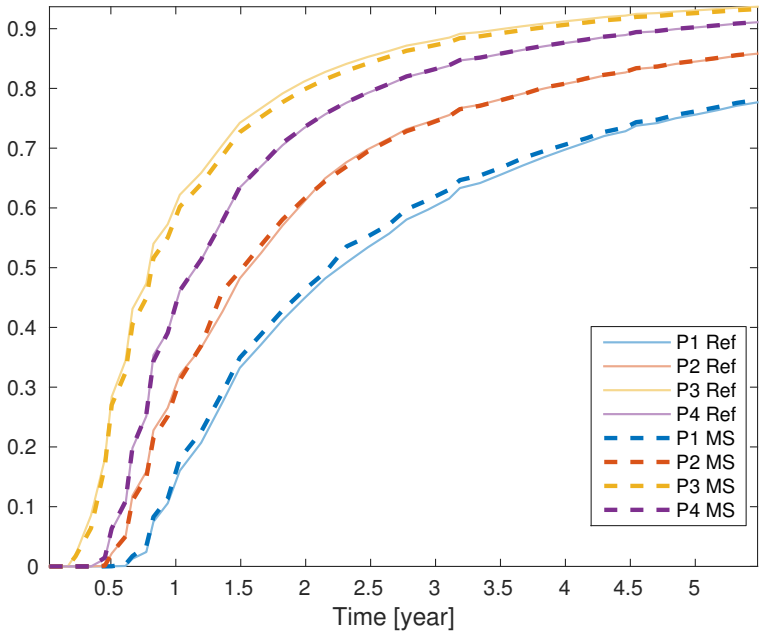

Iterated sequential solver:

- 0.001 pressure increment tolerance
- 10^{-6} tolerance for algebraic multigrid

Iterated multiscale solver:

- 0.005 pressure increment tolerance
- 10^{-2} tolerance for MsRSB solver

Approximate MsRSB solver is ten times faster than baseline sequential

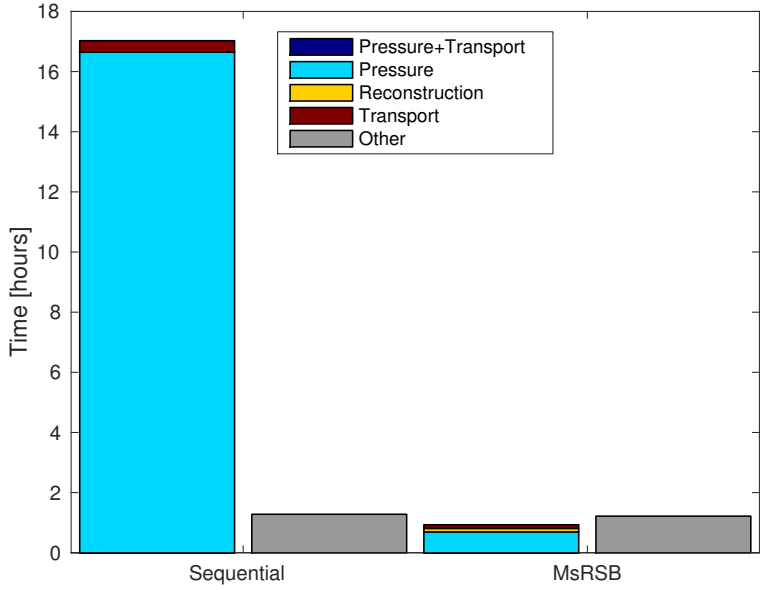

Example: realistic waterflooding

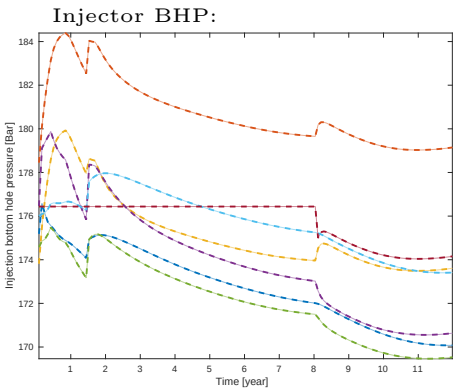

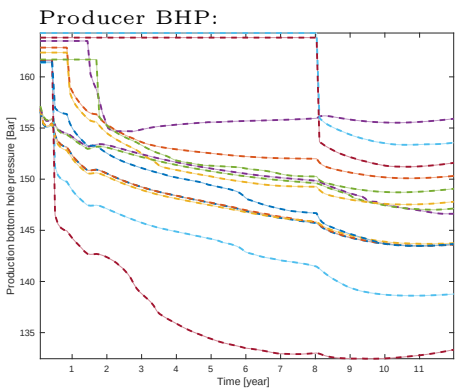

Watt Field: water flooding

415 711 active cells, three rock types

7 injectors, 15 horizontal producers

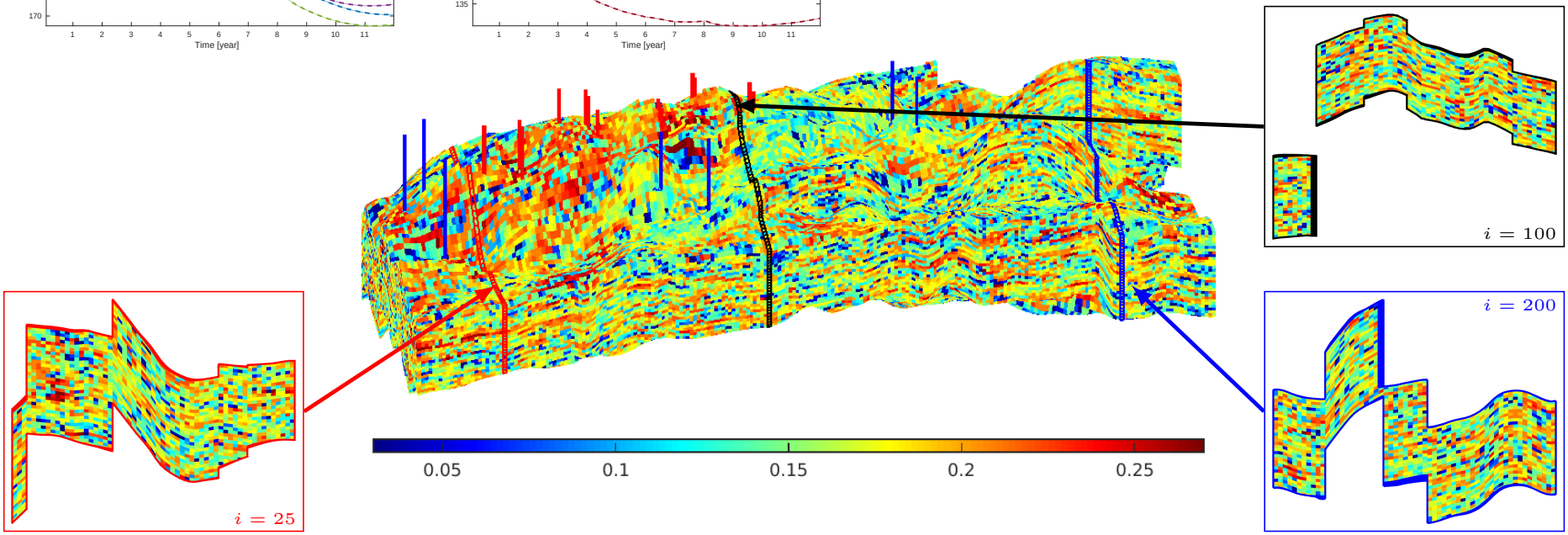

Møyner & Lie, SPE J. (2016)

Example: realistic waterflooding

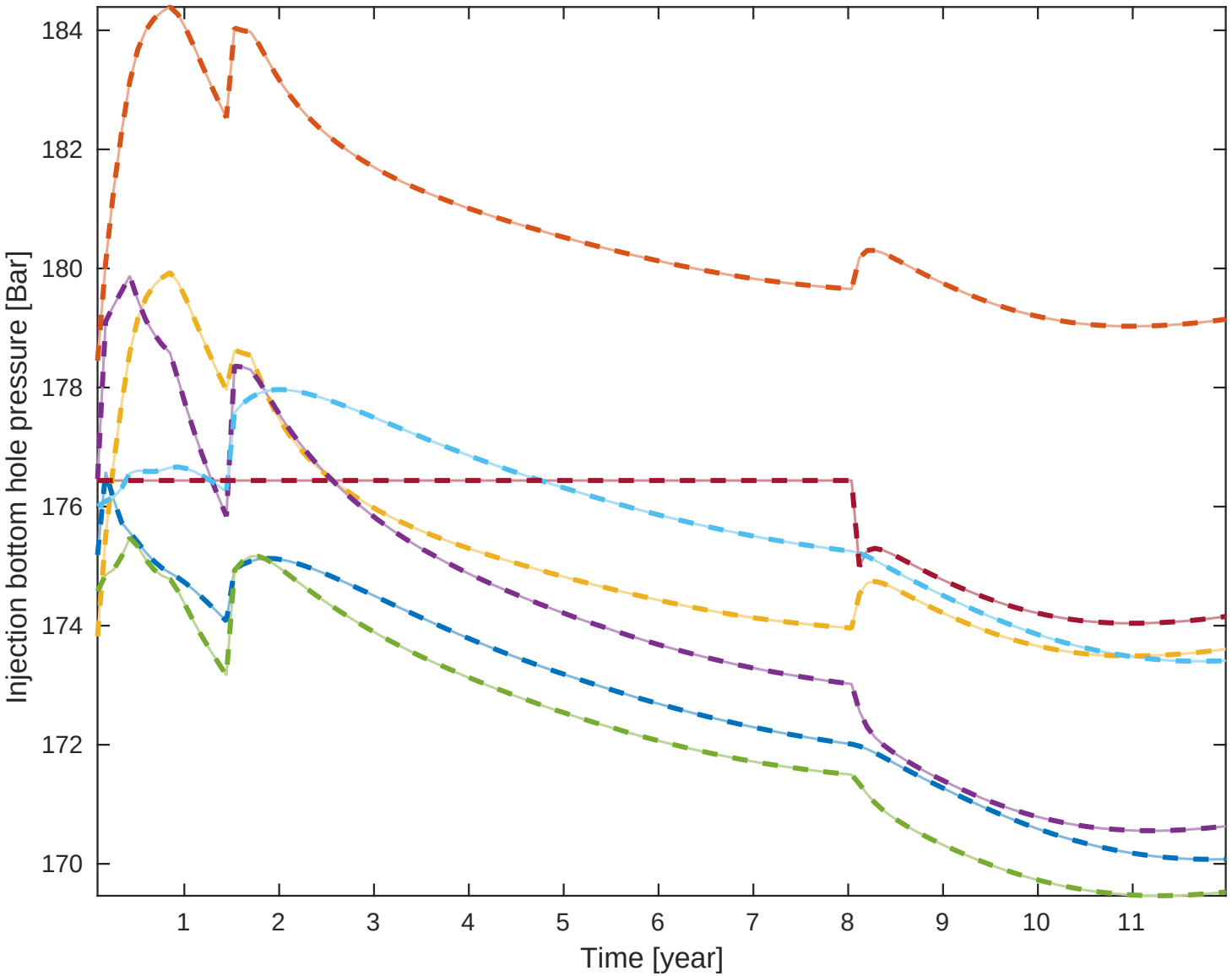

Thin solid: fine-scale solution
Thick dashed: multiscale solution

Multiscale: 800 blocks, tolerance 0.05
Solver speedup: 9×

Møyner & Lie, SPE J. (2016)

Example: 3-phase flow

- Synthetic model with fluid model based on SPE1 benchmark
- Gas is injected at constant rate into a undersaturated reservoir
- Producer at fixed bottom hole pressure
- Highly sensitive to pressure approximation

Gas satuaration at breakthrough

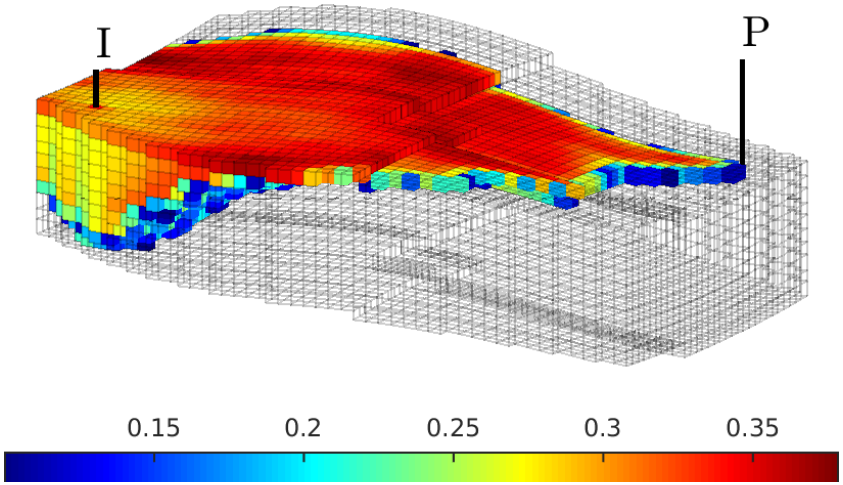

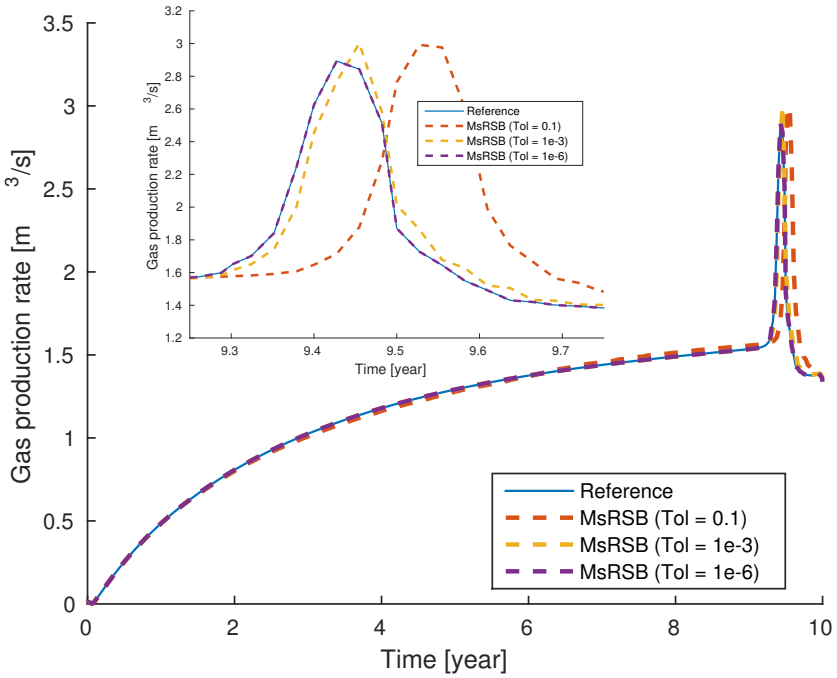

Møyner & Lie, SPE J. (2016)

Example: 3-phase flow

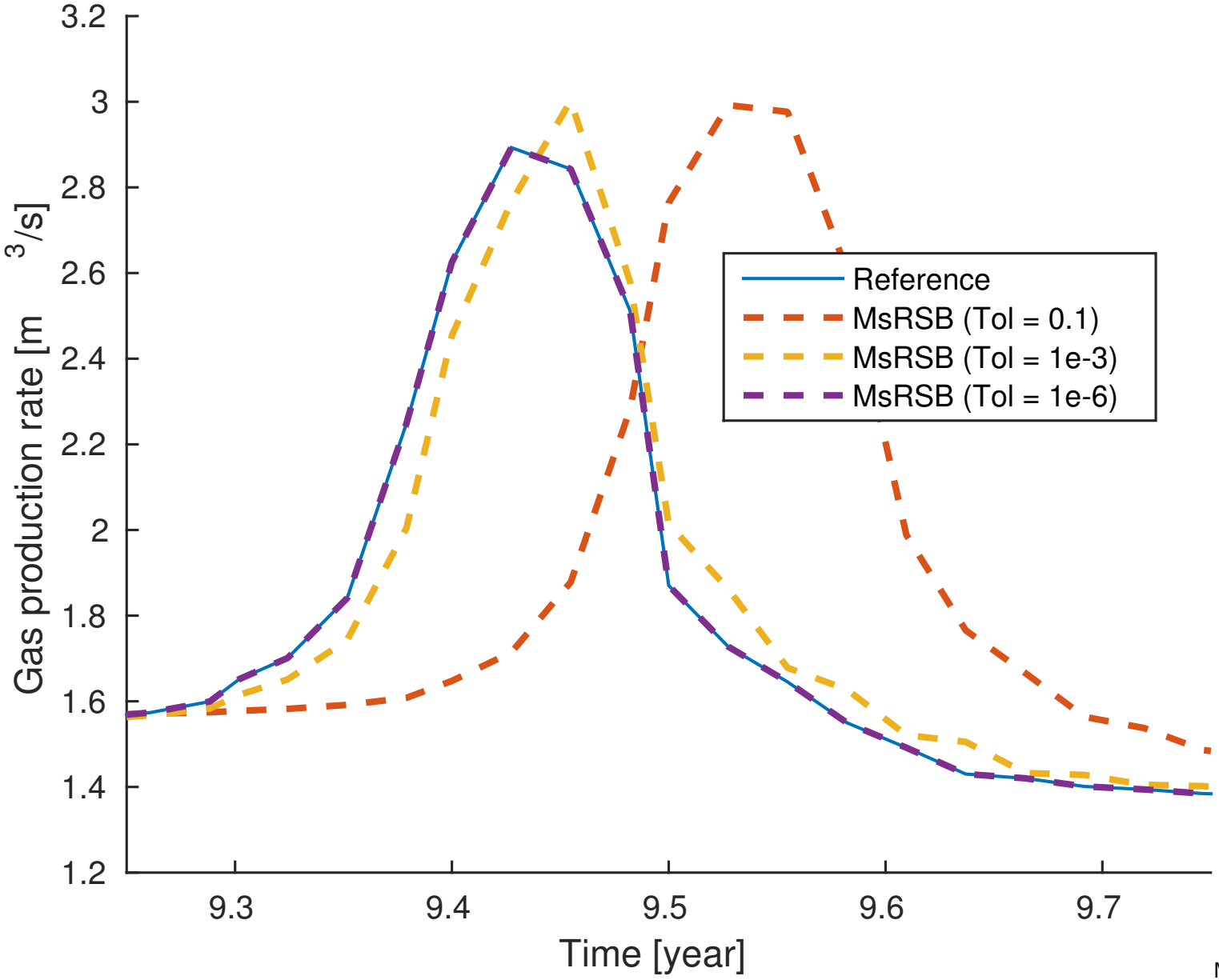

Møyner &

Lie, SPE J. (2016)

Example: INTERSECT Prototype on Gullfaks

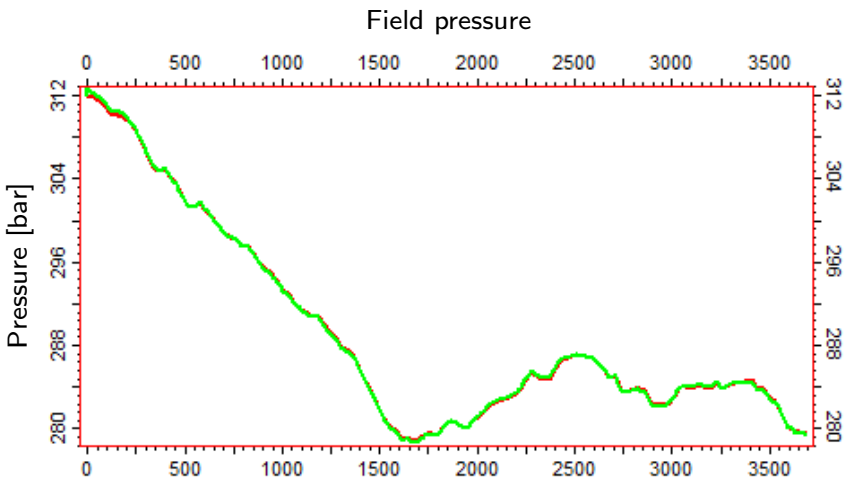

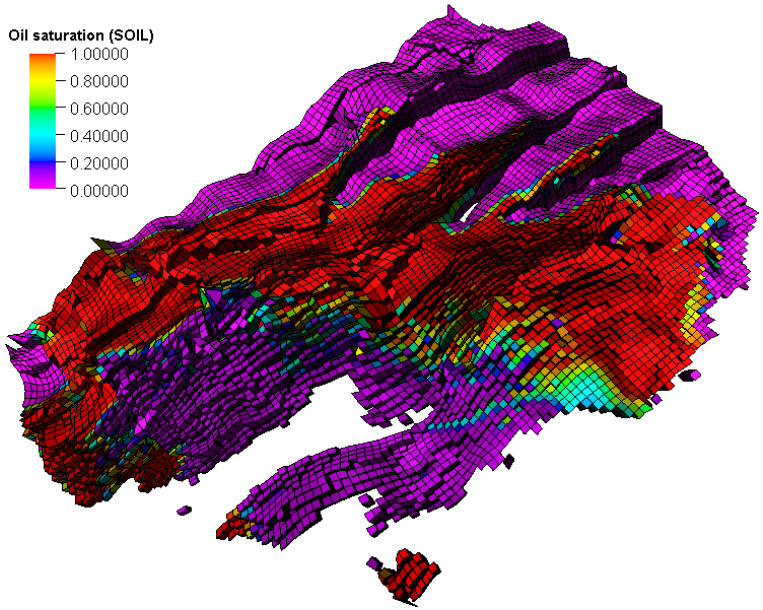

- Giant North Sea field, started production in 1986
- Mainly water injection, but also gas and water-alternating-gas in some areas
- Coarse $80 \times 100 \times 19$ simulation model with real history (3-phase black oil)
- MsRSB basis functions in Intersect R&P Multiscale simulator

Lie, Møyner, Natvig, Kozlova, Bratvedt, S. Watanabe, Z. Li, Successful Application of Multiscale Methods in a Real Reservoir Simulator Environment, Comput. Geosciences 2017

Recent developments: Compositional flow

Compositional flow: Governing equations

Aqueous phase,

$$\mathcal{R}_w = \partial_t(\phi \rho_w S_w) + \nabla \cdot (\rho_w \vec{v}_w) - \rho_w q_w = 0.$$

Component i,

$$\mathcal{R}_i = \partial_t(\phi \left[\rho_l S_l X_i + \rho_v S_v Y_i\right]) + \nabla \cdot (\rho_l X_i \vec{v}_l + \rho_v Y_i \vec{v}_v) - \rho_l X_i q_l - \rho_v Y_i q_v = 0.$$

- Hydrocarbons assumed to exist in vapor/liquid – not in aqueous
- Generalized cubic equation-of-state (Peng-Robinson in examples)
- Lohrenz-Bray-Clark viscosity correlation

Møyner & Tchelepi, SPE RSC (2017)

Isothermal flash

- Flash equations,

$$
\begin{aligned}
f_{il}(p, T, x_1, ..., x_n, Z_l) - f_{iv}(p, T, y_1, ..., y_n, Z_v) = 0, \text{ for } i \in \{1, ..., N\} \\
z_i - Lx_i - (1 - L)y_i = 0, \text{ for } i \in \{1, ..., N\} \\
\sum_{i=1}^{N} x_i - y_i = 0.
\end{aligned}
$$

- Applies in cells with two hydrocarbon phases.
- Overall composition: Flash to be solved at every iteration

Sequential total mass scheme: Pressure

Scheme suggested by Hajibeygi & Tchelepi (SPE J, 2014), where pressure is found by total mass balance,

$$\mathcal{R}_p = \frac{\phi}{\Delta t}\left[R_t^{n+1} - R_t^n\right] + \nabla \cdot \vec{V}_t - Q_t = 0.$$

from unweighted sum over component equations.

Define total density, total mass fluxes

$$R_t = \sum_{\beta=w,l,v} \rho_\beta S_\beta, \quad \vec{V}_t = \sum_{\beta=w,l,v} \rho_\beta \vec{v}_\beta, \quad Q_t = \sum_{\beta=w,l,v} \rho_\beta q_\beta.$$

Total mass does not change during transport – *reasonable?*

Sequential-implicit total mass scheme: Transport

Transport equation for hydrocarbon component i,

$$\mathcal{R}_{ti} = \frac{\phi}{\Delta t}\left[(X_i R_l)^{n+1} + (Y_i R_v)^{n+1} - (X_i R_l)^n - (Y_i R_v)^n\right] + \nabla \cdot \left(X_i \vec{V}_l + Y_i \vec{V}_v\right) - X_i Q_l - Y_i Q_v = 0.$$

Where we have used fixed masses to obtain,

$$R_\alpha = \frac{\rho_\alpha S_\alpha}{\sum\limits_{\beta=w,l,v} \rho_\beta S_\beta} R_t, \quad Q_\alpha = \frac{\rho_\alpha \lambda_\alpha}{\sum\limits_{\beta=w,l,v} \rho_\beta \lambda_\beta} Q_t,$$

$$\vec{V}_\alpha = \frac{\lambda_\alpha \rho_\alpha}{\sum\limits_{\beta=w,l,v} \lambda_\beta \rho_\beta} (\vec{V}_t + K \sum_{\beta=w,l,v} \rho_\beta \lambda_\beta (\rho_\beta - \rho_\alpha) \vec{g} \nabla z)$$

Sequential total volume scheme: Pressure

Pressure equation as total volume balance

Defined weighted sum (see Watts, 1986 or review by Coats, 2000)

$$\mathcal{R}_p = \sum_{i=1}^{N} w_i \mathcal{R}_i$$

Weights (partial component volumes) chosen such that accumulation

$$A_p = \frac{\partial}{\partial t} \left[\sum_{i=1}^{N} w_i (\rho_l S_l X_i + \rho_v S_v Y_i) \right]$$

has zero derivatives w.r.t. all primary variables except pressure.

Sequential-implicit total volume scheme: Transport

Transport equation for hydrocarbon component i,

$$\mathcal{R}_{ti} = \partial_t(\phi\left[\rho_l S_l X_i + \rho_v S_v Y_i\right]) + \nabla\cdot(\rho_l X_i \vec{v}_l + \rho_v Y_i \vec{v}_v) - \rho_l X_i q_l - \rho_v Y_i q_v = 0.$$

Phase velocity by fractional flow, keeping total velocity fixed

$$\vec{v}_\alpha = \frac{\lambda_\alpha}{\sum\limits_{\beta=w,l,v} \lambda_\beta}(\vec{v}_t + K \sum_{\beta=w,l,v} \lambda_\beta(\rho_\beta - \rho_\alpha)\vec{g}\nabla z)$$

CO_2 injection: Layer of SPE 10 Model 2

- Six component fluid from Mallison et al (2005)
- Initial concentration
  - N_2+CH_4: 0.463
  - CO_2: 0.01640
  - C_{2-5}: 0.20520
  - C_{6-13}: 0.19108
  - C_{14-24}: 0.08113
  - C_{25-80}: 0.04319
- CO_2 and water injected at opposite corners

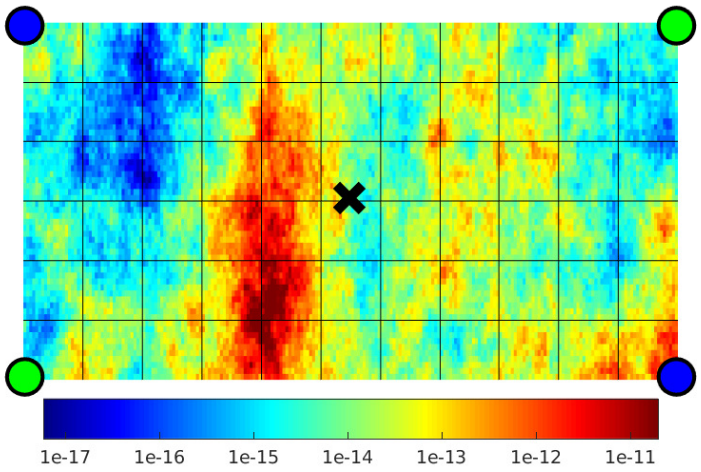

Water and gas injection

CO_2 injection: Layer of SPE 10 Model 2

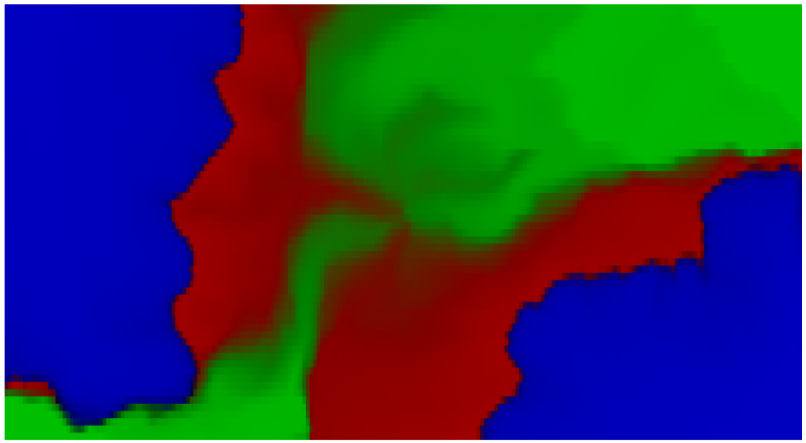

Sequential saturation at 2/3 PVI

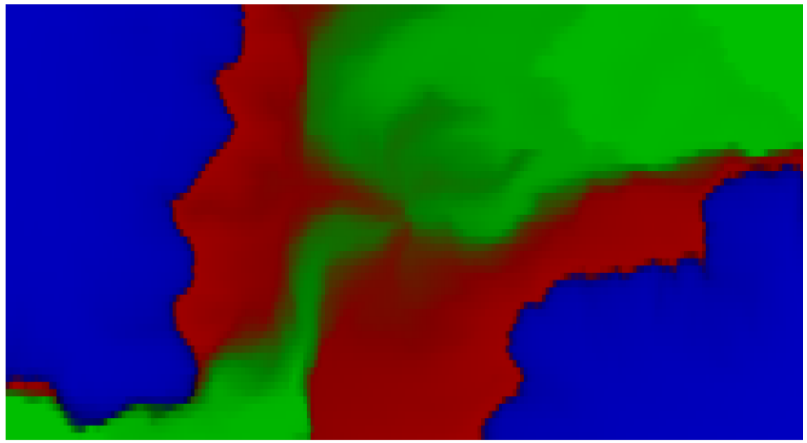

MsRSB saturation at 2/3 PVI

CO_2 injection: Layer of SPE 10 Model 2

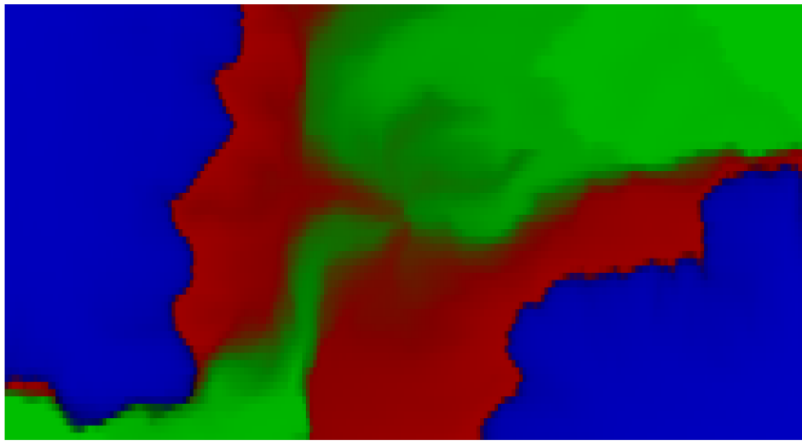

Sequential saturation at 2/3 PVI

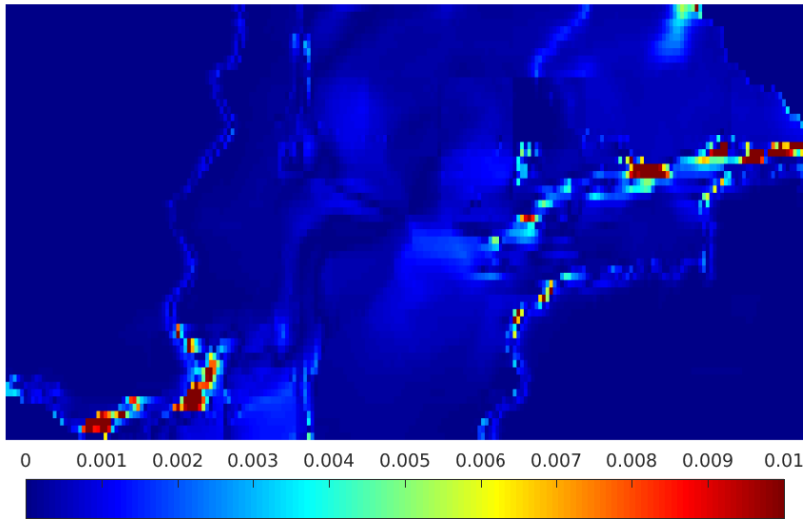

$|S_{ms} - S|$ at 2/3 PVI

CO_2 injection: Layer of SPE 10 Model 2

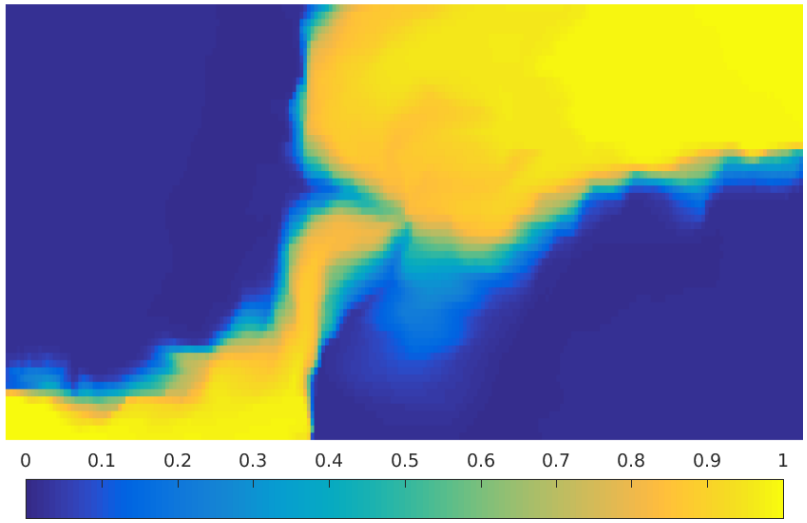

CO_2 concentration at 2/3 PVI

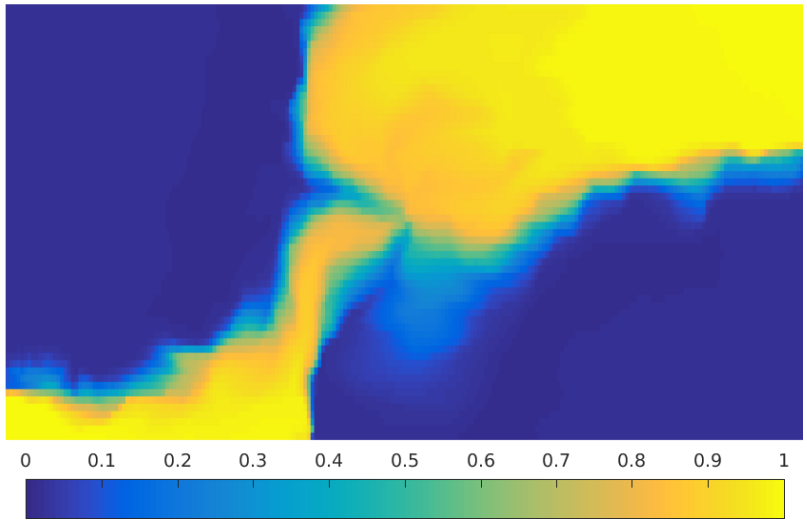

CO_2 concentration at 2/3 PVI

CO_2 injection: Layer of SPE 10 Model 2

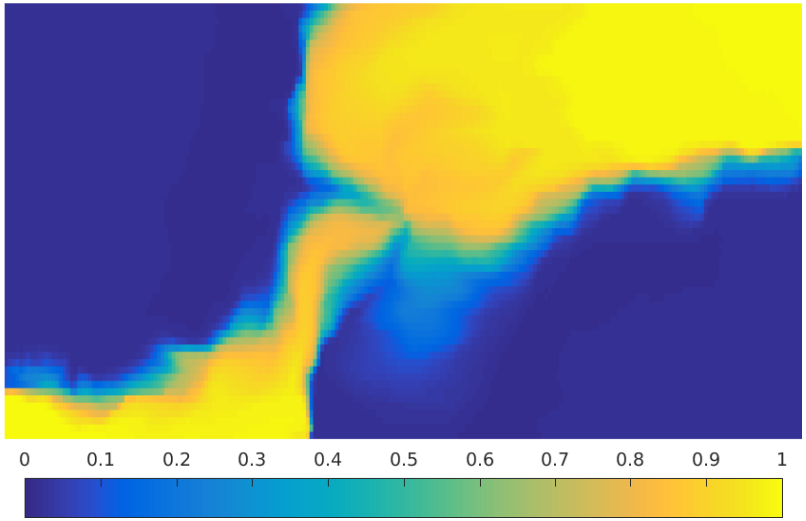

CO_2 concentration at 2/3 PVI

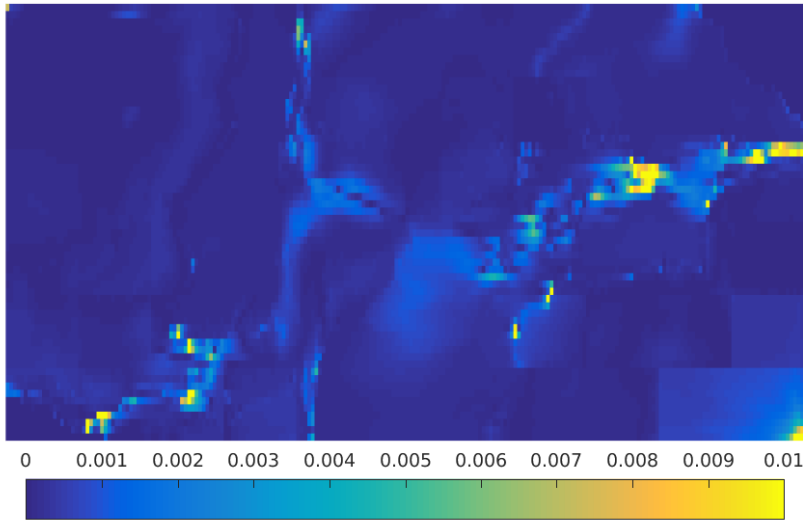

$|z_{ms} - z|$ at 2/3 PVI

CO_2 injection: Layer of SPE 10 Model 2

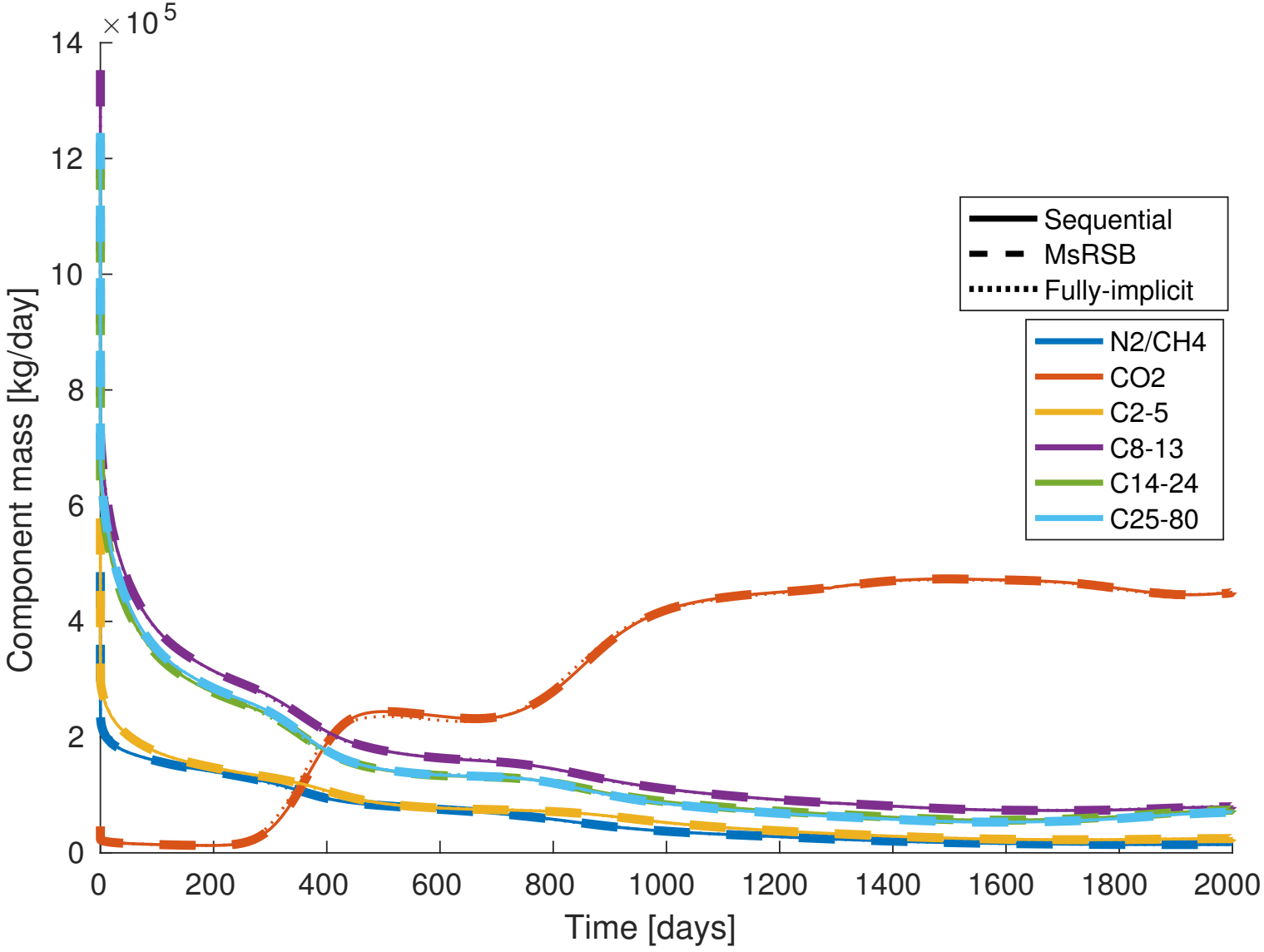

Component rates

CO_2 injection: Layer of SPE 10 Model 2

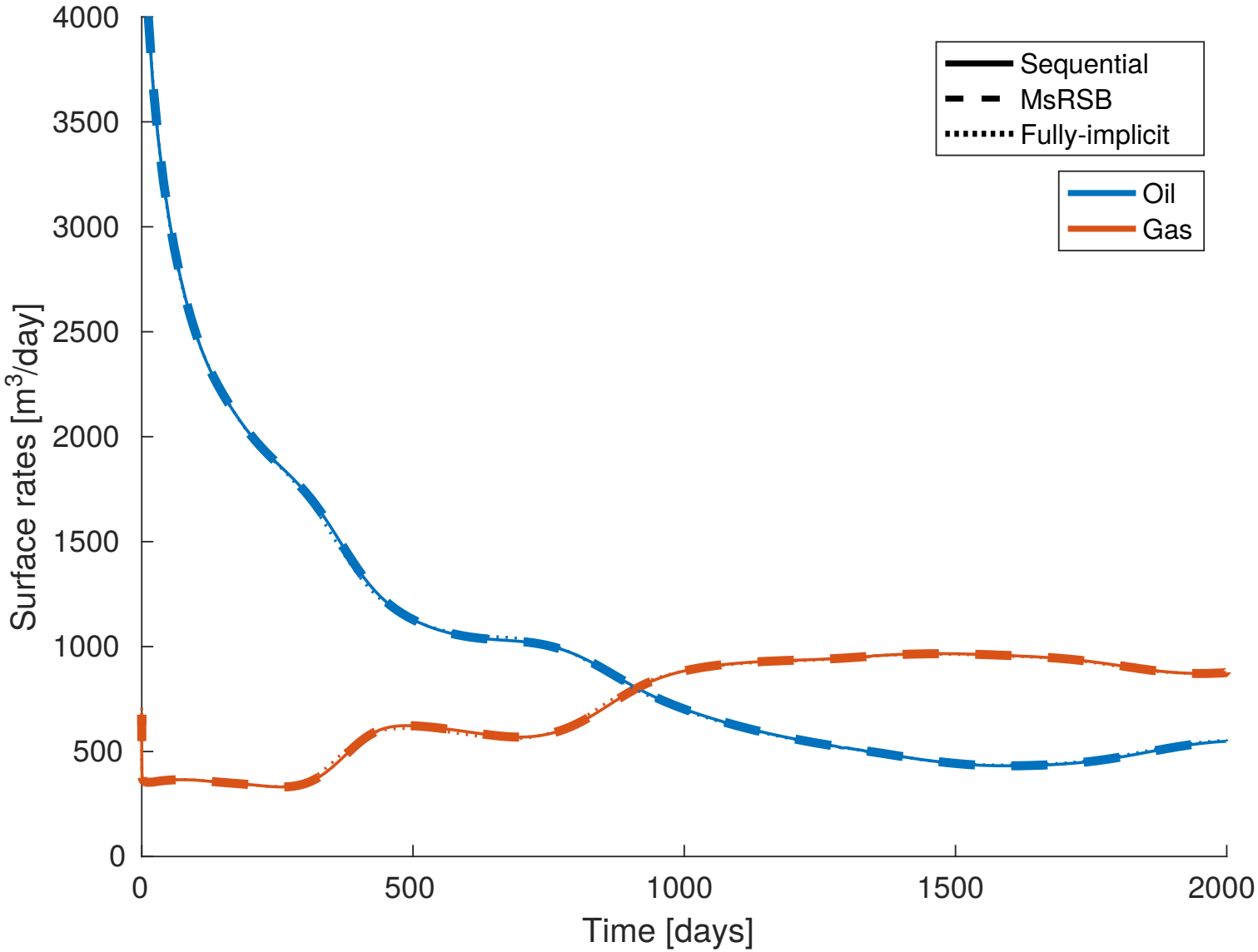

Gas and oil production

Example: Norne field

- Subset of Norne field model
- Synthetic wells injecting N_2
- Reservoir contains Methane, n-Pentane and n-Decane
- Low field pressure makes phase behavior sensitive
- Model contains faults, anisotropy, pinched cells, ...
- 40,000 fine cells, 200 coarse blocks

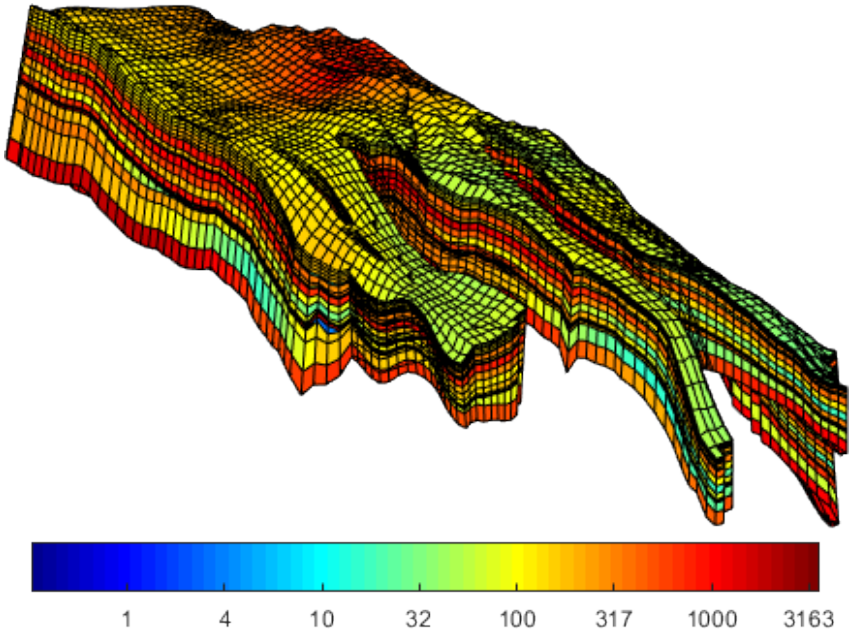

Permeability (millidarcy)

Example: Norne field

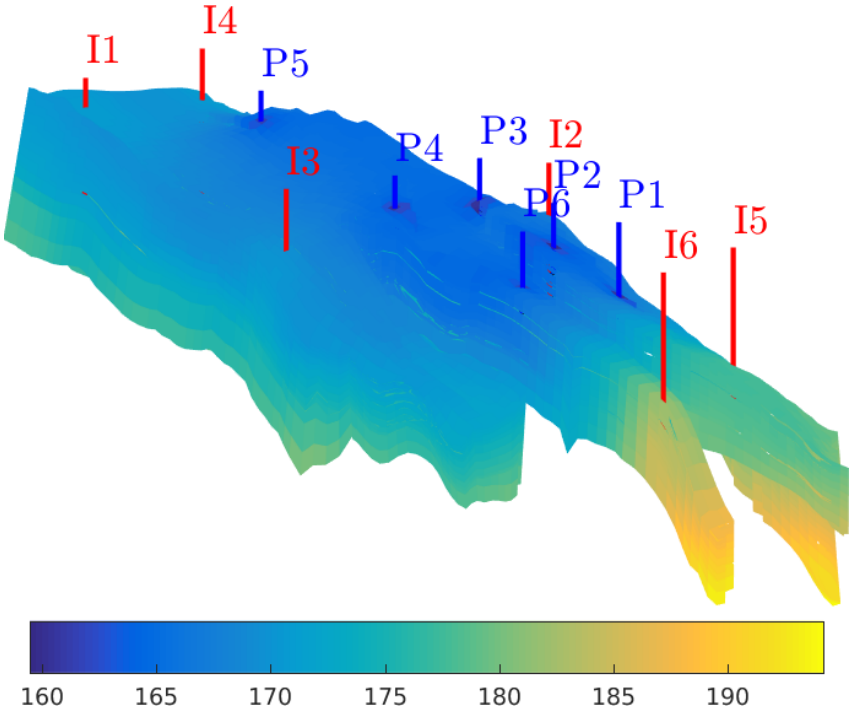

Field pressure

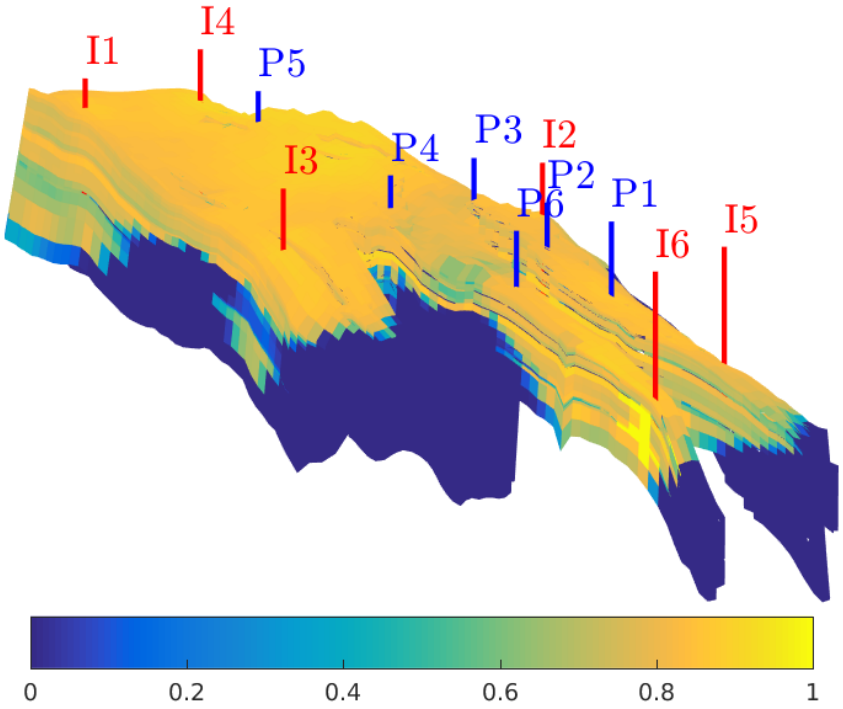

Gas saturation

Example: Norne field

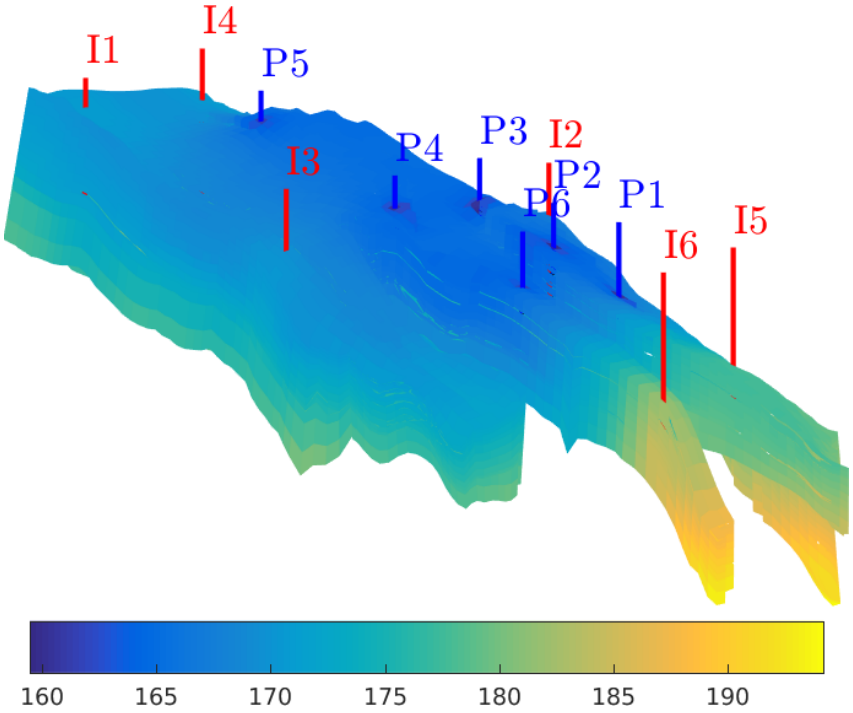

Field pressure

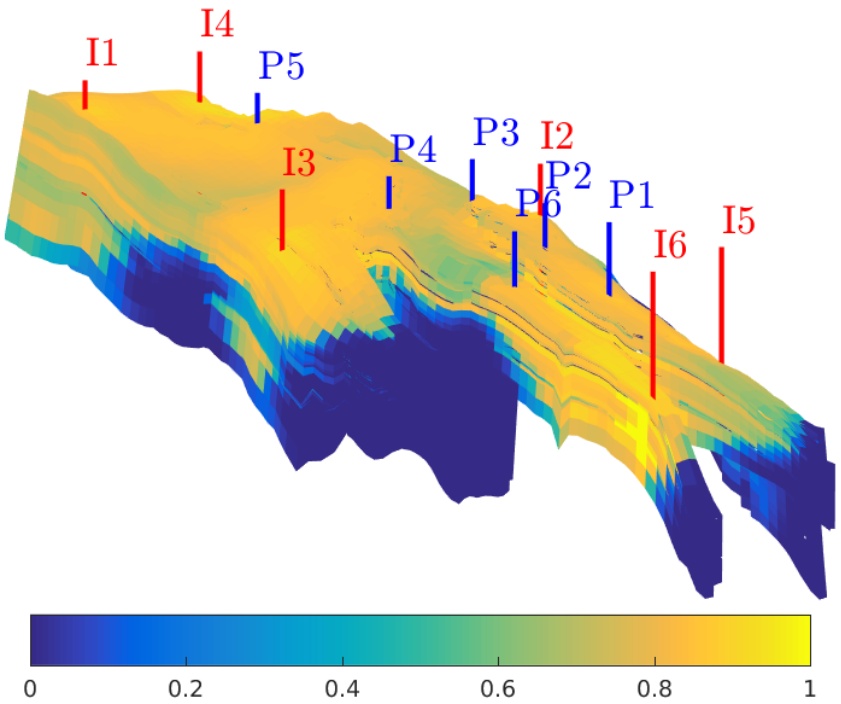

N_2 concentration

Example: Norne field

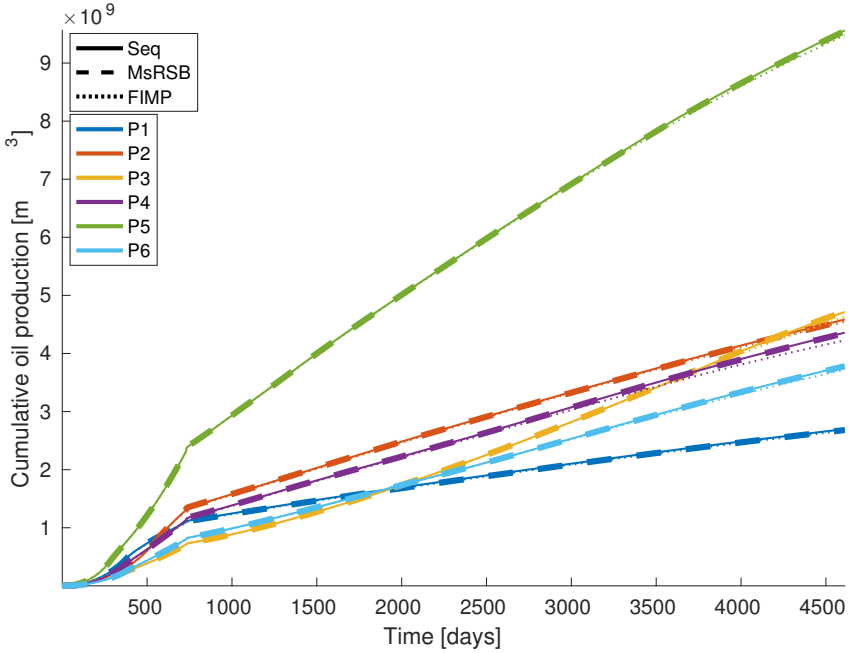

Cumulative oil production

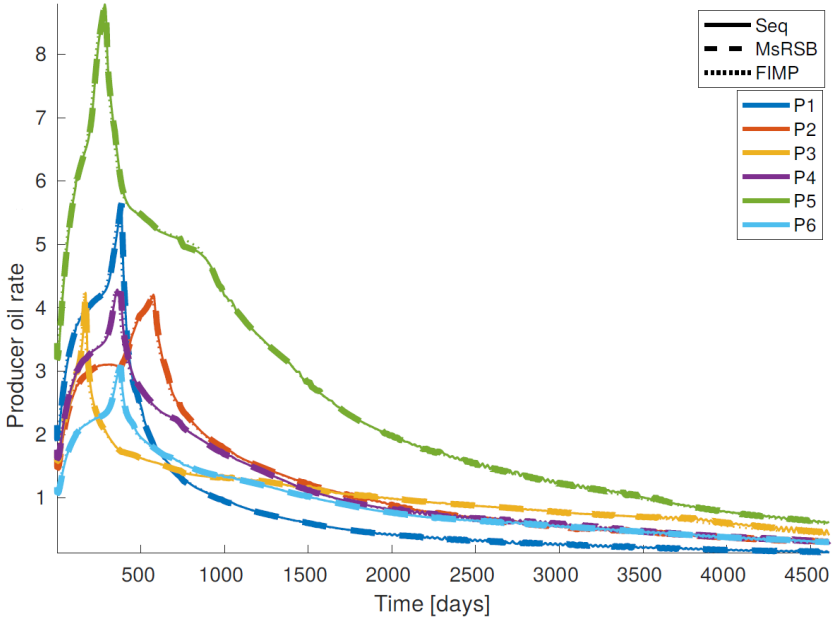

Oil production

Example: Norne field

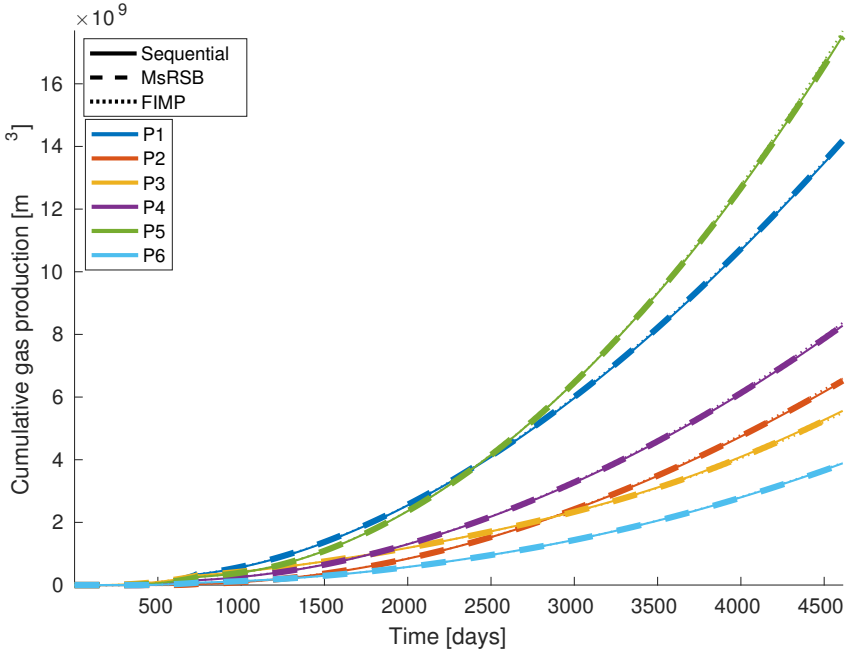

Cumulative gas production

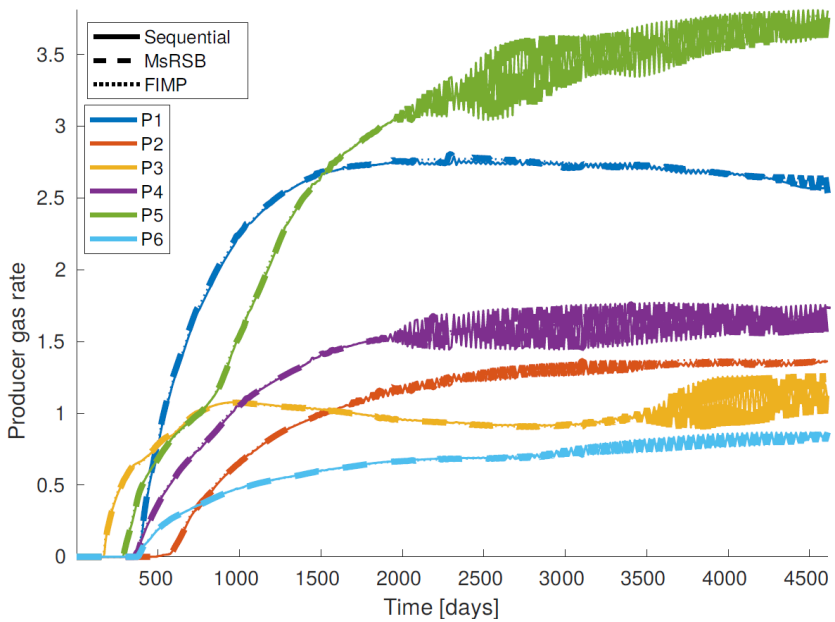

Gas production

Example: Norne field

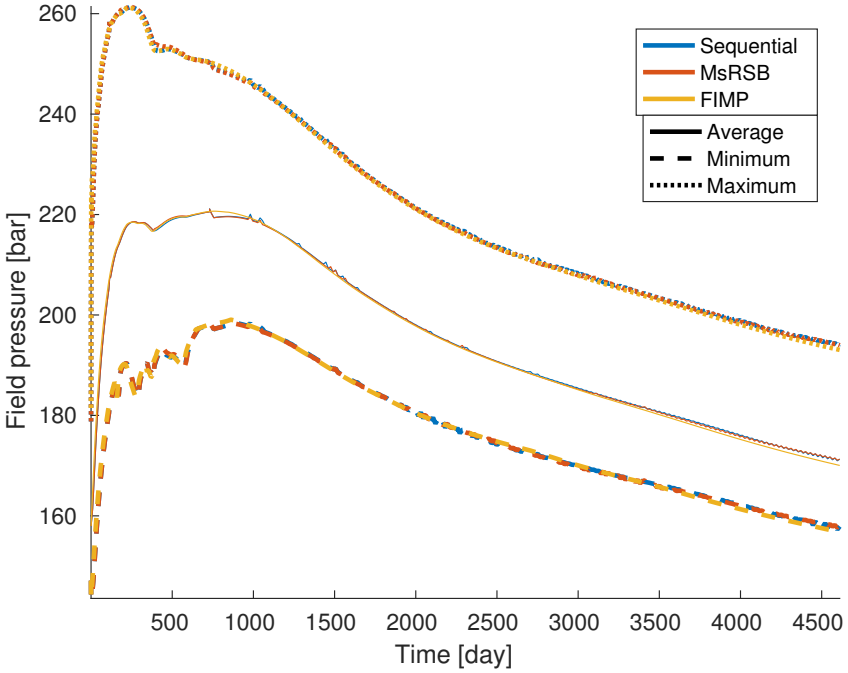

Field pressure

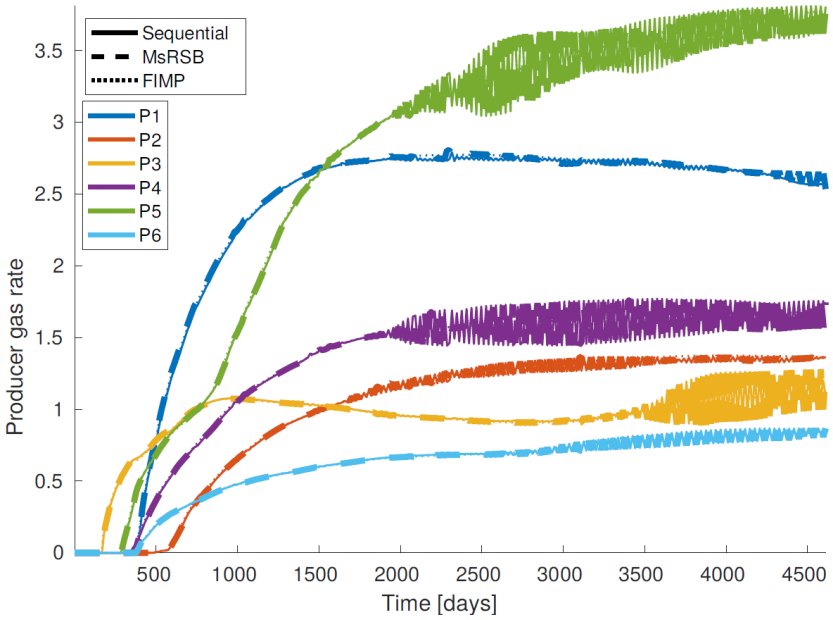

Gas production

Example: Nitrogen test

- SPE 10 model with very thin layer
- Use same fluid as for Norne field
- Constructed to produce oscillations in mass-scheme
- Compare total mass and total volume schemes

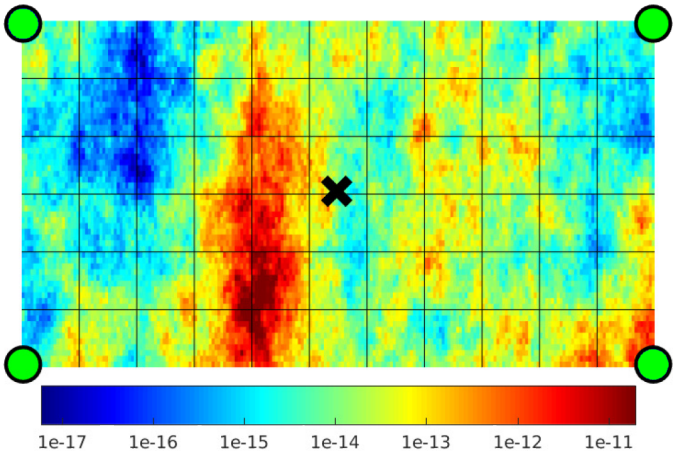

Configuration

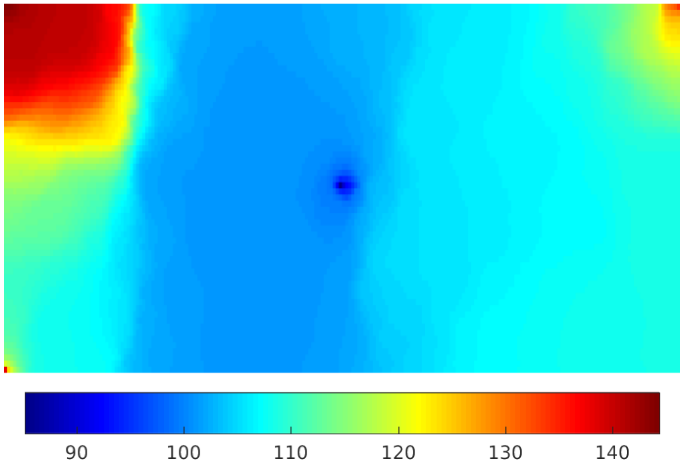

Pressure

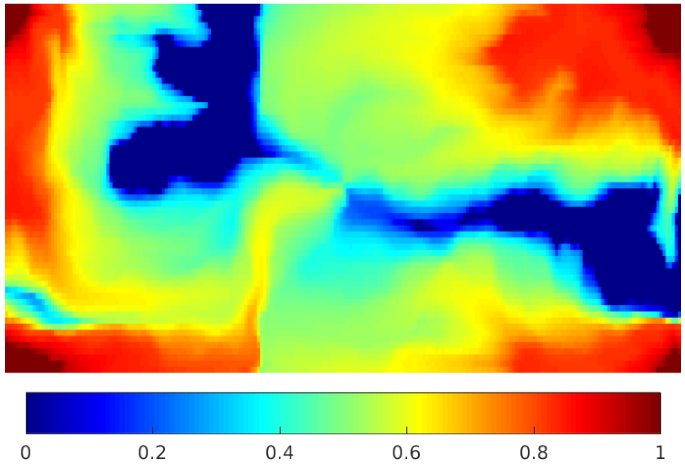

Gas saturation

Example: Nitrogen test

Fully implicit

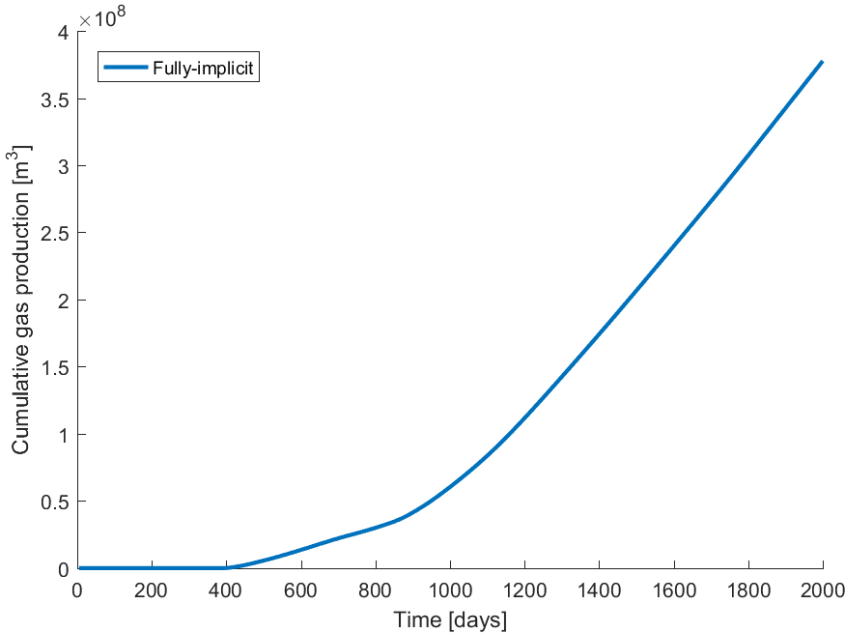

Cumulative gas production

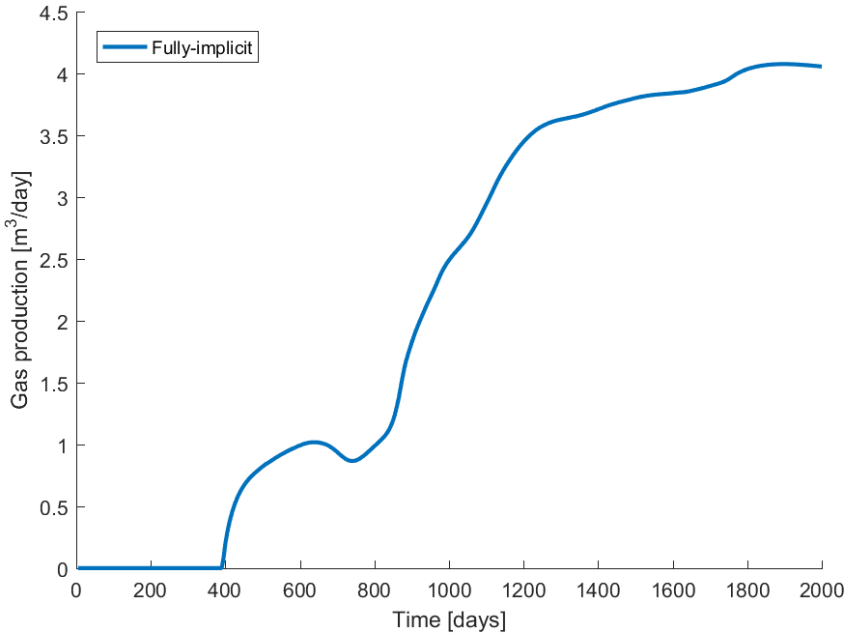

Gas production

Example: Nitrogen test

Total mass splitting

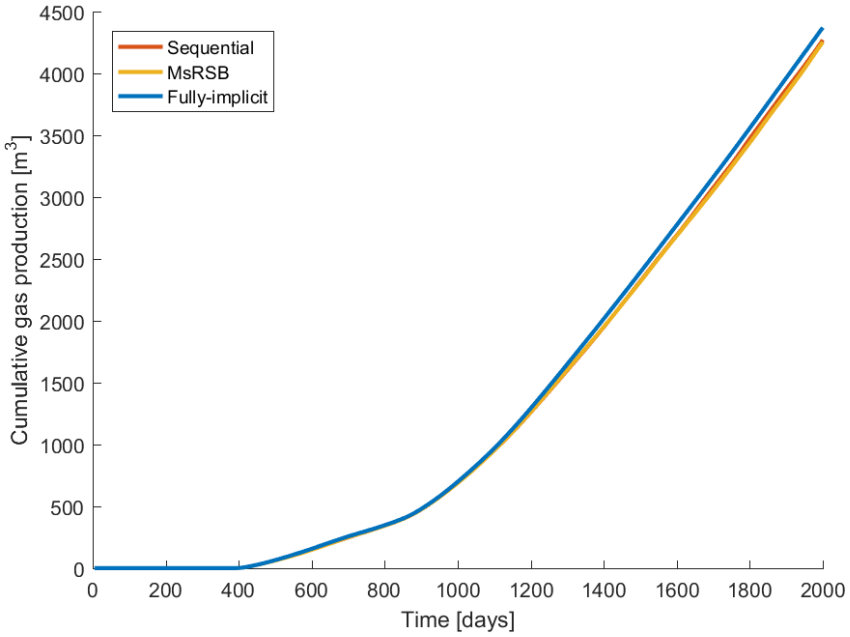

Cumulative gas production

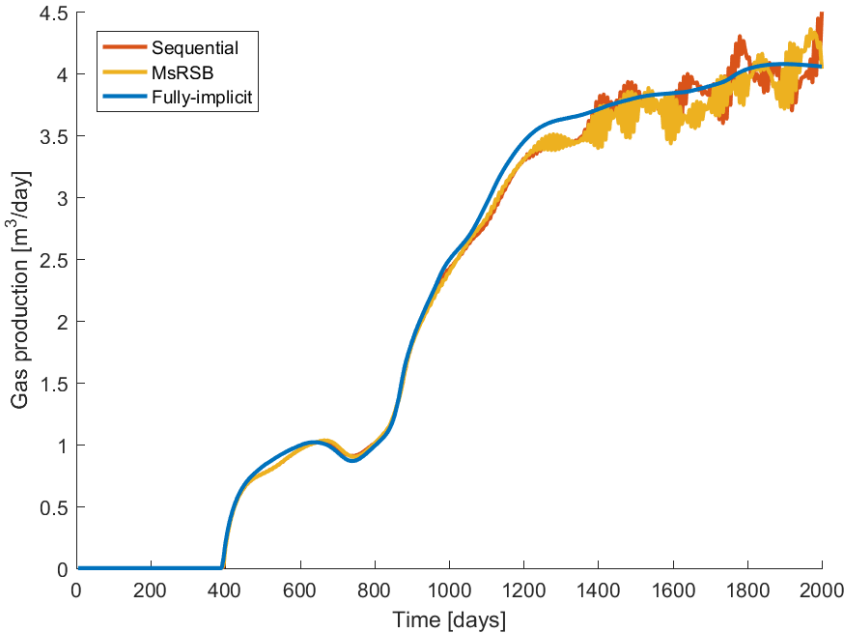

Gas production

Example: Nitrogen test

Total volume splitting

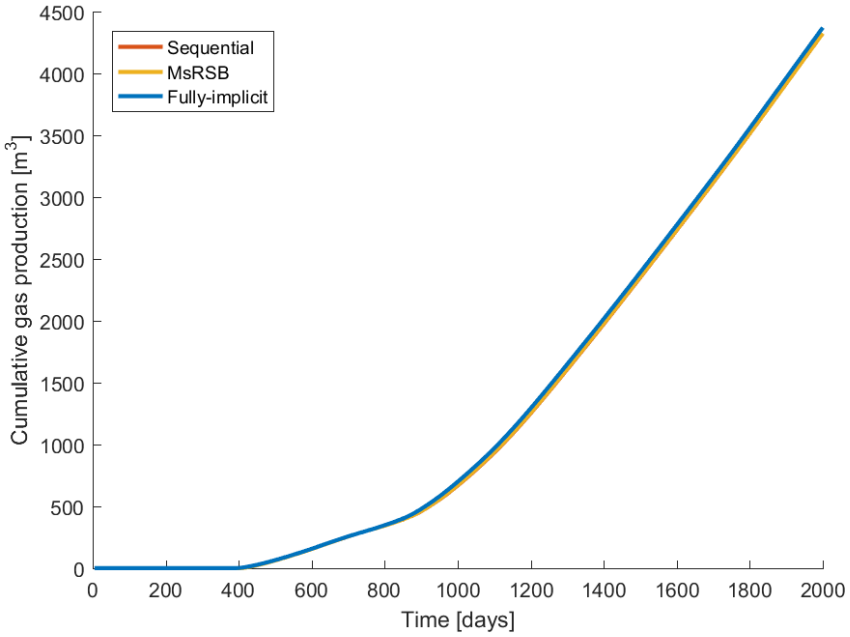

Cumulative gas production

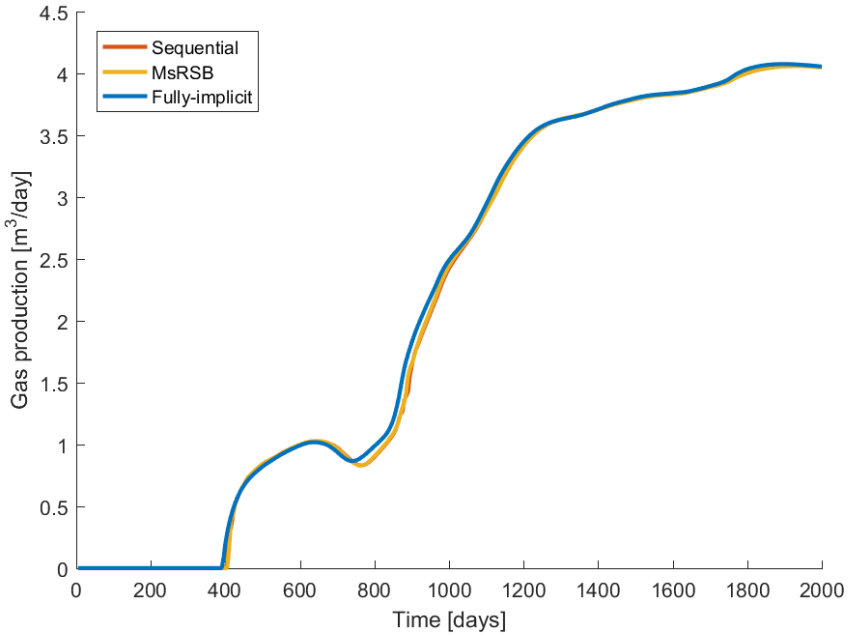

Gas production

Example: Nitrogen test

Producer gas-oil-ratio

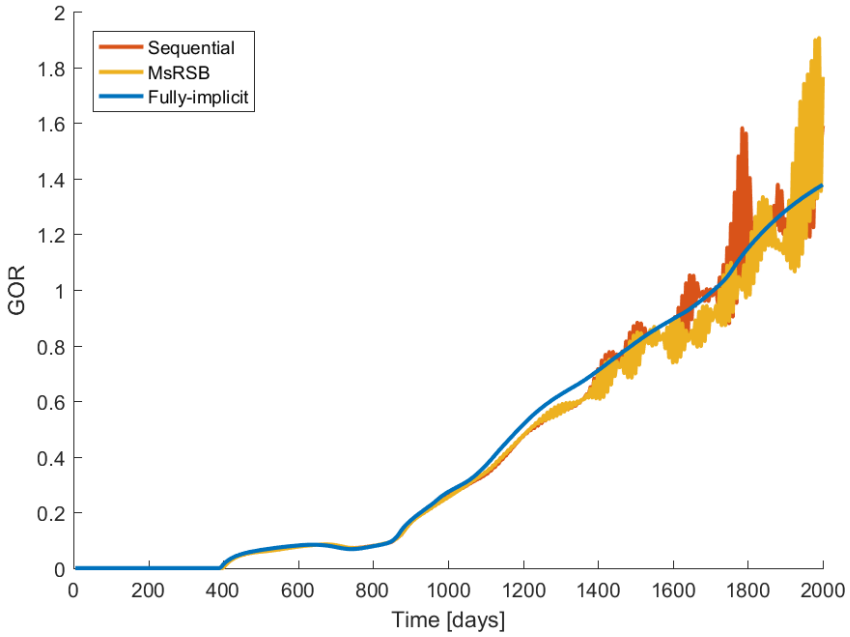

Total mass splitting

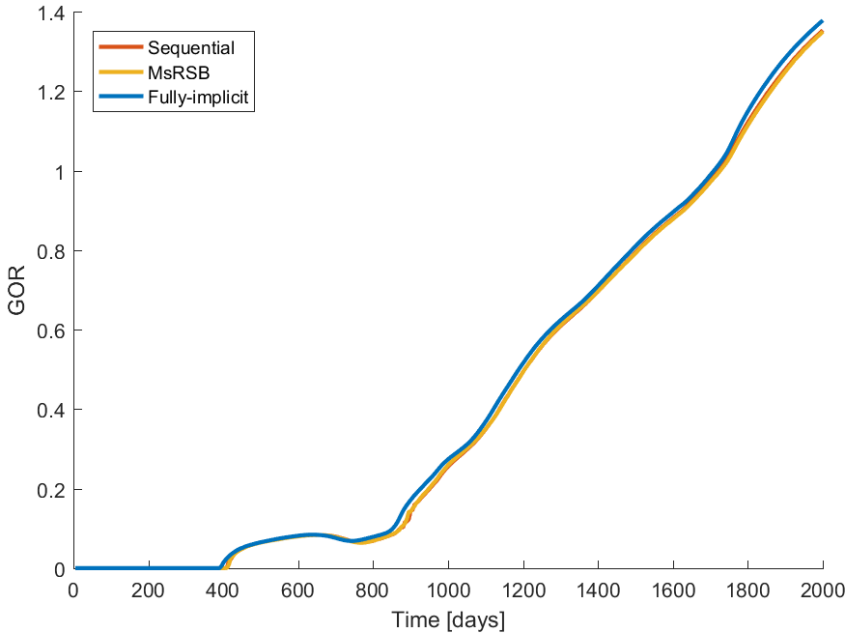

Total volume splitting

Recent developments: Feature-enrichment

Room for improvements

- Slow convergence in certain cases with strong contrasts and long correlation lengths
- Desire to adapt coarse grid to geological features
- Want improved resolution near wells
- Flux reconstruction for transport can be expensive

Previous work:

- generalized multiscale element methods (Efendiev et al)
- hybrid finite-volume/Galerkin method (Cortinovis and Jenny)

New idea: multiple multiscale operators

Assume N prolongation operators $P^1, \ldots, P^N$ that may come from different coarse grids and support regions, or different multiscale methods (MsRSB, MsFV,. . .)

Likewise, there are N restriction operators $R^1, \ldots, R^N$

New idea: multiple multiscale operators

Assume N prolongation operators $P^1, \ldots, P^N$ that may come from different coarse grids and support regions, or different multiscale methods (MsRSB, MsFV,. . .)

Likewise, there are N restriction operators $R^1, \ldots, R^N$

Multiplicative multistep method:

$$p^* = p^{k+(\ell-1)/N} + S(q - Ap^{k+(\ell-1)/N})$$

$$p^{k+\ell/N} = p^* + P^\ell(\underbrace{R^\ell A P^\ell}_{A^\ell_{ms}})^{-1} R^\ell(q - Ap^*),$$

Example setup: P^1 is *general* and covers domain evenly, whereas $P^2, \ldots, P^N$ are *feature specific*

Lie, Møyner, Natvig, SPE RSC 2017

Minimal assumptions on operators

1. P^ℓ and R^ℓ are constructed from a non-overlapping partition of the fine grid. Each column j in $\boldsymbol{P}^\ell$ is called a *basis function* and is associated with a coarse grid block $\overline{\Omega}_j^\ell$
2. The support S_j^ℓ of each basis function is compact and contains $\overline{\Omega}_j^\ell$
3. The columns of P^ℓ form a partition of unity, i.e., each row in P^ℓ has unit row sum

Examples of partition types

- Rectilinear or structured subdivisions
- Adapting to facies, rock types, saturation regions, etc
- Partitions adapting to faults, fractures,. . .
- From block-structured grids, LGR,. . .
- Unstructured graph-based partitions
- Amalgamations based on indicators
- Adapting dynamically to flow
- Separating near-well and far-field
- . . .

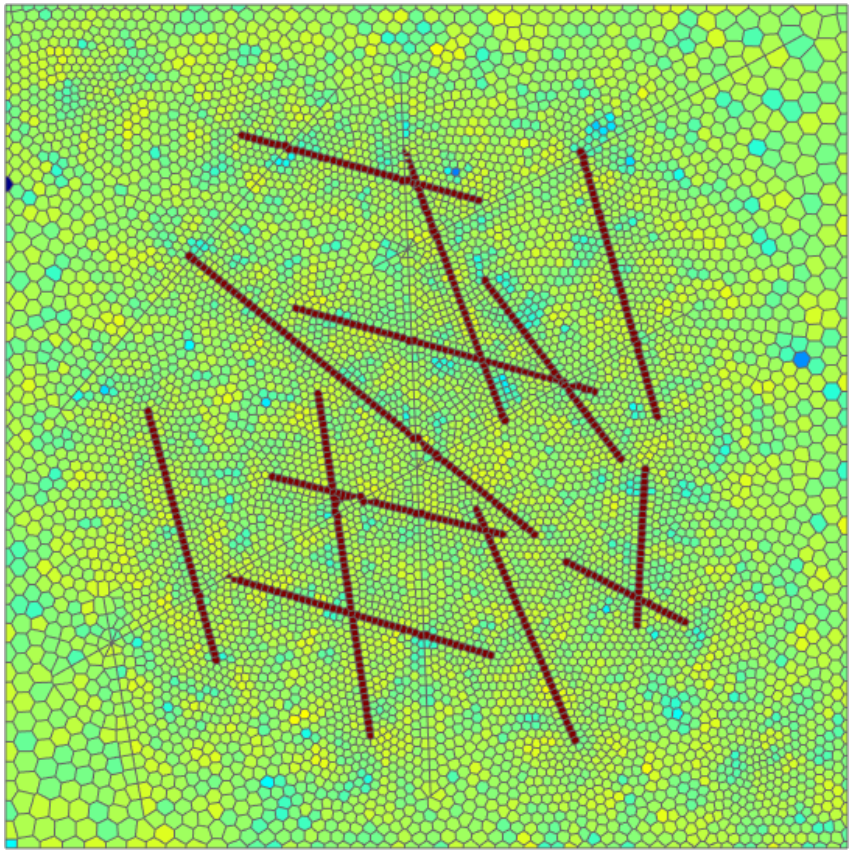

Examples of partition types

- Rectilinear or structured subdivisions
- Adapting to facies, rock types, saturation regions, etc
- Partitions adapting to faults, fractures,. . .
- From block-structured grids, LGR,. . .
- Unstructured graph-based partitions
- Amalgamations based on indicators
- Adapting dynamically to flow
- Separating near-well and far-field
- . . .

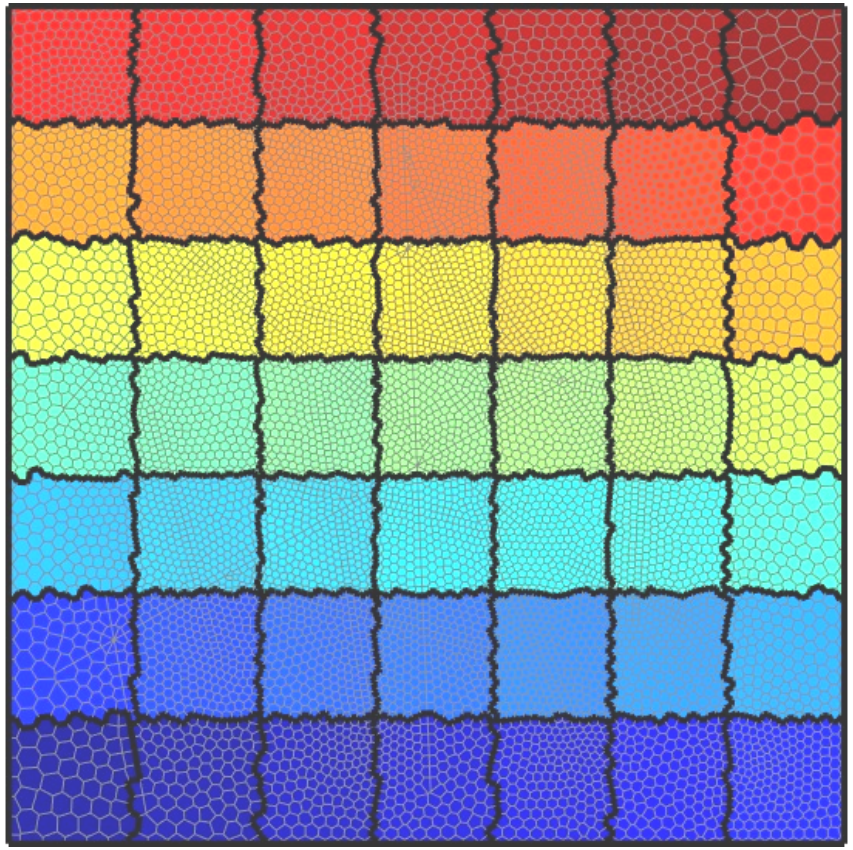

Examples of partition types

- Rectilinear or structured subdivisions
- Adapting to facies, rock types, saturation regions, etc
- Partitions adapting to faults, fractures,. . .
- From block-structured grids, LGR,. . .
- Unstructured graph-based partitions
- Amalgamations based on indicators
- Adapting dynamically to flow
- Separating near-well and far-field
- . . .

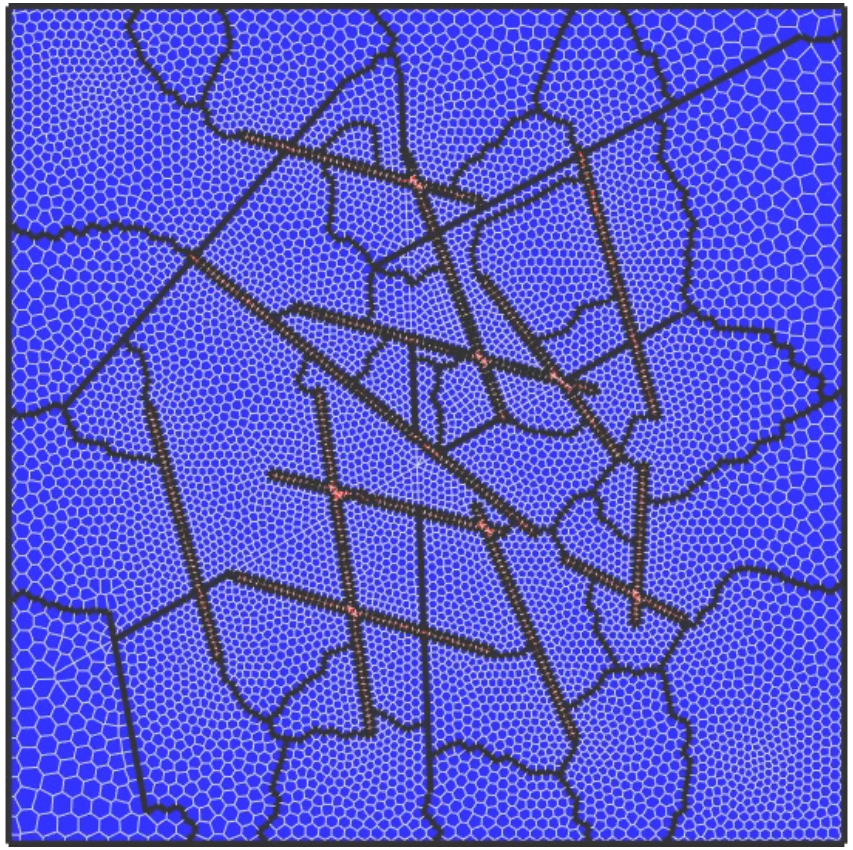

Examples of partition types

- Rectilinear or structured subdivisions
- Adapting to facies, rock types, saturation regions, etc
- Partitions adapting to faults, fractures,. . .
- From block-structured grids, LGR,. . .
- Unstructured graph-based partitions
- Amalgamations based on indicators
- Adapting dynamically to flow
- Separating near-well and far-field
- . . .

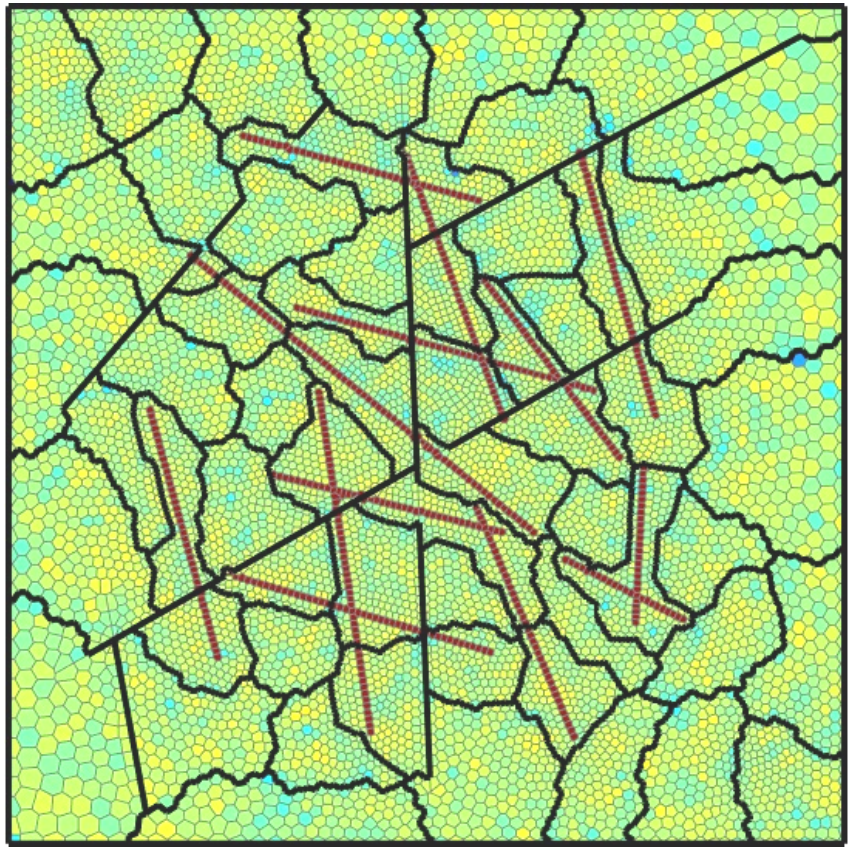

Examples of partition types

- Rectilinear or structured subdivisions
- Adapting to facies, rock types, saturation regions, etc
- Partitions adapting to faults, fractures,. . .
- From block-structured grids, LGR,. . .
- Unstructured graph-based partitions
- Amalgamations based on indicators
- Adapting dynamically to flow
- Separating near-well and far-field
- . . .

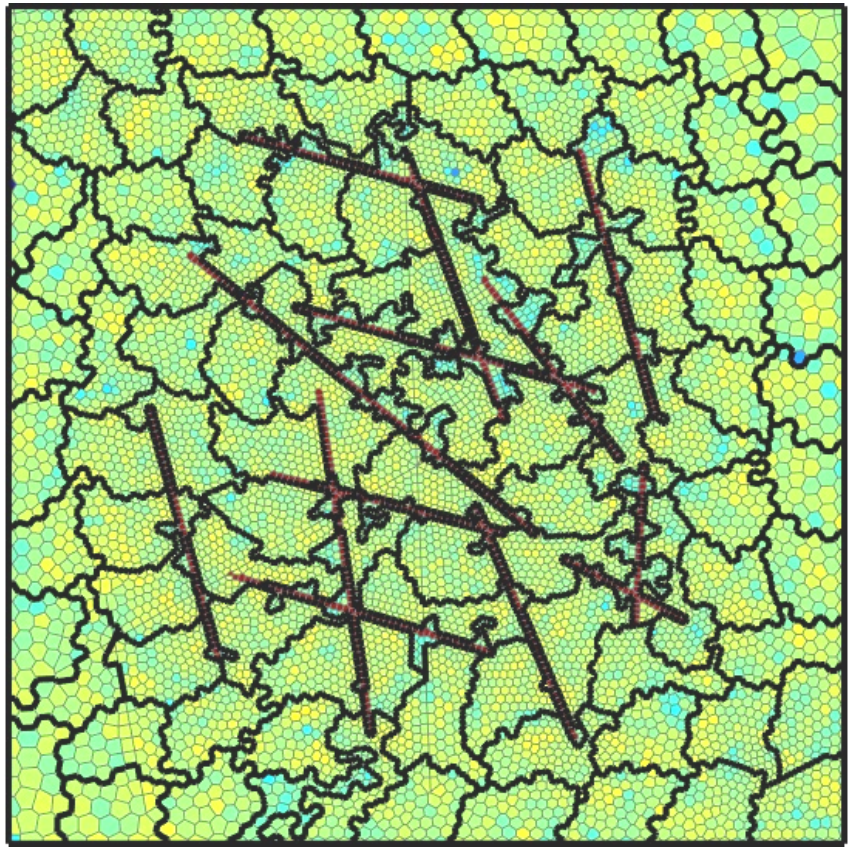

Examples of partition types

- Rectilinear or structured subdivisions
- Adapting to facies, rock types, saturation regions, etc
- Partitions adapting to faults, fractures,. . .
- From block-structured grids, LGR,. . .
- Unstructured graph-based partitions
- Amalgamations based on indicators
- Adapting dynamically to flow
- Separating near-well and far-field
- . . .

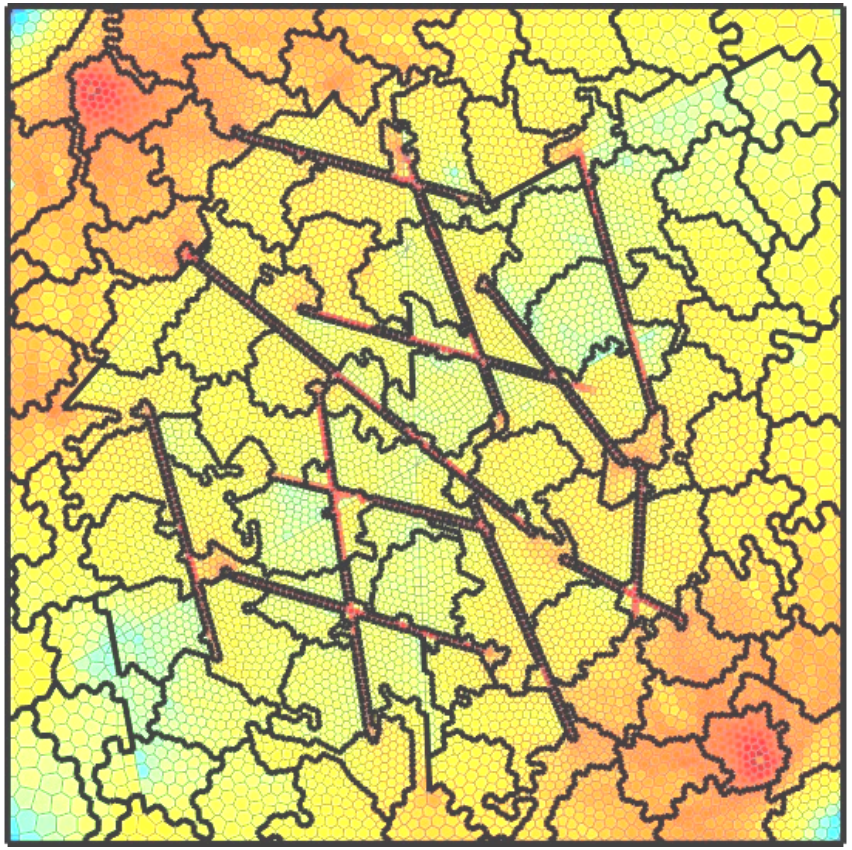

Examples of partition types

- Rectilinear or structured subdivisions
- Adapting to facies, rock types, saturation regions, etc
- Partitions adapting to faults, fractures,. . .
- From block-structured grids, LGR,. . .
- Unstructured graph-based partitions
- Amalgamations based on indicators
- Adapting dynamically to flow
- Separating near-well and far-field
- . . .

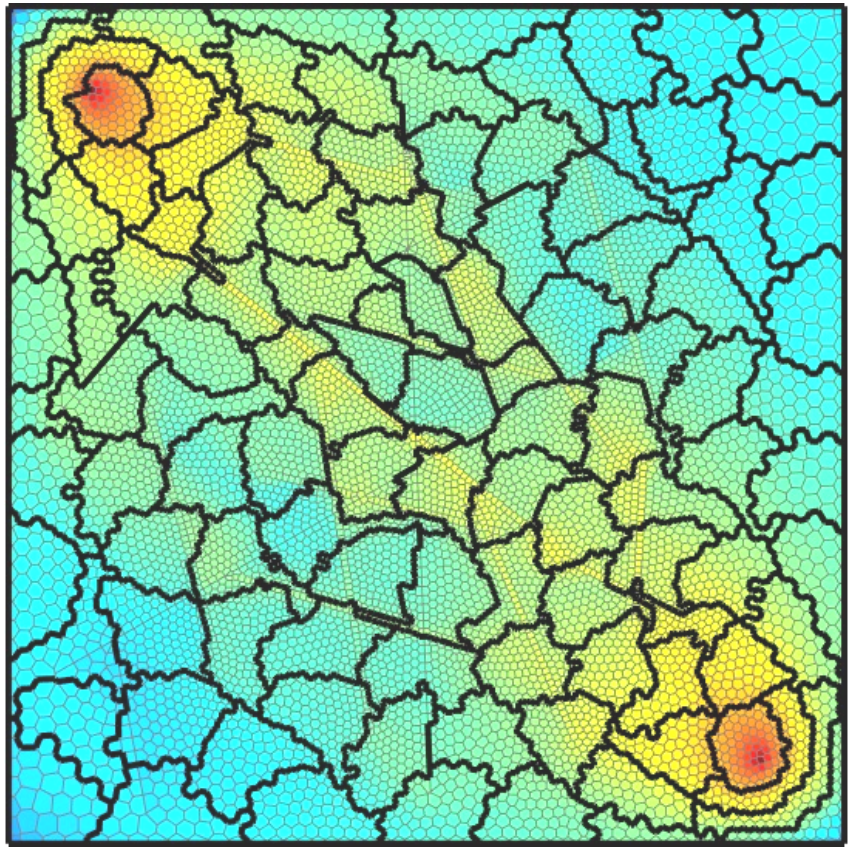

Examples of partition types

- Rectilinear or structured subdivisions
- Adapting to facies, rock types, saturation regions, etc
- Partitions adapting to faults, fractures,. . .
- From block-structured grids, LGR,. . .
- Unstructured graph-based partitions
- Amalgamations based on indicators
- Adapting dynamically to flow
- Separating near-well and far-field
- . . .

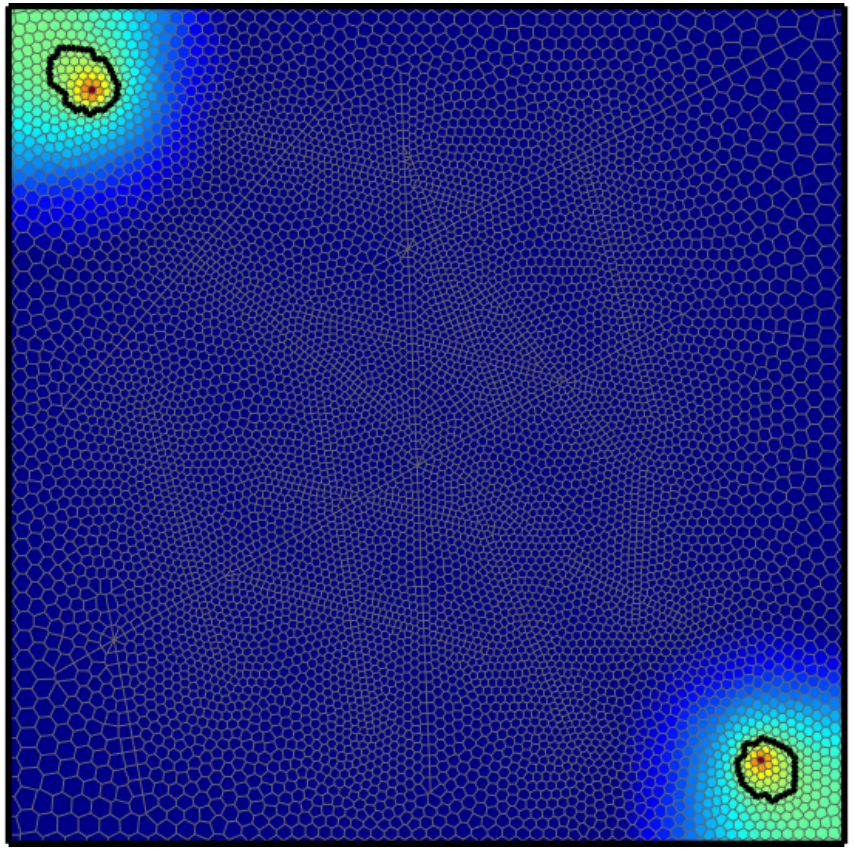

Numerical example: SPE10

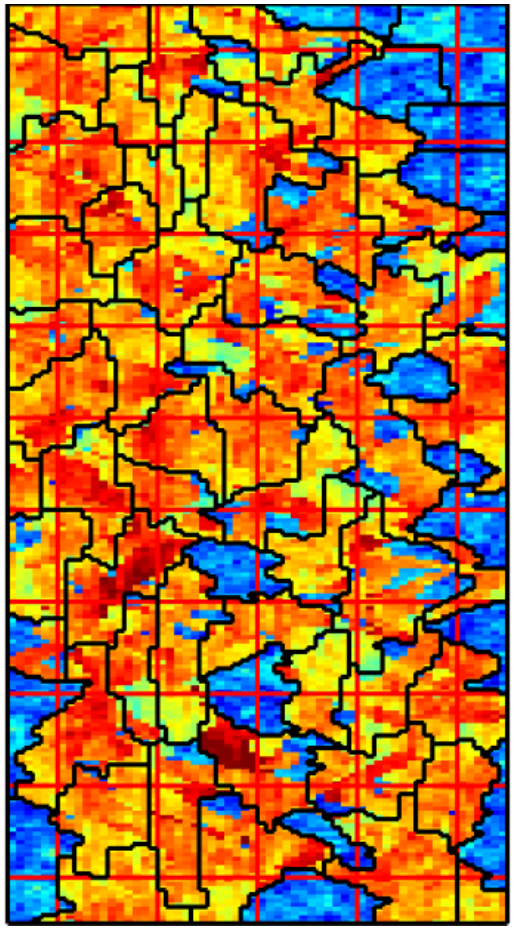

Layer 85: 220×60 subsample, pressure drop from north to south, linear relperms, equal viscosities

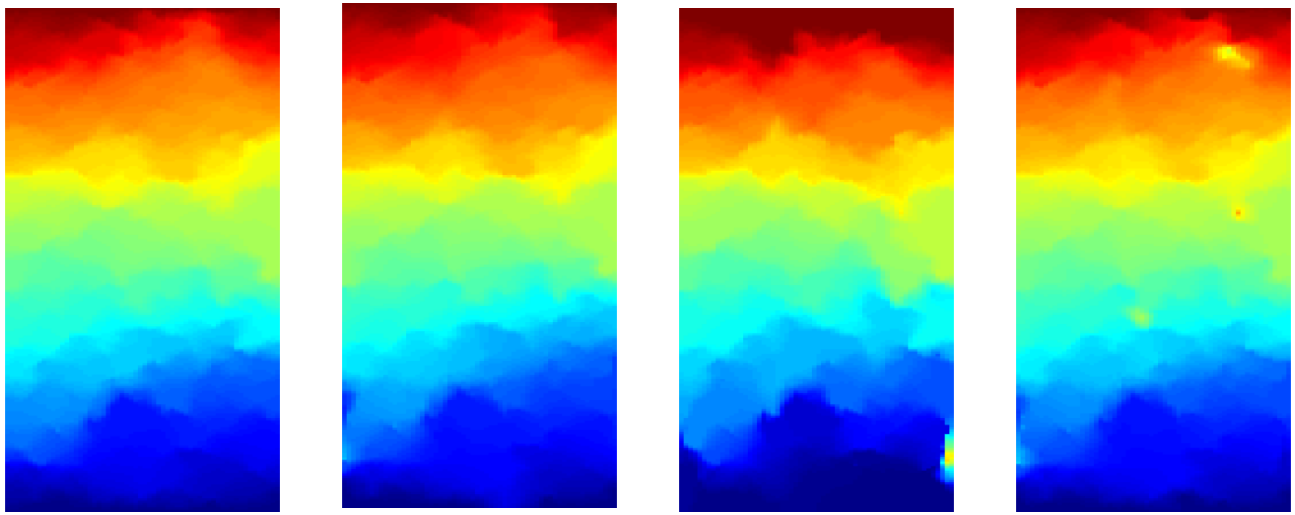

fine rectangular metis combined

Partition	L^2	L^∞
Rectangular	0.0307	0.1782
Metis	0.0791	0.5506
Combined	0.0293	0.2929

Numerical example: SPE10

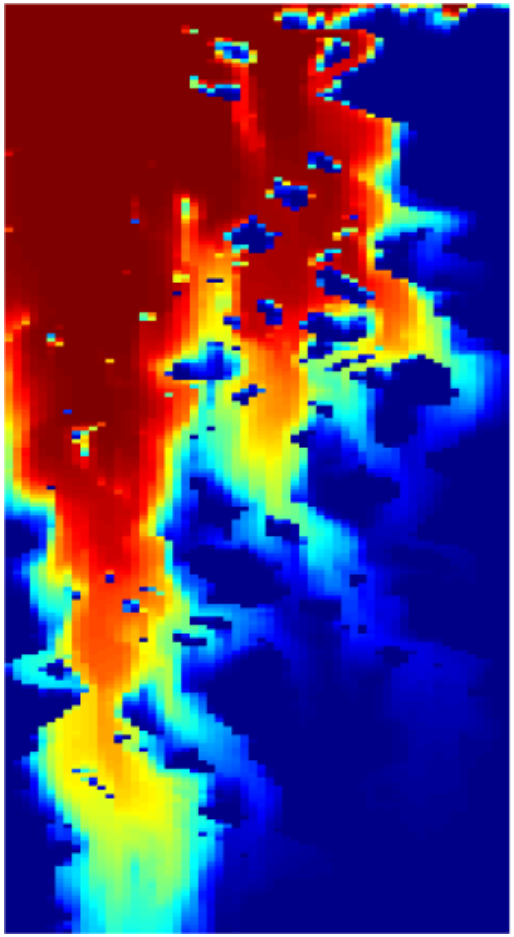

Layer 85: 220×60 subsample, pressure drop from north to south, linear relperms, equal viscosities

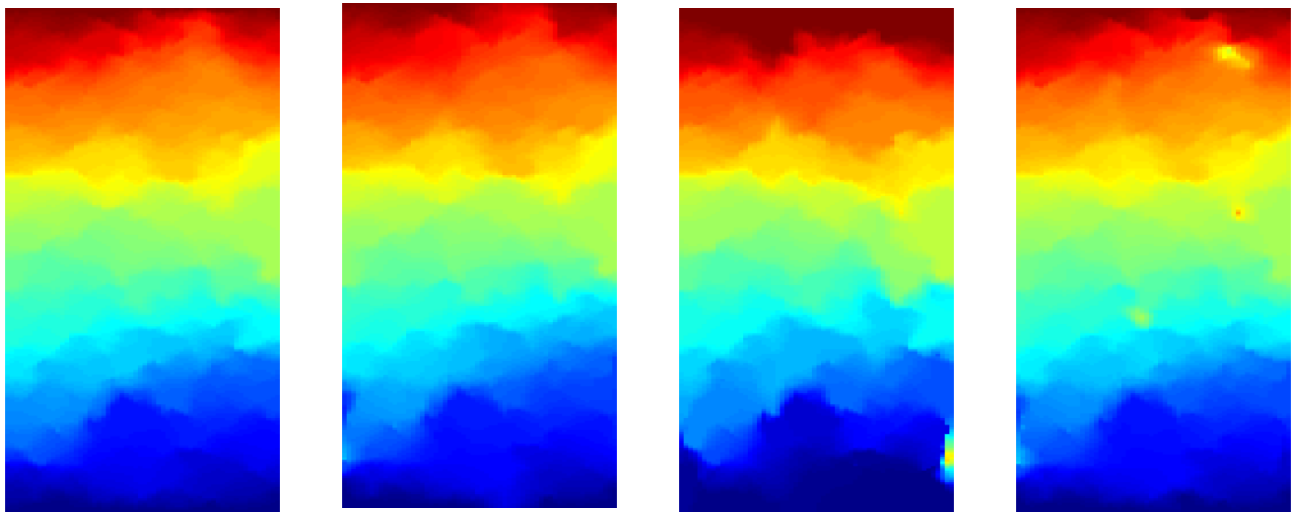

fine rectangular metis combined

Partition	L^2	L^∞
Rectangular	0.0307	0.1782
Metis	0.0791	0.5506
Combined	0.0293	0.2929

Numerical example: SPE10

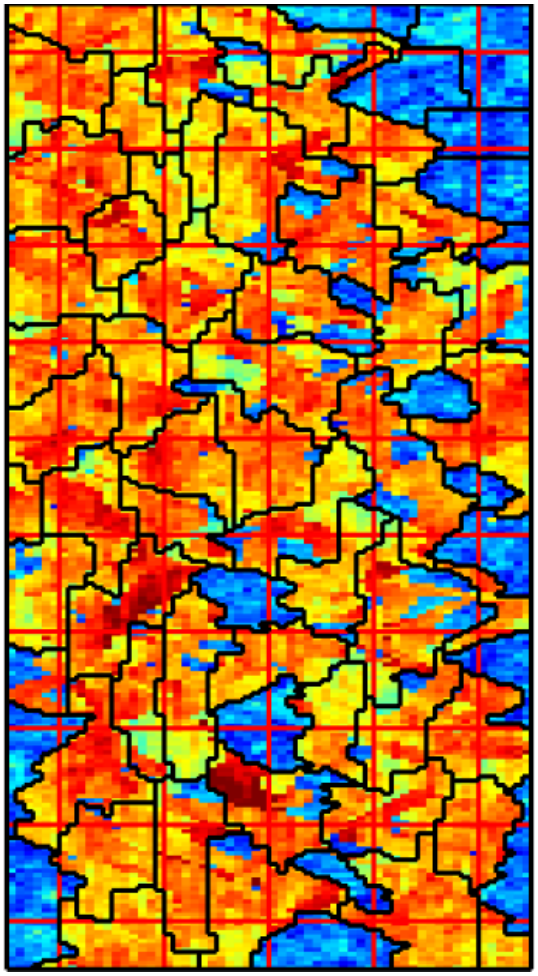

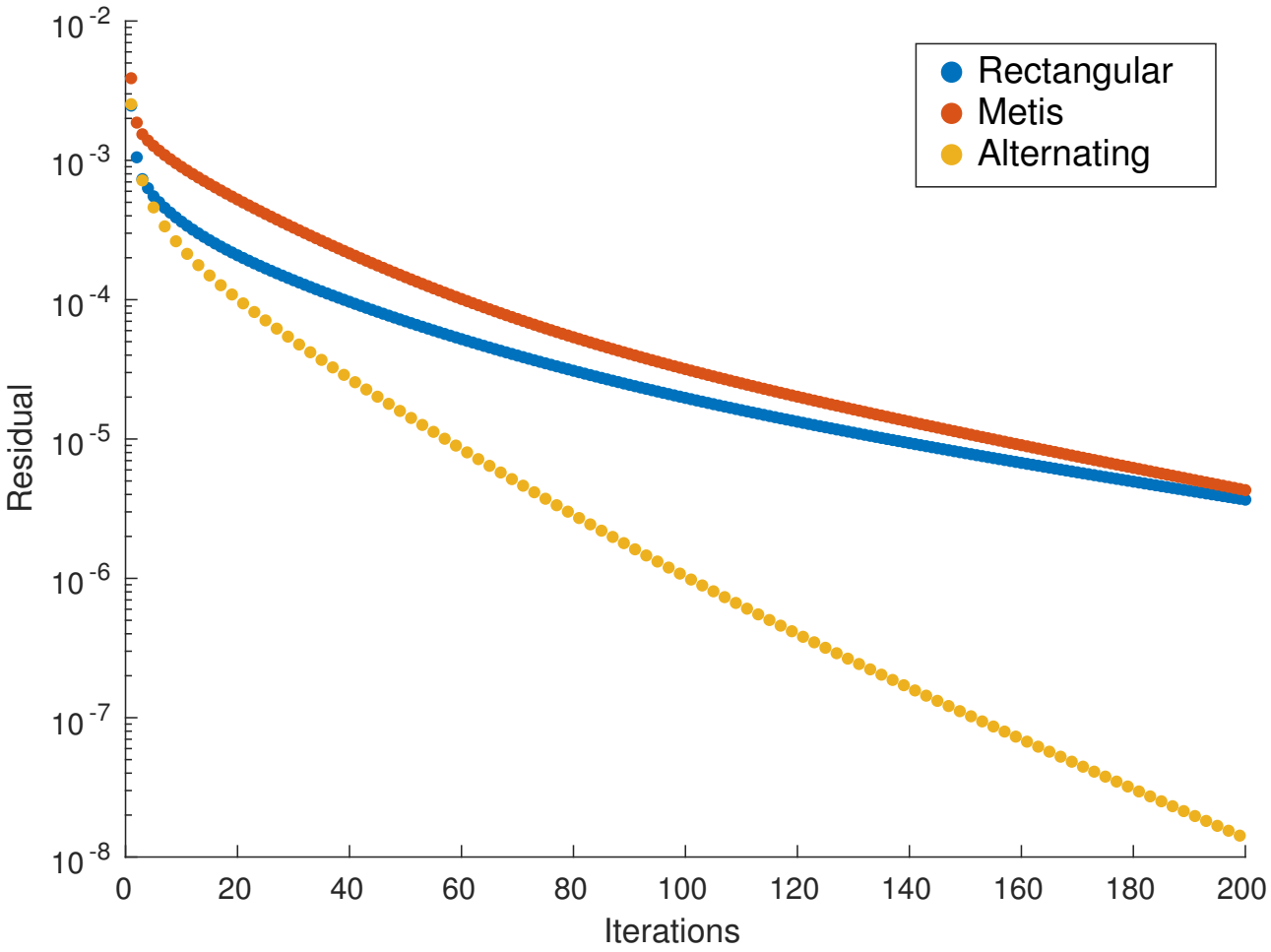

Numerical example: SPE10

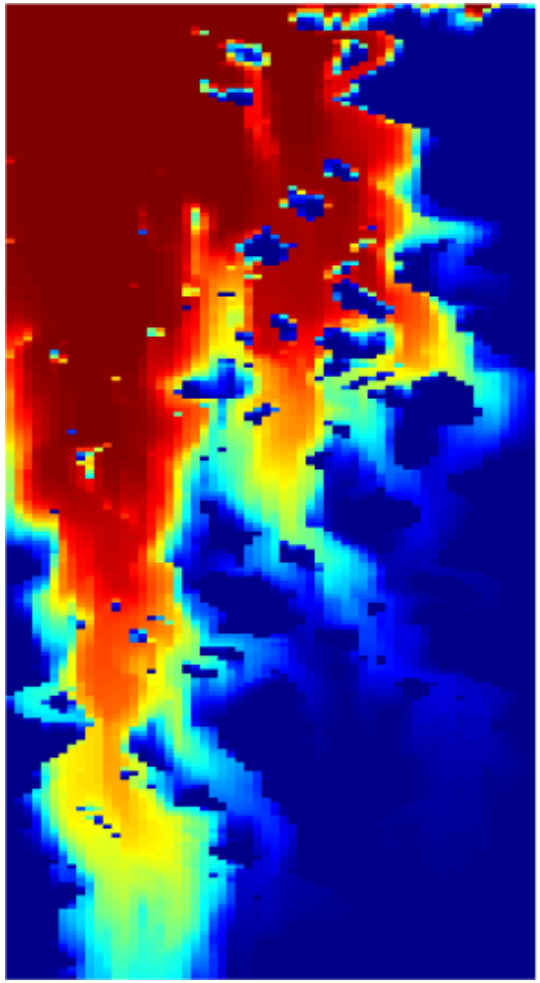

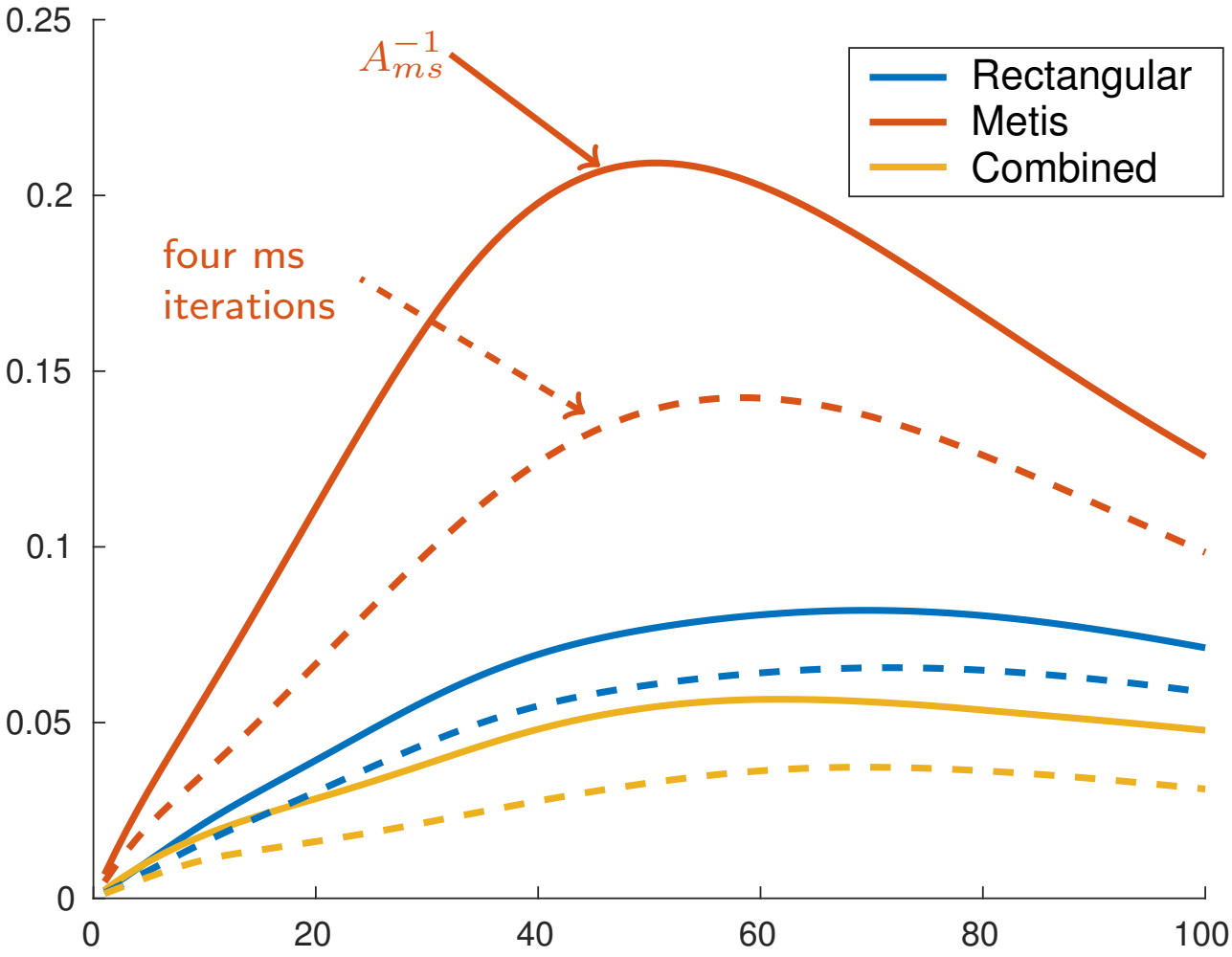

Numerical example: Unstructured grid

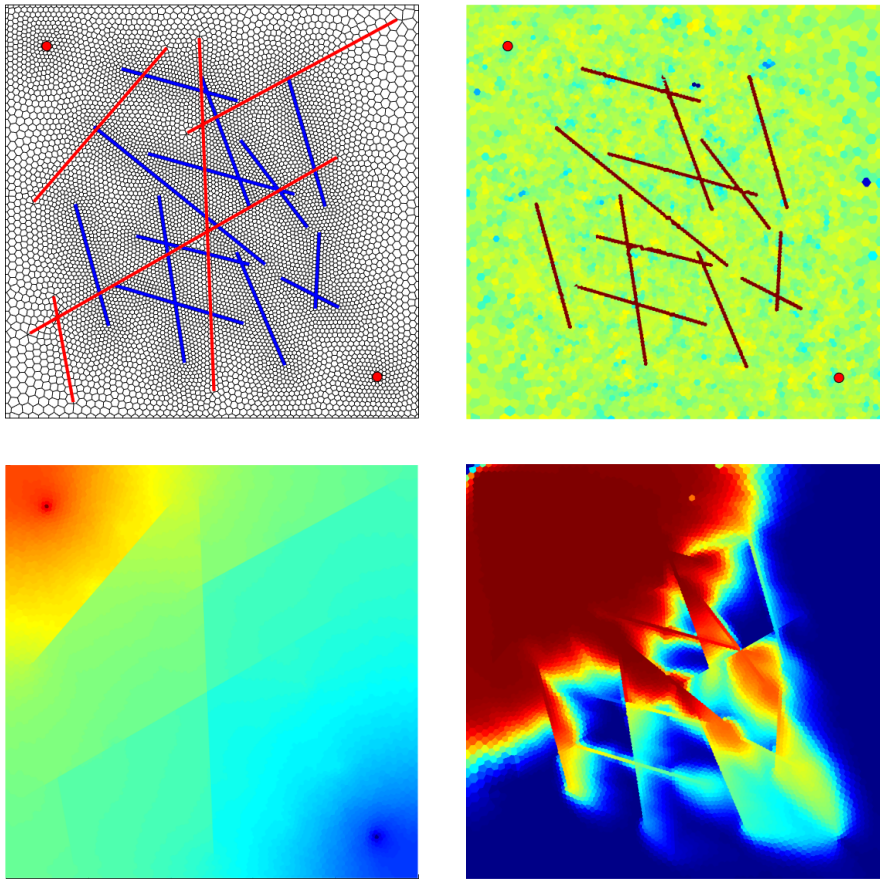

PEBI grid adapting to five faults and thirteen volumetric fractures.

Faults: 0.01 trans. multiplier
Fractures: 5 darcy
Background: average 100 md
Wells:
- injector, bhp: 500 bar
- producer, bhp: 200 bar

Numerical example: Unstructured grid

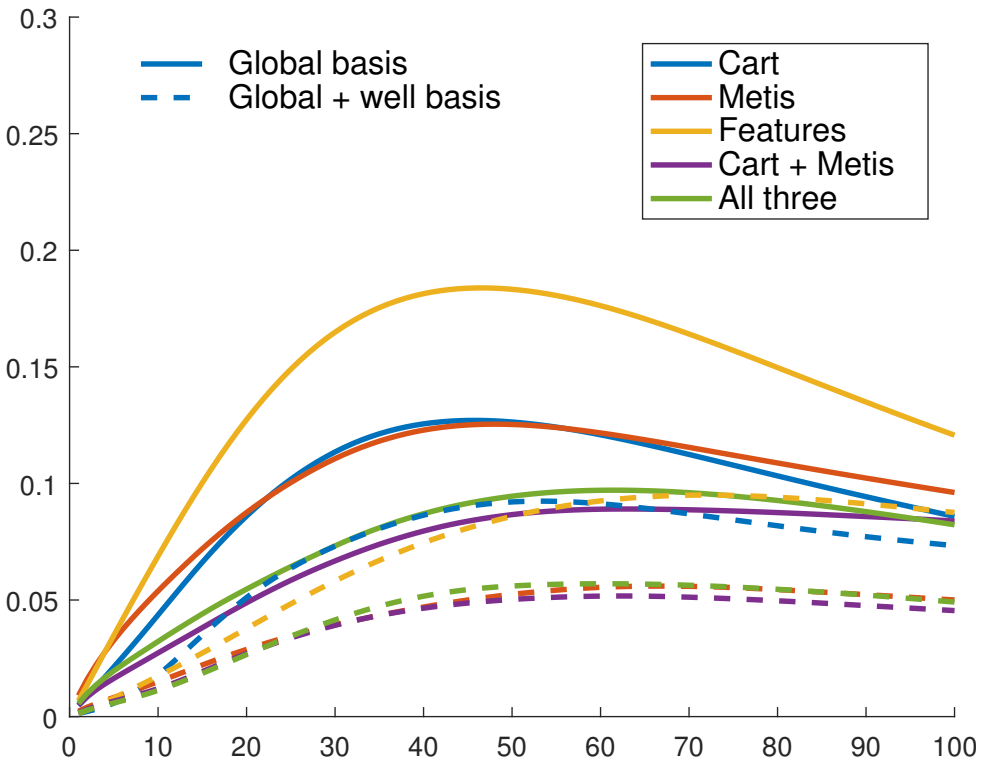

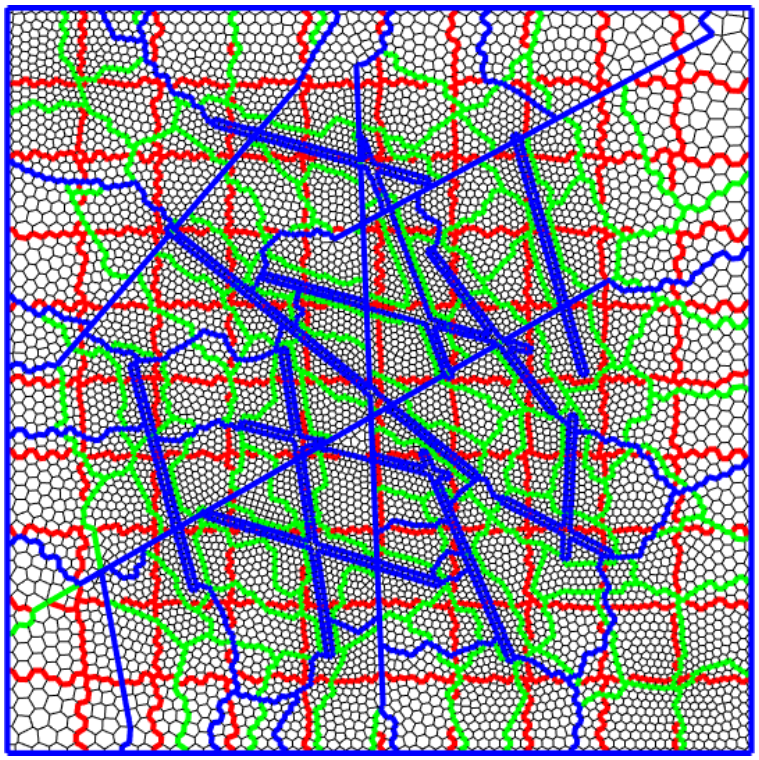

Numerical example: Unstructured grid

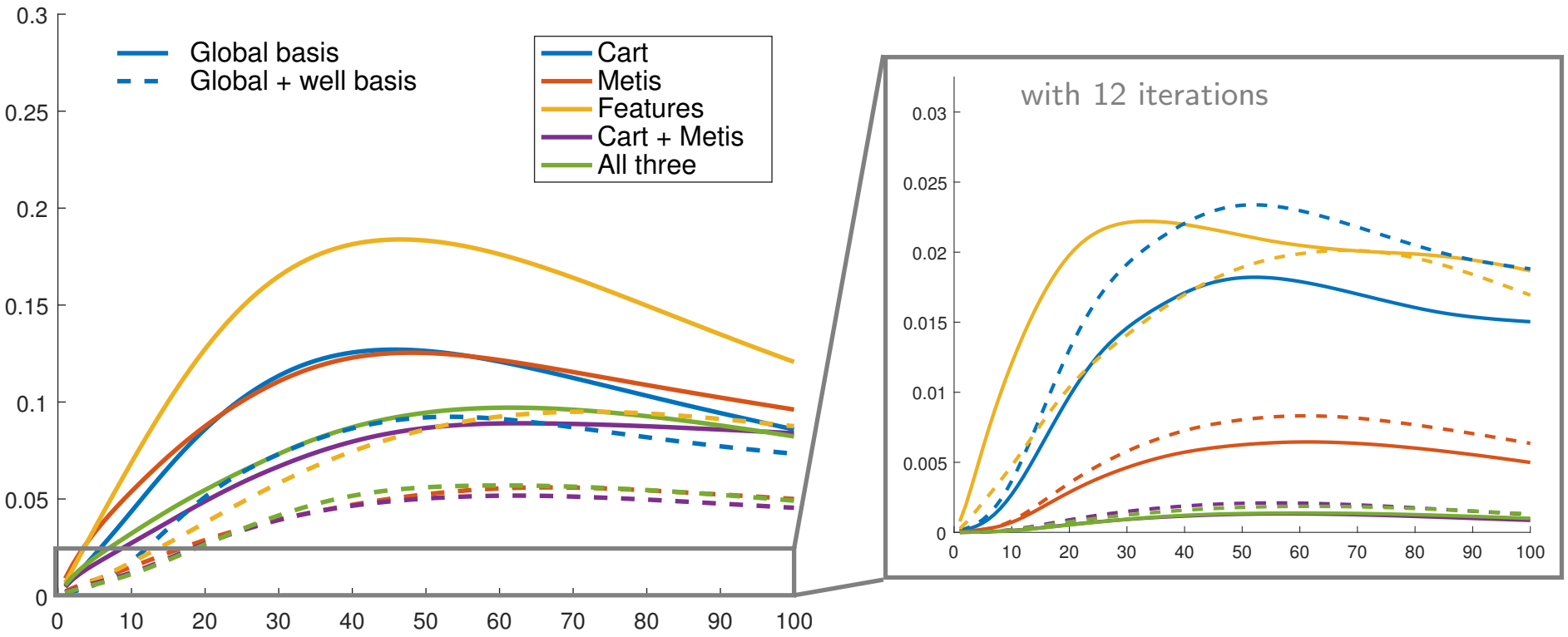

Numerical example: Gullfaks

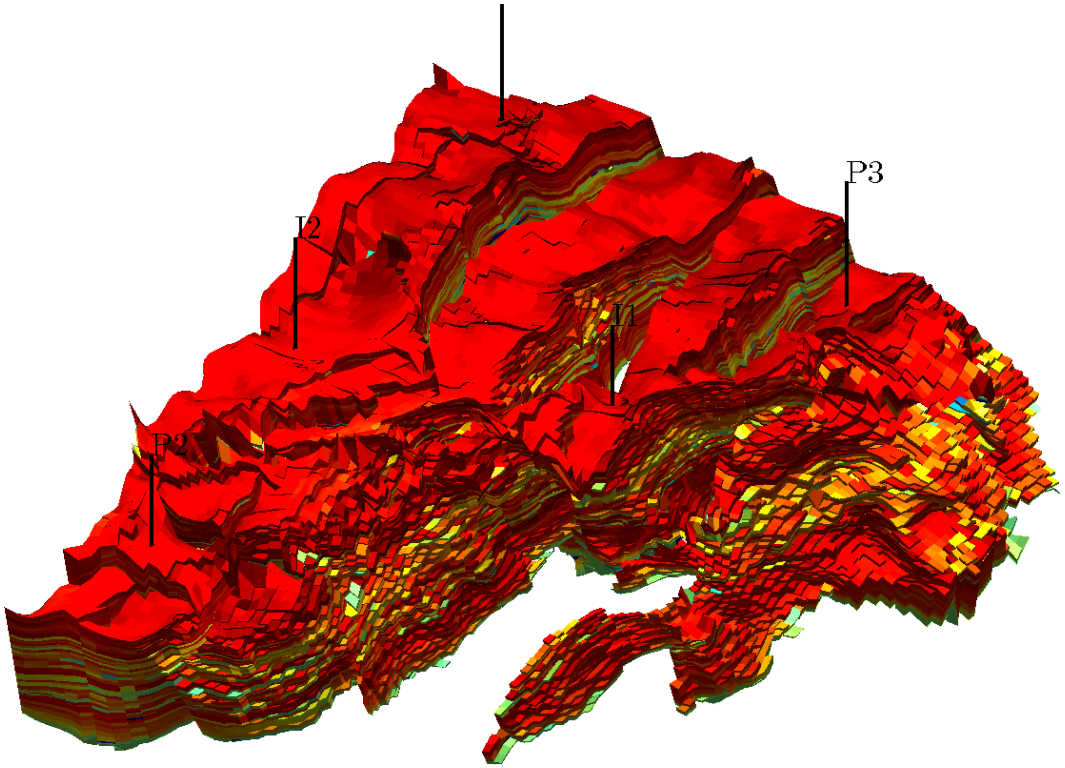

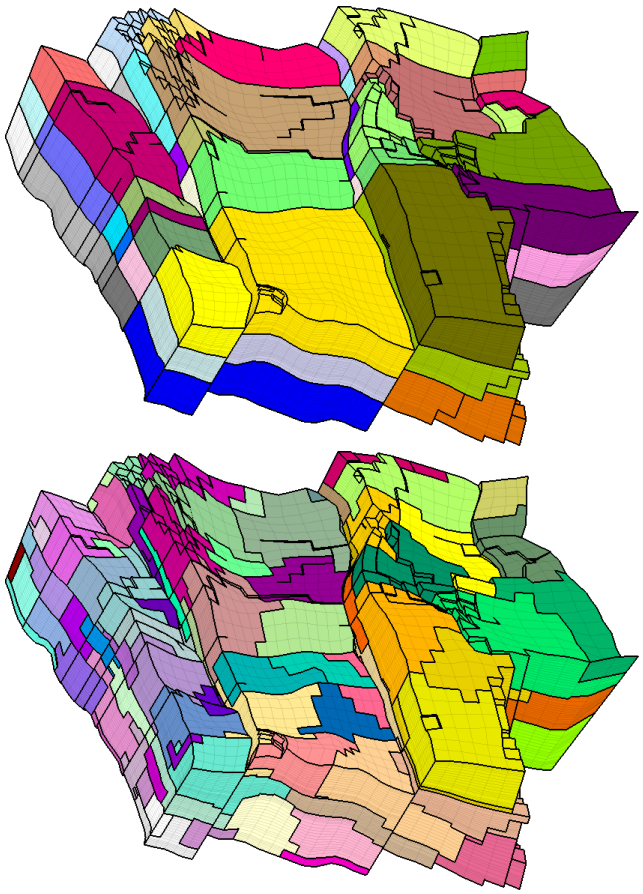

Higher resolution: $80 \times 100 \times 52$ cells, 416 000 active
Partition: rectangular (upper) and by Metis (lower)

Numerical example: Gullfaks

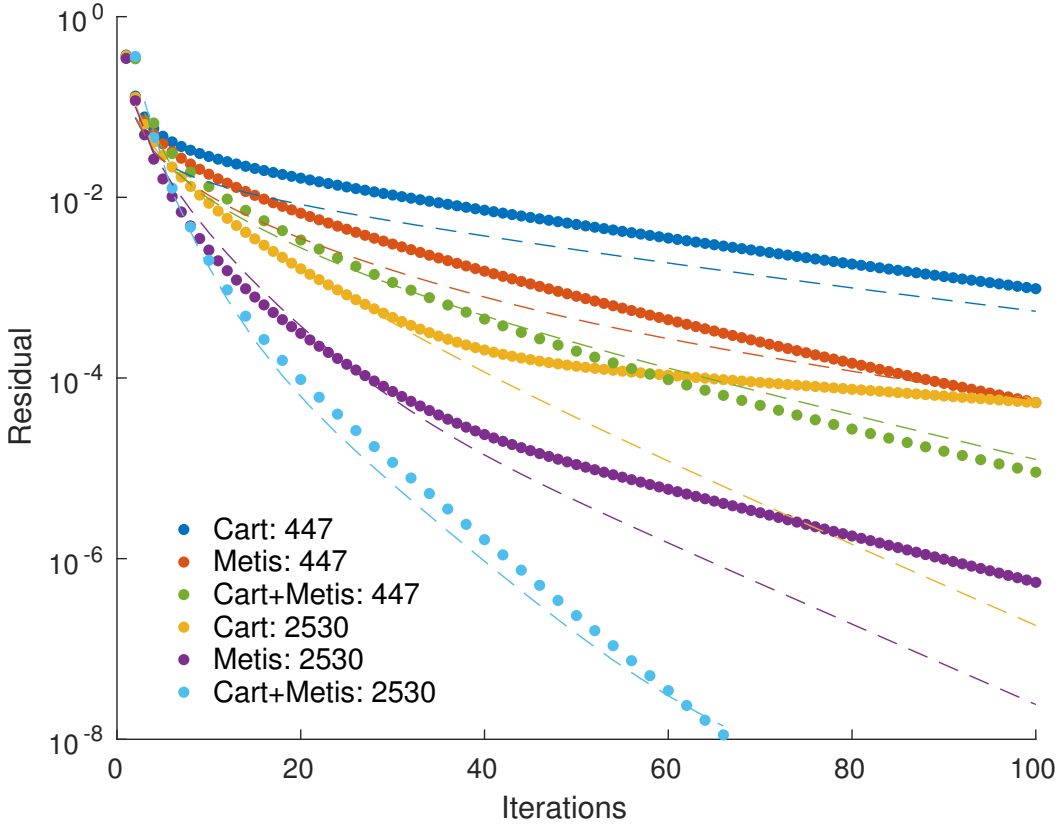

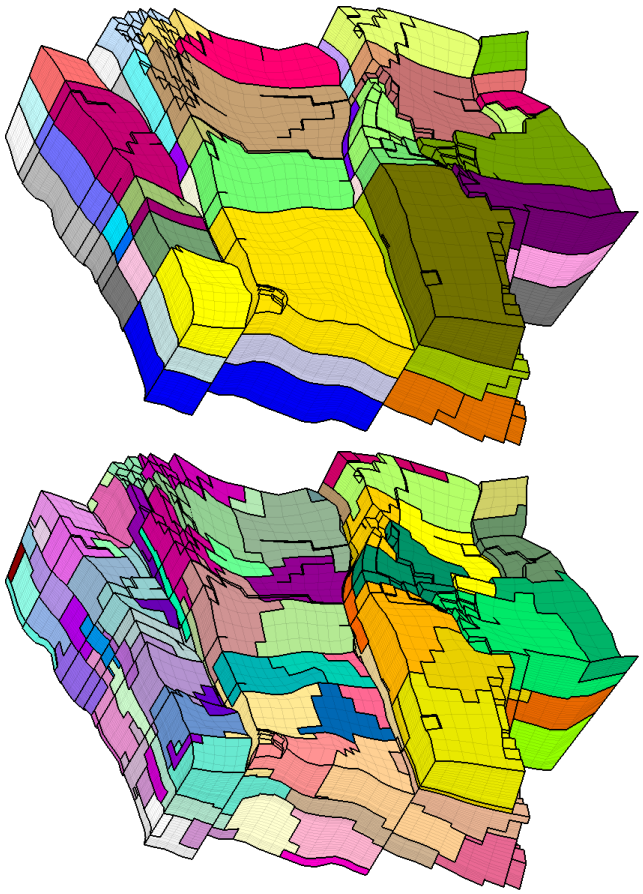

Conclusion

- Multiscale basis functions for pressure, fully unstructured
- Applicable to wide range of flow problems through finite-volume framework
- Emphasis on robust local method for fine-scale transport
- Unstructured coarsening allows for adaption to features
- Very simple to implement regardless of grid complexity
- Prototype in commercial simulator and MRST

Backup slides

Basis functions: MsFV vs MsRSB

MsFV, $\mathbf{K}_x = \mathbf{K}_y$

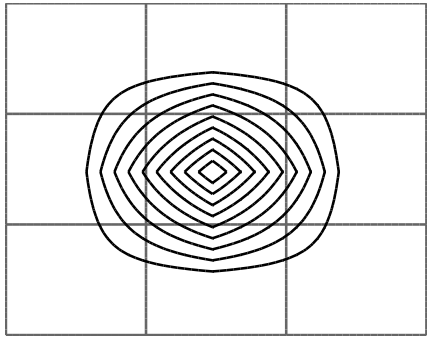

$$\begin{bmatrix} -0.08 & -0.16 & -0.09 \\ -0.18 & & -0.16 \\ -0.08 & -0.17 & -0.08 \end{bmatrix}$$

MsRSB, $\mathbf{K}_x = \mathbf{K}_y$

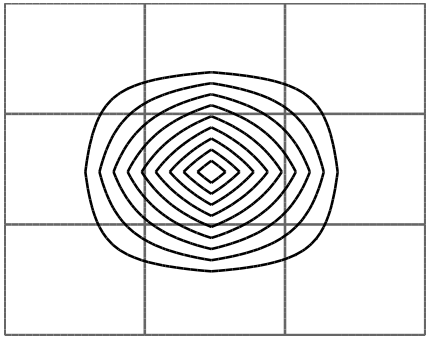

$$\begin{bmatrix} -0.08 & -0.16 & -0.09 \\ -0.17 & & -0.16 \\ -0.08 & -0.17 & -0.08 \end{bmatrix}$$

MsFV, $\mathbf{K}_x = 8\mathbf{K}_y$

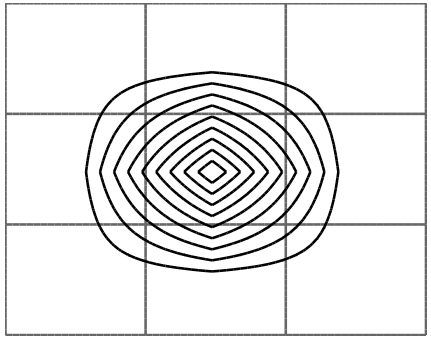

$$\begin{bmatrix} -0.09 & +0.17 & -0.09 \\ -0.49 & & -0.49 \\ -0.07 & +0.14 & -0.08 \end{bmatrix}$$

MsRSB, $\mathbf{K}_x = 8\mathbf{K}_y$

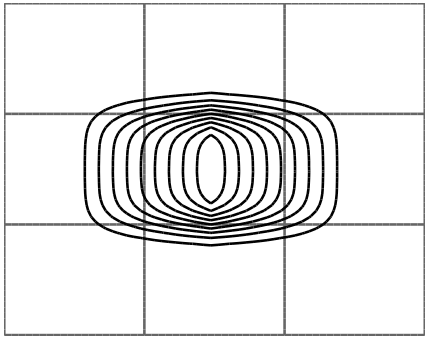

$$\begin{bmatrix} -0.03 & +0.05 & -0.04 \\ -0.48 & & -0.48 \\ -0.03 & +0.05 & -0.04 \end{bmatrix}$$

MsFV, Tarbert

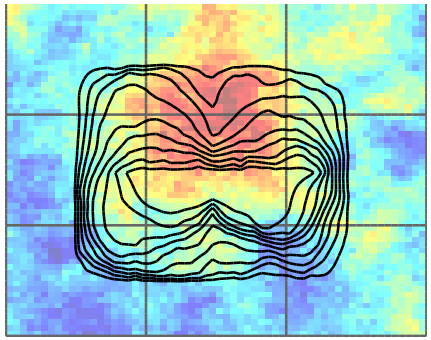

$$\begin{bmatrix} -0.01 & -0.96 & -0.02 \\ -0.00 & & +0.00 \\ -0.00 & -0.01 & -0.00 \end{bmatrix}$$

MsRSB, Tarbert

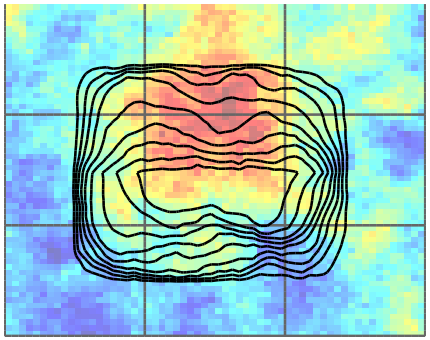

$$\begin{bmatrix} -0.01 & -0.97 & -0.01 \\ -0.00 & & +0.01 \\ -0.00 & -0.01 & -0.00 \end{bmatrix}$$

MsFV, Upper Ness

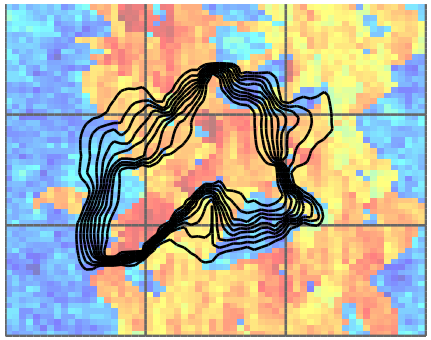

$$\begin{bmatrix} -0.00 & -0.55 & -0.02 \\ -0.00 & & -0.32 \\ -0.00 & -0.09 & -0.01 \end{bmatrix}$$

MsRSB, Upper Ness

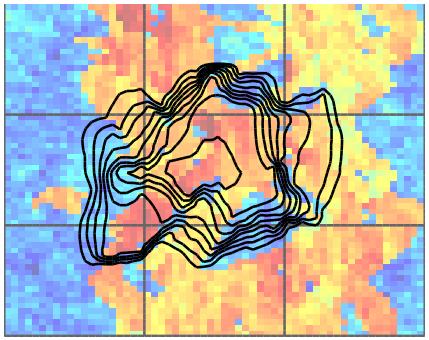

$$\begin{bmatrix} -0.18 & -0.31 & -0.02 \\ -0.04 & & -0.17 \\ -0.15 & -0.12 & -0.01 \end{bmatrix}$$

The matrices report the net fluxes into or out of the neighboring coarse blocks induced by a unit pressure differential

Example: water-based EOR

- Full Eclipse 100 polymer model with adsorption, Todd-Langstaff mixing, inaccessible pore volume, and permeability reduction
- Polymer concentration changes water viscosity to achieve better sweep
- Model includes shear thinning, i.e., water-polymer viscosity depends on the velocity.
- Non-Newtonian fluid rheology makes the pressure equation highly nonlinear

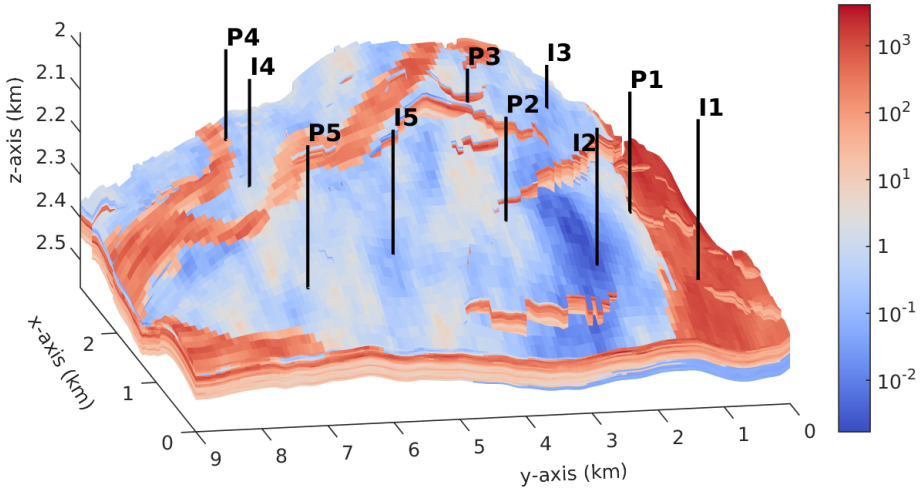

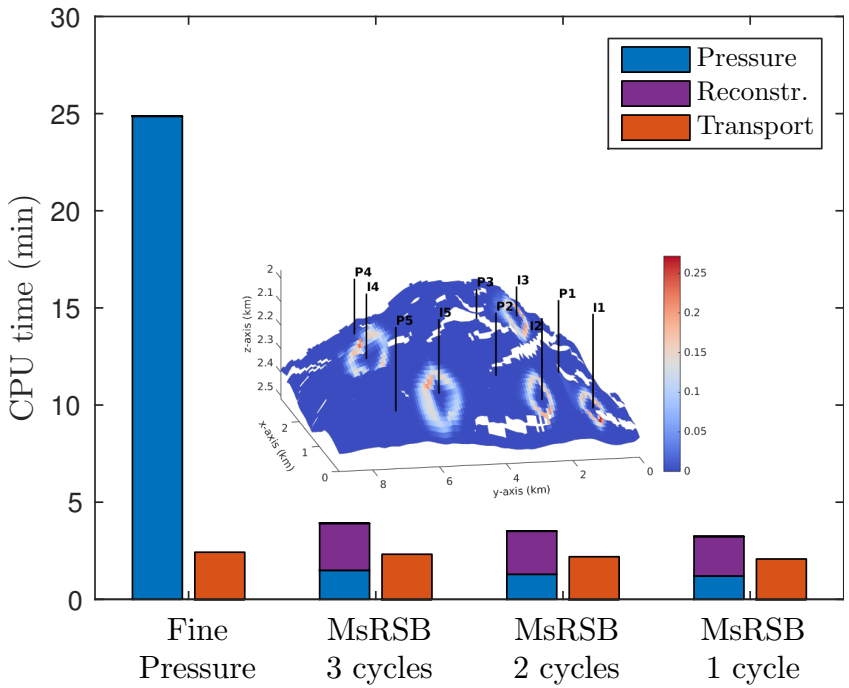

Example: validation on SPE10 layers

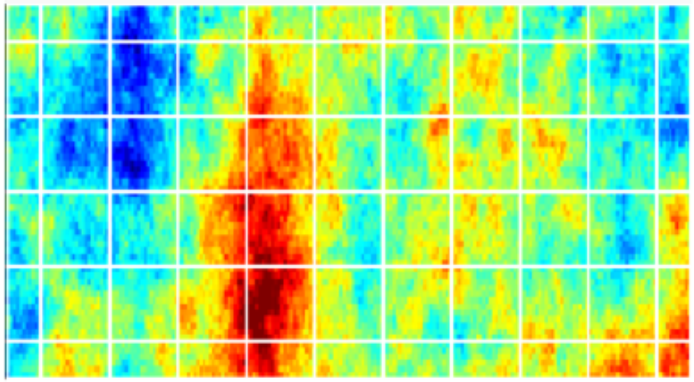

Permeability

Reference solution

MsRSB

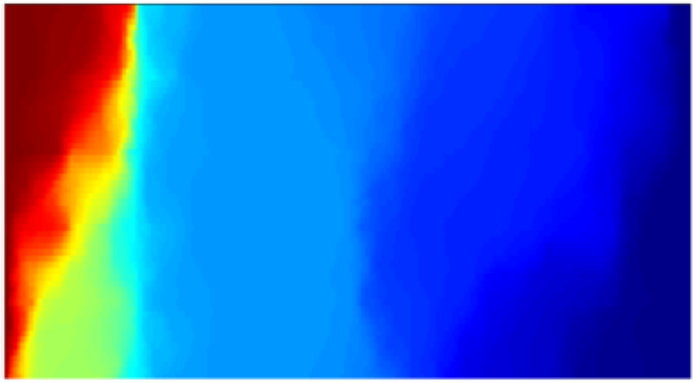

MsFV

Error	Grid	p (L^2)	p (L^∞)	v (L^2)	v (L^∞)
MsFV	6×11	0.0313	0.0910	0.1138	0.4151
MsRSB	6×11	0.0204	0.0766	0.0880	0.4071

Example: validation on SPE10 layers

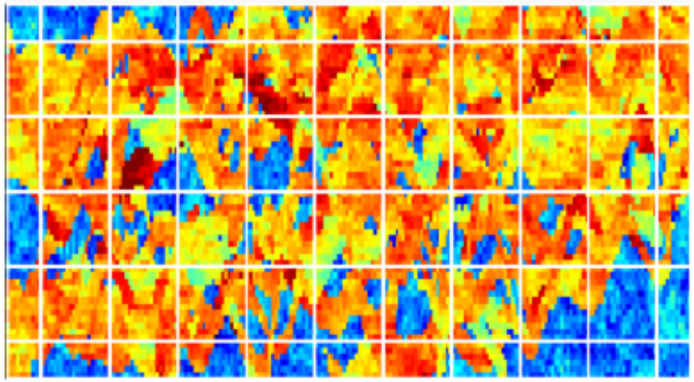

Permeability

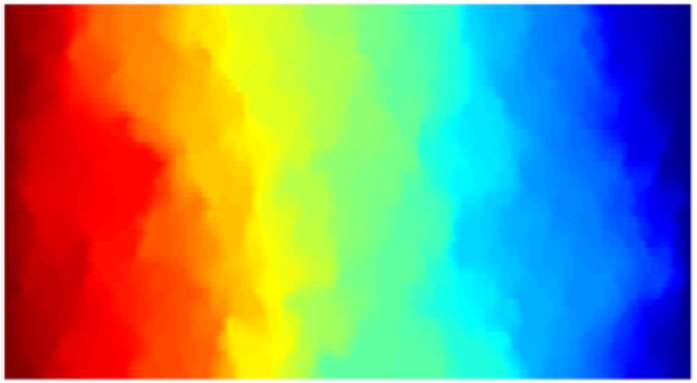

Reference solution

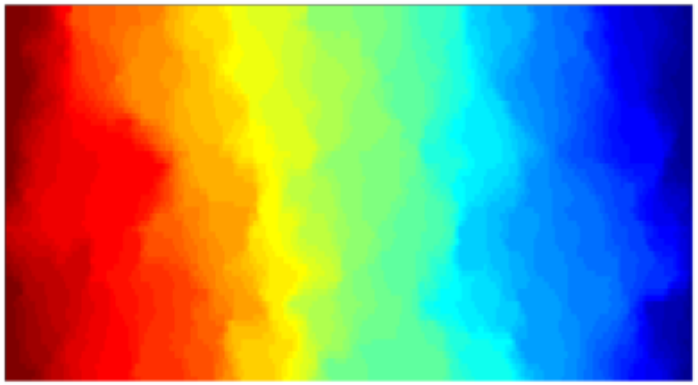

MsRSB

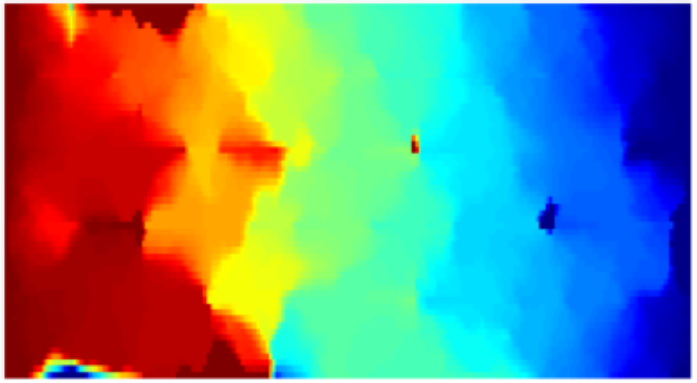

MsFV

Error	Grid	p (L^2)	p (L^∞)	v (L^2)	v (L^∞)
MsFV	6×11	0.2299	2.0725	0.4913	0.7124
MsRSB	6×11	0.0232	0.0801	0.1658	0.3240

Numerical example: well basis

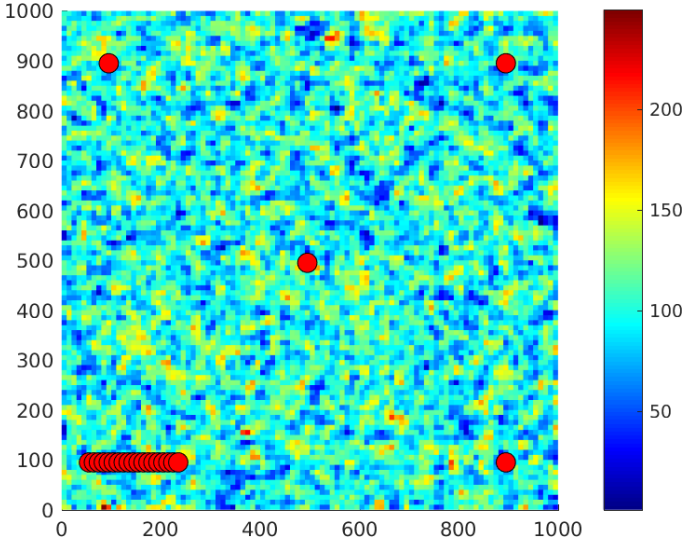

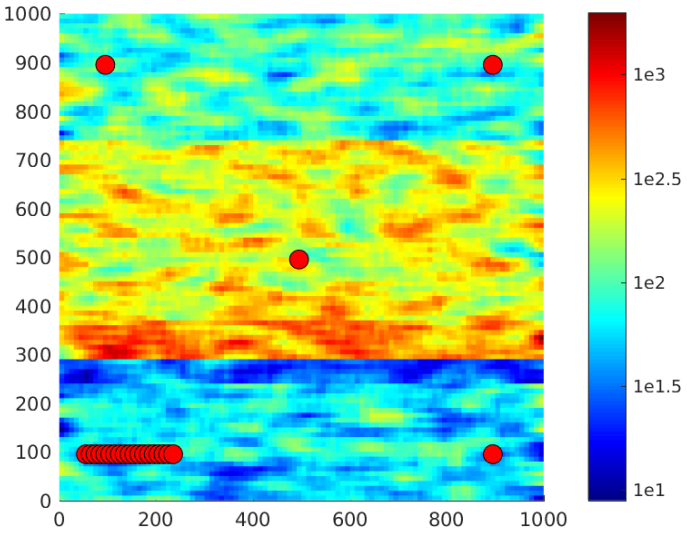

Basis	Gaussian L^2	Gaussian L^∞	Layered L^2	Layered L^∞
6×6	0.0641	0.1679	0.0619	0.1750
Well basis	0.0760	0.1131	0.1015	0.1215
Well basis $+ 6 \times 6$	0.0303	0.1136	0.0280	0.0634

Example: Validation of compositional simulator

Compare MRST implementation to AD-GPRS research simulator

- Simple one dimensional example
- Pressure drop of 50 bar over domain
- Compare different schemes to validate

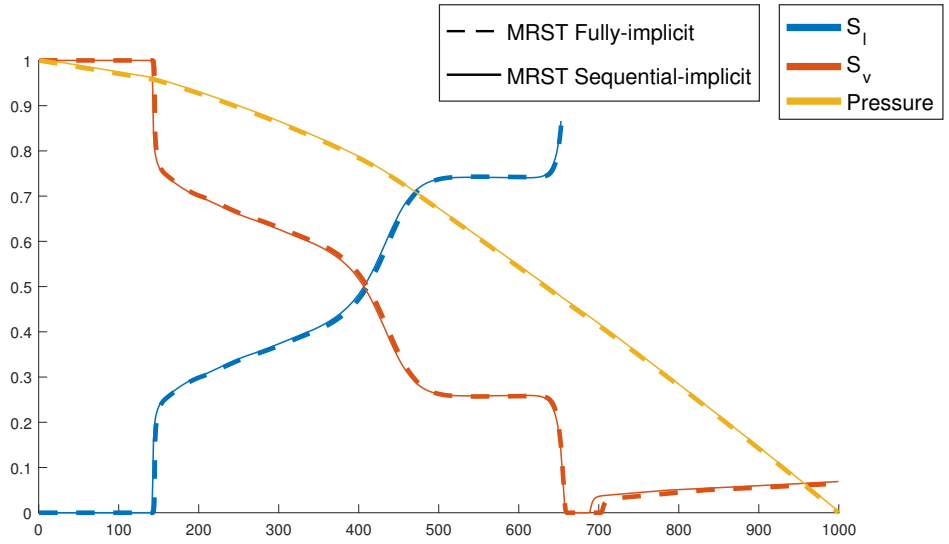

Reservoir quantities, $p_{min} = 75$ bar

Example: Validation of compositional simulator

Compare MRST implementation to AD-GPRS research simulator

- Simple one dimensional example
- Pressure drop of 50 bar over domain
- Compare different schemes to validate

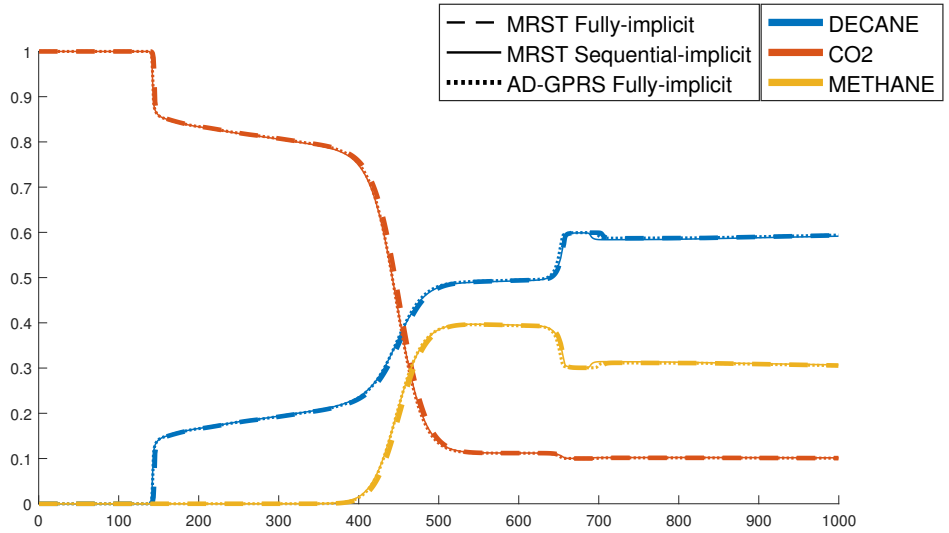

Mole fractions, $p_{min} = 75$ bar

Example: Validation of compositional simulator

Compare MRST implementation to AD-GPRS research simulator

- Simple one dimensional example
- Pressure drop of 50 bar over domain
- Compare different schemes to validate

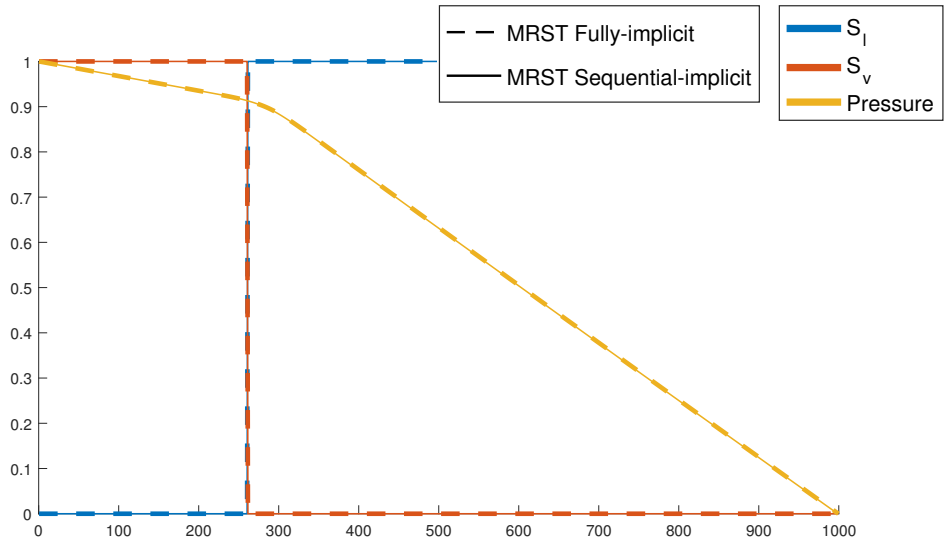

Reservoir quantities, $p_{min} = 275$ bar

Example: Validation of compositional simulator

Compare MRST implementation to AD-GPRS research simulator

- Simple one dimensional example
- Pressure drop of 50 bar over domain
- Compare different schemes to validate

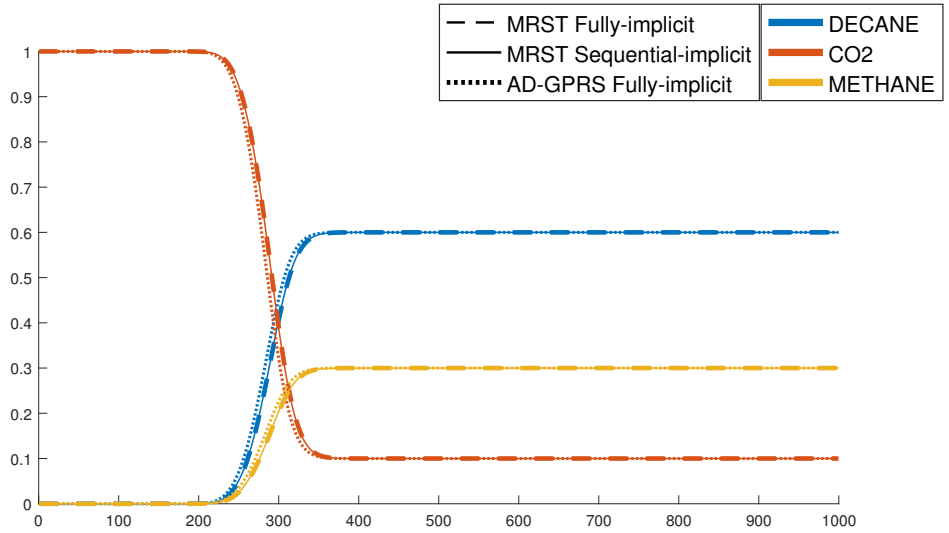

Mole fractions, $p_{min} = 275$ bar

Example: unstructured PEBI grid

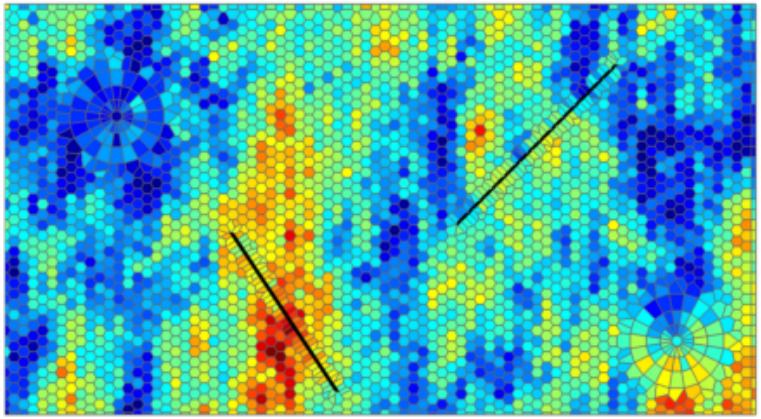

Porosity and grid

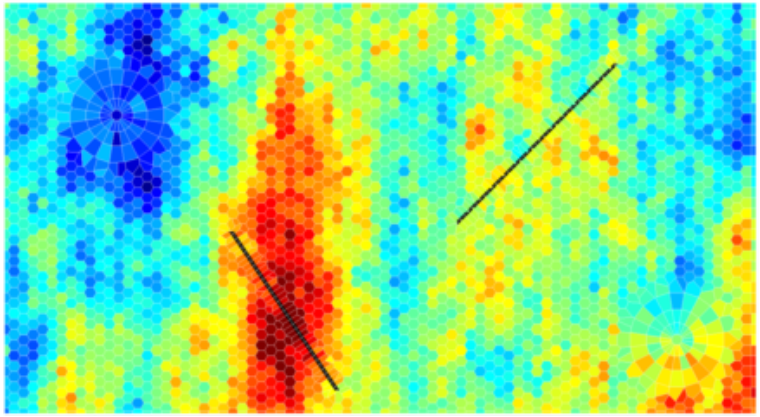

Permability from SPE 10, Layer 35

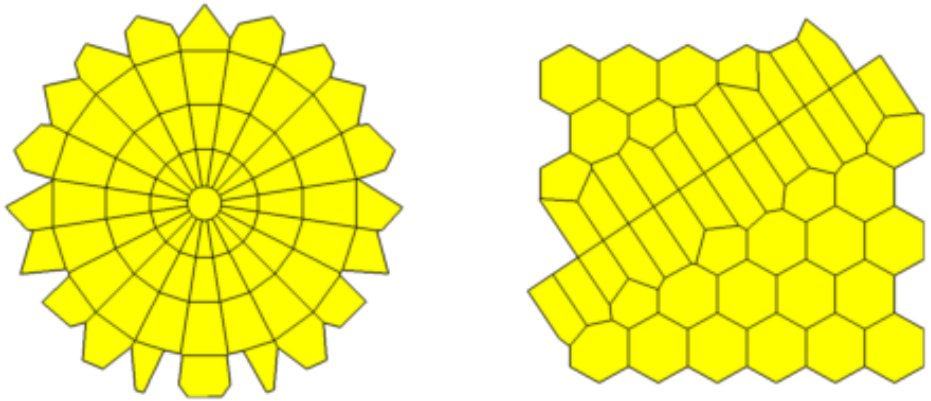

Detailed view of refinement

- Unstructured grid designed to minimize grid orientation effects
- Two embedded radial grids near wells
- Fine grid adapts to faults
- The faults are sealed, i.e. allow no fluid flow through

Example: unstructured PEBI grid

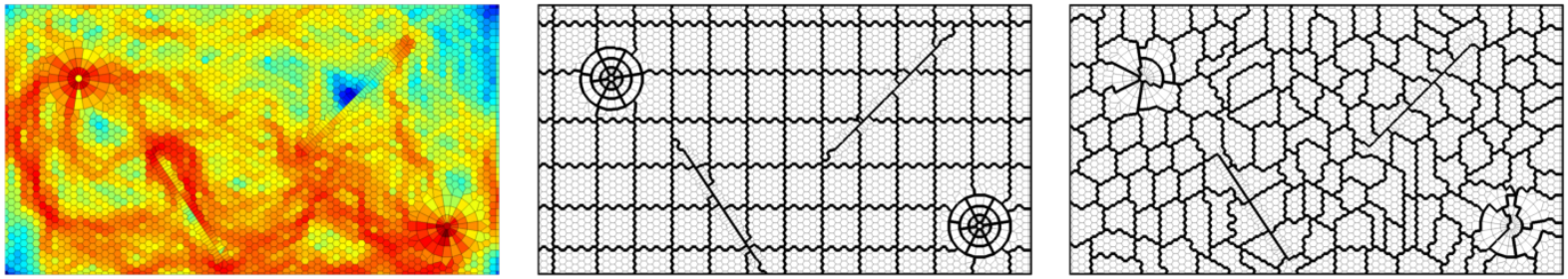

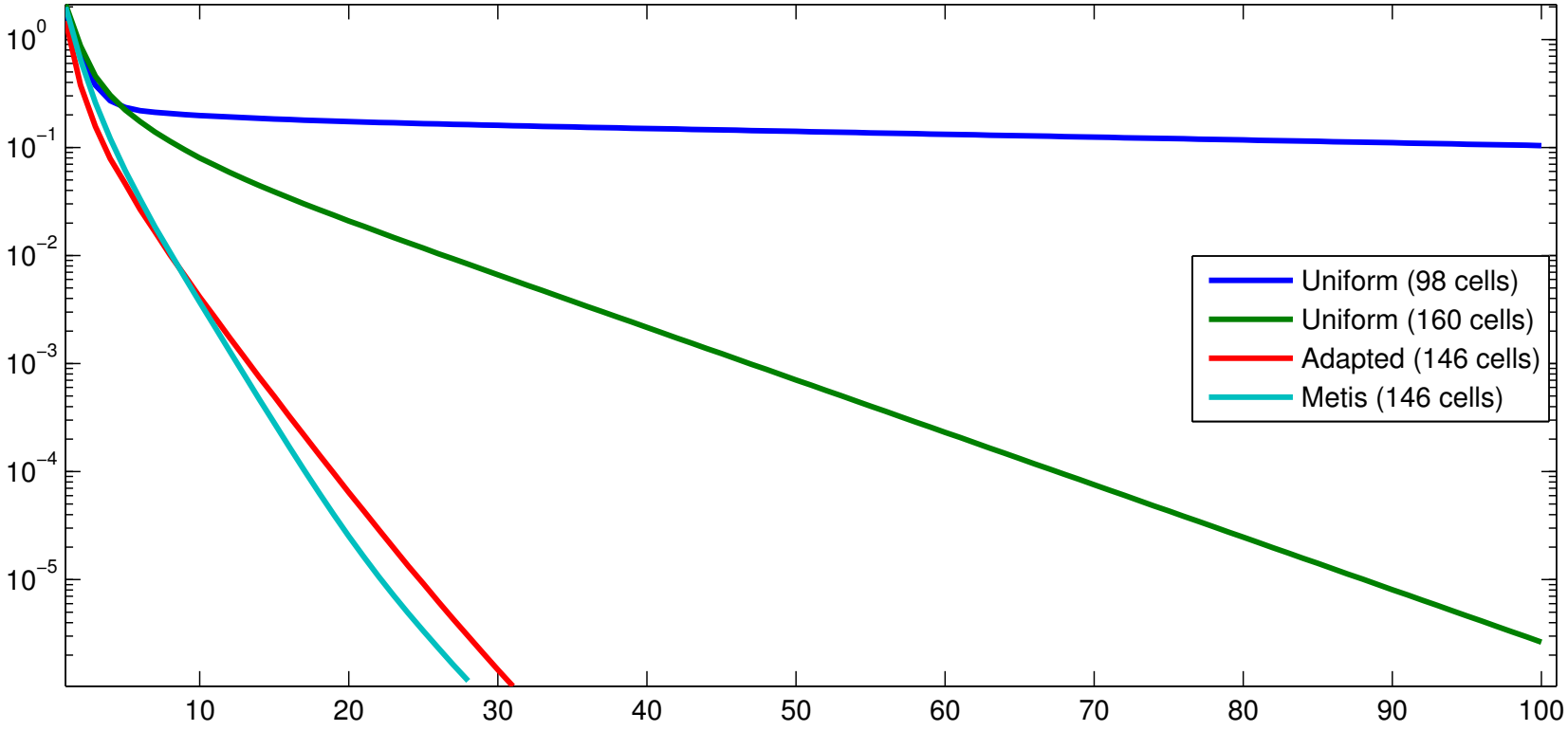

Two-step preconditioner, ILU(0) as 2nd stage, Richardson iterations

Example: unstructured PEBI grid

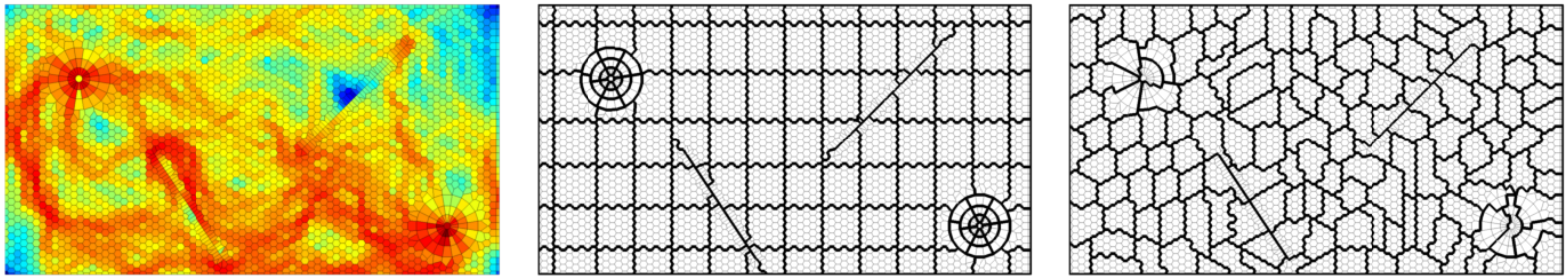

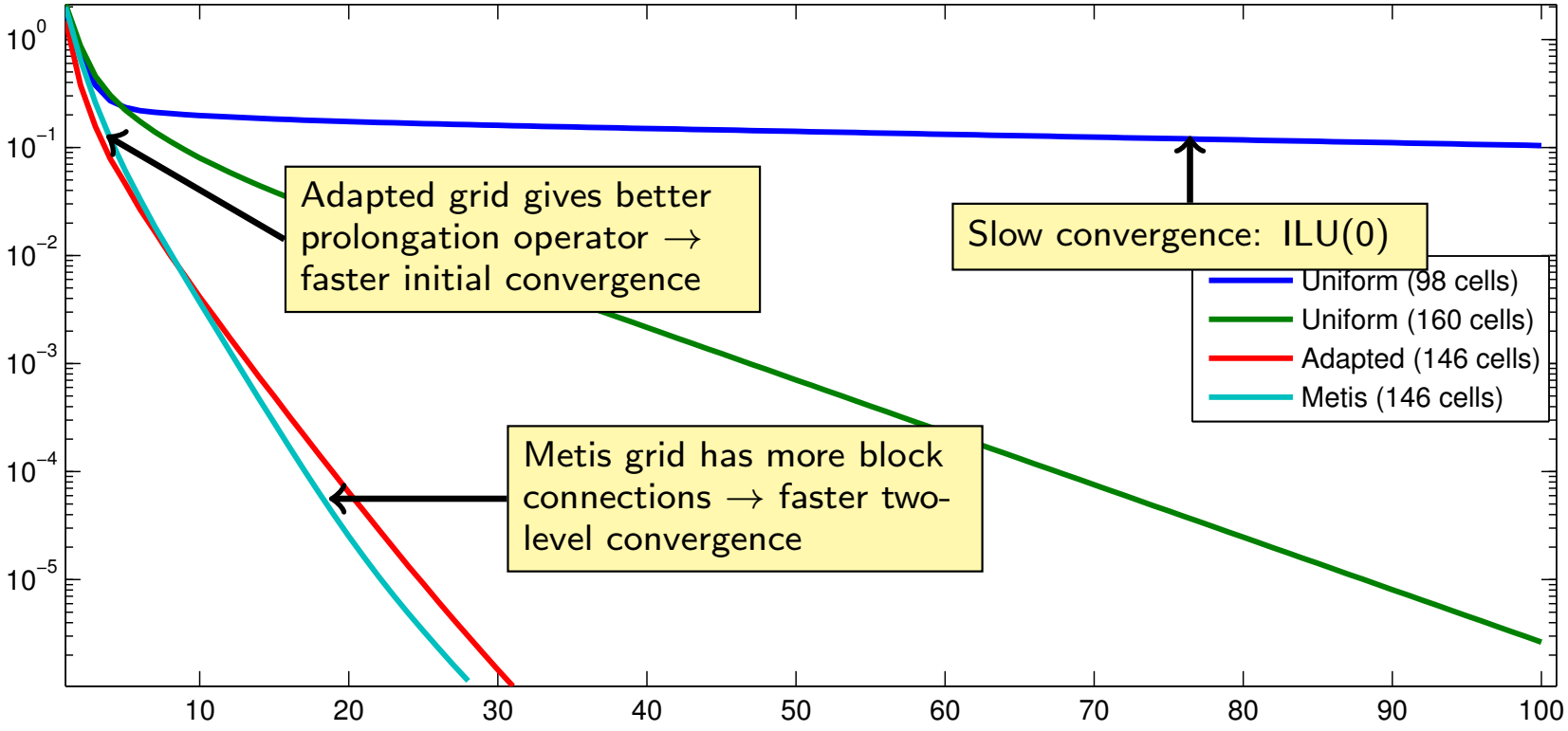

Two-step preconditioner, ILU(0) as 2nd stage, Richardson iterations

Example: unstructured PEBI grid

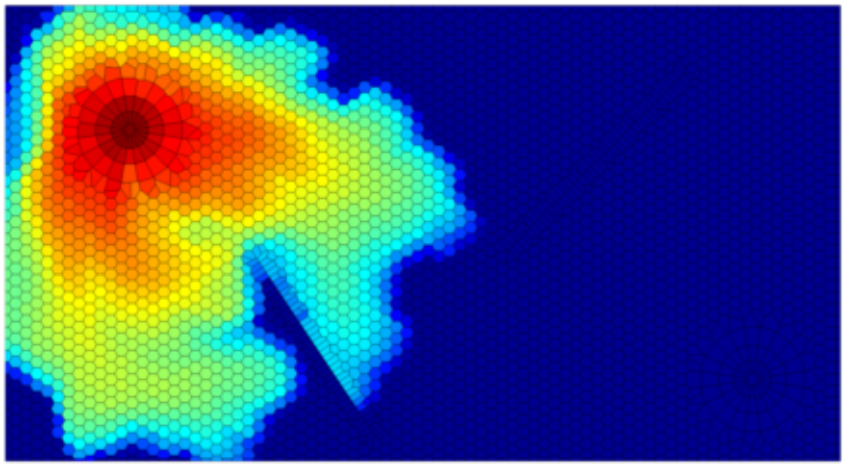

Water front, fine-scale solution

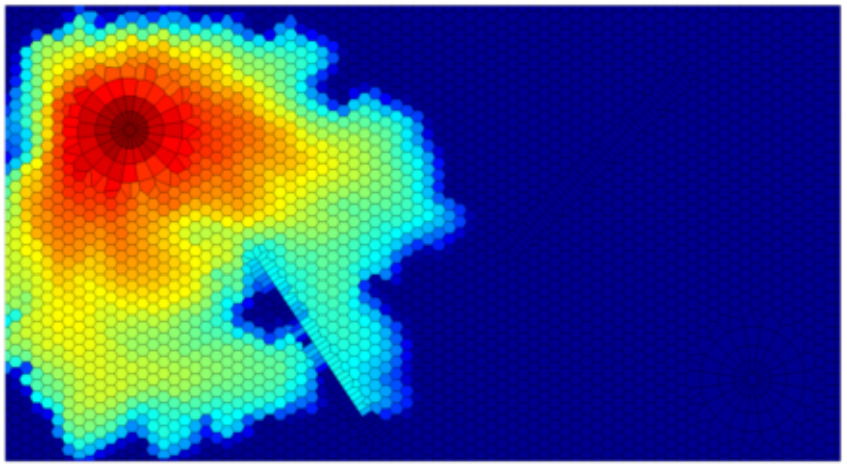

Water front, multiscale solution

- Injector: 1 PVI at constant rate. Producer: fixed bottom-hole pressure.
- Relative mobility: $\lambda_{rw} = s_w^2$, $\lambda_{ro} = (1 - s_w)^2/5$
- Basis functions: adapted grid, updated by reapplying smoother

Example: unstructured PEBI grid

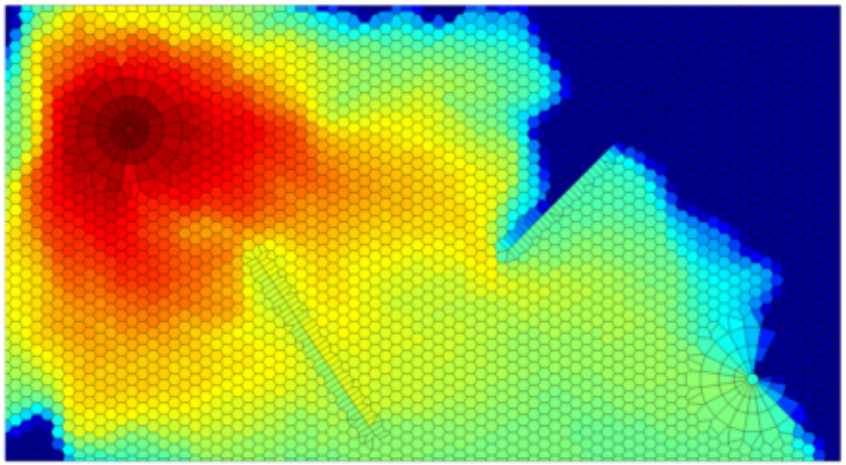

Water front, fine-scale solution

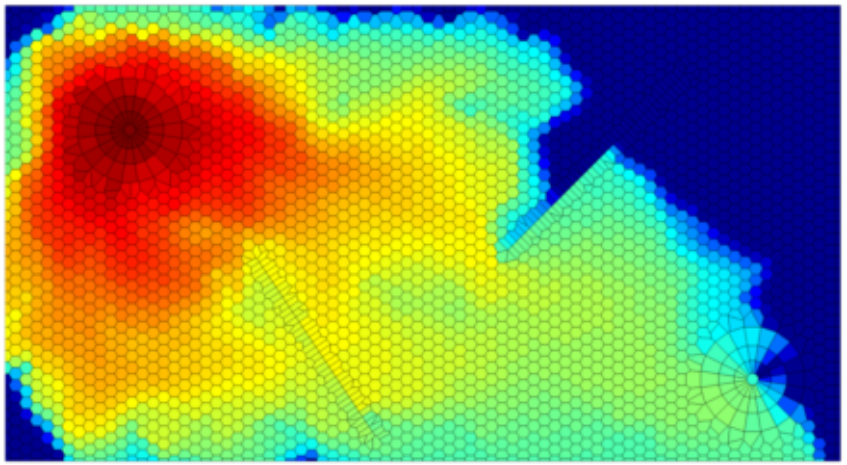

Water front, multiscale solution

- Injector: 1 PVI at constant rate. Producer: fixed bottom-hole pressure.
- Relative mobility: $\lambda_{rw} = s_w^2$, $\lambda_{ro} = (1 - s_w)^2/5$
- Basis functions: adapted grid, updated by reapplying smoother

Example: unstructured PEBI grid

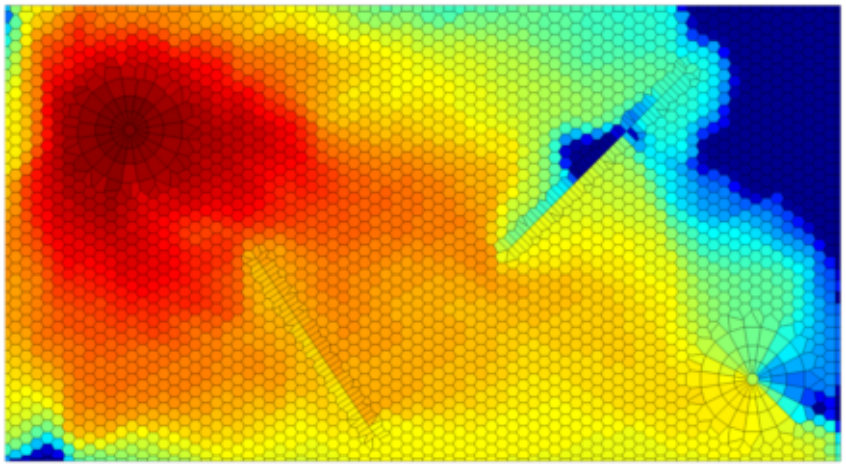

Water front, fine-scale solution

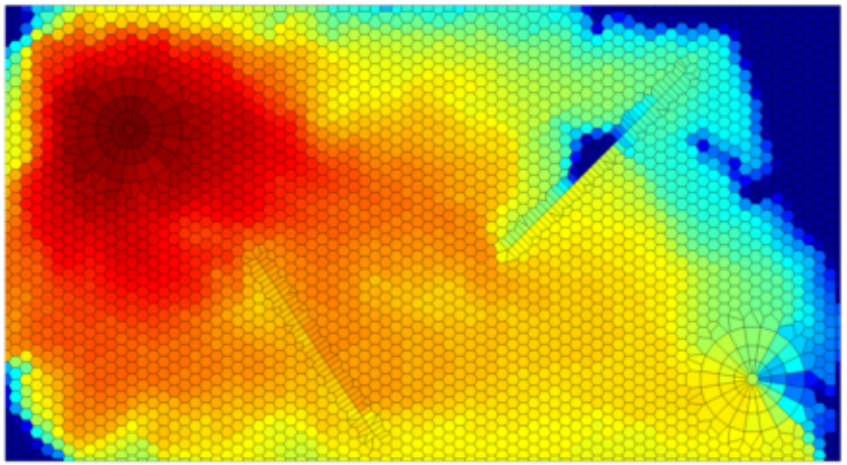

Water front, multiscale solution

- Injector: 1 PVI at constant rate. Producer: fixed bottom-hole pressure.
- Relative mobility: $\lambda_{rw} = s_w^2$, $\lambda_{ro} = (1 - s_w)^2/5$
- Basis functions: adapted grid, updated by reapplying smoother

MsRSB: computing basis functions

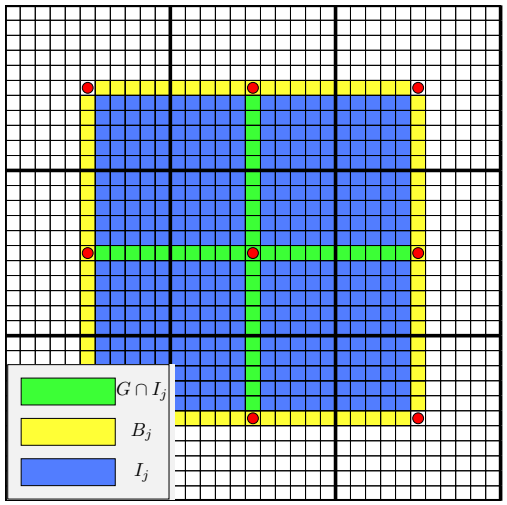

Divide set of fine cells F into m coarse blocks,

$$C_j \subseteq F, \quad C_j \cap C_i = \emptyset \quad \forall \quad i \neq j, \quad i, j \in [1, m], \quad |F| = n.$$

Define support I_j and its boundary B_j for each block,

$$P_j(\boldsymbol{x}) > 0, \quad \boldsymbol{x} \in I_j \qquad P_j(\boldsymbol{x}) = 0 \text{ otherwise.}$$

For convenience, define global boundary/dual as union of all boundaries

$$G = B_1 \cup B_2 \cup \ldots \cup B_{m-1} \cup B_m.$$

For cells in G, let H_i be the set of blocks where it is active,

$$H_i = \{j \,|\, i \in I_j, i \in G\}.$$

MsRSB: computing basis functions

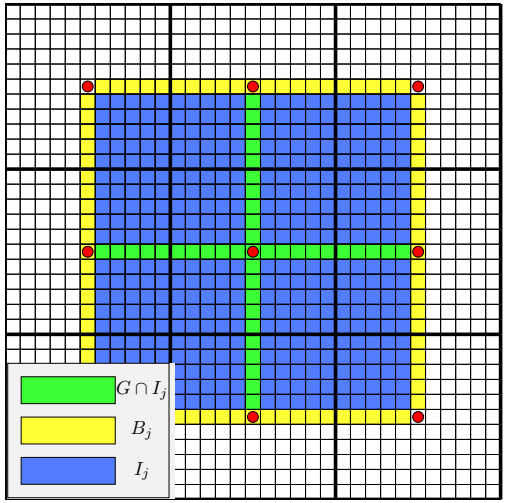

Define preliminary update by Jacobi relaxation,

$$\widehat{\mathbf{d}}_j = -\omega D^{-1} A P_j^n.$$

Modify the update according to cell category,

$$d_{ij} = \begin{cases} \frac{\widehat{d}_{ij} - P_{ij}^n \sum_{k \in H_i} \widehat{d}_{ik}}{1 + \sum_{k \in H_i} \widehat{d}_{ik}}, & i \in I_j, i \in G, \\ \widehat{d}_{ij}, & i \in I_j, i \notin G, \\ 0, & i \notin I_j. \end{cases}$$

Finally, apply the update and proceed to next iteration

$$P_{ij}^{n+1} = P_{ij}^n + d_{ij}$$

MsRSB: computing basis functions

- Jacobi iterations ensures algebraic smoothness
- Limited support by construction
- Does the proposed basis functions have partition of unity?

Two cases: $i \in G$ and $i \notin G$. First, consider $i \notin G$:

$$\begin{aligned}\sum_j P_{ij}^{n+1} =& \sum_j P_{ij}^n - \frac{\omega}{A_{ii}} \sum_j \sum_k A_{ik} P_{kj}^n \\ =& 1 - \frac{\omega}{A_{ii}} \sum_k A_{ik} \left(\sum_j P_{kj}^n \right) \\ =& 1 - \frac{\omega}{A_{ii}} \sum_k A_{ik} = 1.\end{aligned}$$

We have used that $\sum_{j \in H_i} P_{ij}^n = 1$ by assumption and that P_{ij}^n is nonzero only in H_i.

MsRSB: computing basis functions

- Jacobi iterations ensures algebraic smoothness
- Limited support by construction
- Does the proposed basis functions have partition of unity?

Two cases: $i \in G$ and $i \notin G$. Next, consider $i \in G$.

$$\begin{aligned}
\sum_{j\in\{1,\dots,m\}} P_{ij}^{n+1} &= \sum_{j\in H_i}\left(P_{ij}^n + \frac{\widehat{d}_{ij} - P_{ij}^n \sum_{k\in H_i}\widehat{d}_{ik}}{1+\sum_{k\in H_i}\widehat{d}_{ik}}\right) \\
&= 1 + \sum_{j\in H_i} \frac{\widehat{d}_{ij} - P_{ij}^n \sum_{k\in H_i}\widehat{d}_{ik}}{1+\sum_{k\in H_i}\widehat{d}_{ik}} \\
&= 1 + \frac{\sum_{k\in H_i}\widehat{d}_{ik}}{1+\sum_{k\in H_i}\widehat{d}_{ik}} - \frac{\sum_{k\in H_i}\widehat{d}_{ik}}{1+\sum_{k\in H_i}\widehat{d}_{ik}} \sum_{j\in H_i} P_{ij}^n = 1.
\end{aligned}$$

We have used that $\sum_{j\in H_i} P_{ij}^n = 1$ by assumption and that P_{ij}^n is nonzero only in H_i.